

Supplementary Figures and Tables

Table S1. Record of all DNA microarrays hybridized for *Saccharomyces cerevisiae* BY4741 wild type, $\Delta cin5$, $\Delta gln3$, $\Delta hmo1$, and $\Delta zap1$. For those rows that contain information about a GCAT array, the first column labeled “GCAT” designates if the data comes from the top half or the bottom half of the microarray. This information is necessary to perform the normalization procedure described by Sherbina (2014a).

GCAT	File Name	Strain	Sample	Flask	Dye Orientation
Top	Slide82_20060620_0635_Top_Nonnormalized_data.gpr	wild type	t15/t0	1	Cy5/Cy3
Bottom	Slide82_20060620_0635_Bottom_Nonnormalized_data.gpr	wild type	t15/t0	1	Cy5/Cy3
	13669355_2008-01-31_0635_Nonnormalized_data.gpr	wild type	t15/t0	2	Cy5/Cy3
	13664282_2007-10-30_0635_Nonnormalized_data.gpr	wild type	t15/t0	3	Cy3/Cy5
	13664286_2007-09-14_0635_Nonnormalized_data.gpr	wild type	t15/t0	4	Cy3/Cy5
Top	Slide55_20060420_0635_Top_Nonnormalized_data.gpr	wild type	t30/t0	0	Cy5/Cy3
Bottom	Slide55_20060420_0635_Bottom_Nonnormalized_data.gpr	wild type	t30/t0	0	Cy5/Cy3
Top	Slide83_20060620_0635_Top_Nonnormalized_data.gpr	wild type	t30/t0	1	Cy5/Cy3
Bottom	Slide83_20060620_0635_Bottom_Nonnormalized_data.gpr	wild type	t30/t0	1	Cy5/Cy3
	13669354_2008-01-31_0635_Nonnormalized_data.gpr	wild type	t30/t0	2	Cy5/Cy3
	13669406_2007-10-30_0635_Nonnormalized_data.gpr	wild type	t30/t0	3	Cy3/Cy5
	13664283_2007-09-24_0635_Nonnormalized_data.gpr	wild type	t30/t0	4	Cy3/Cy5
Top	Slide56_20060420_0635_Top_Nonnormalized_data.gpr	wild type	t60/t0	0	Cy5/Cy3
Bottom	Slide56_20060420_0635_Bottom_Nonnormalized_data.gpr	wild type	t60/t0	0	Cy5/Cy3
Top	Slide79_20060614_0635_Top_Nonnormalized_data.gpr	wild type	t60/t0	1	Cy5/Cy3
Bottom	Slide79_20060614_0635_Bottom_Nonnormalized_data.gpr	wild type	t60/t0	1	Cy5/Cy3
	13669353_2008-01-31_0635_Nonnormalized_data.gpr	wild type	t60/t0	2	Cy5/Cy3
	13669404_2007-10-30_0635_Nonnormalized_data.gpr	wild type	t60/t0	3	Cy3/Cy5
Top	Slide57_20060420_0635_Top_Nonnormalized_data.gpr	wild type	t90/t0	0	Cy5/Cy3
Bottom	Slide57_20060420_0635_Bottom_Nonnormalized_data.gpr	wild type	t90/t0	0	Cy5/Cy3
Top	Slide84_20060620_0635_Top_Nonnormalized_data.gpr	wild type	t90/t0	1	Cy5/Cy3
Bottom	Slide84_20060620_0635_Bottom_Nonnormalized_data.gpr	wild type	t90/t0	1	Cy5/Cy3
	13669350_2008-01-31_0635_Nonnormalized_data.gpr	wild type	t90/t0	2	Cy5/Cy3
	13669401_2007-10-30_0635_Nonnormalized_data.gpr	wild type	t90/t0	3	Cy3/Cy5

	13664284_2007-09-24_0635_Nonnormalized_data.gpr	wild type	t90/t0	4	Cy3/Cy5
Top	Slide58_20060420_0635_Top_Nonnormalized_data.gpr	wild type	t120/t0	0	Cy5/Cy3
Bottom	Slide58_20060420_0635_Bottom_Nonnormalized_data.gpr	wild type	t120/t0	0	Cy5/Cy3
Top	Slide81_20060614_0635_Top_Nonnormalized_data.gpr	wild type	t120/t0	1	Cy5/Cy3
Bottom	Slide81_20060614_0635_Bottom_Nonnormalized_data.gpr	wild type	t120/t0	1	Cy5/Cy3
	13669352_2008-01-31_0635_Nonnormalized_data.gpr	wild type	t120/t0	2	Cy5/Cy3
	13669358_2007-10-30_0635_Nonnormalized_data.gpr	wild type	t120/t0	3	Cy3/Cy5
	13664285_2007-09-10_0635_Nonnormalized_data.gpr	wild type	t120/t0	4	Cy3/Cy5
	13721688_2008-05-21_0635_Nonnormalized_data.gpr	$\Delta cin5$	t15/t0	1	Cy3/Cy5
	13669344_2007-11-02_0635_Nonnormalized_data.gpr	$\Delta cin5$	t15/t0	2	Cy5/Cy3
	13669346_2008-02-21_0635_Nonnormalized_data.gpr	$\Delta cin5$	t15/t0	3	Cy5/Cy3
	13721677_2008-03-20_0635_Nonnormalized_data.gpr	$\Delta cin5$	t15/t0	4	Cy3/Cy5
	13721684_2008-05-21_0635_Nonnormalized_data.gpr	$\Delta cin5$	t30/t0	1	Cy3/Cy5
	13669345_2007-11-02_0635_Nonnormalized_data.gpr	$\Delta cin5$	t30/t0	2	Cy5/Cy3
	13669348_2008-02-21_0635_Nonnormalized_data.gpr	$\Delta cin5$	t30/t0	3	Cy5/Cy3
	13724271_2008-03-20_0635_Nonnormalized_data.gpr	$\Delta cin5$	t30/t0	4	Cy3/Cy5
	13721687_2008-05-21_0635_Nonnormalized_data.gpr	$\Delta cin5$	t60/t0	1	Cy3/Cy5
	13669342_2007-11-02_0635_Nonnormalized_data.gpr	$\Delta cin5$	t60/t0	2	Cy5/Cy3
	13669351_2008-02-21_0635_Nonnormalized_data.gpr	$\Delta cin5$	t60/t0	3	Cy5/Cy3
	13721678_2008-03-20_fullscan_0635_Nonnormalized_data.gpr	$\Delta cin5$	t60/t0	4	Cy3/Cy5
	13721686_2008-05-21_0635_Nonnormalized_data.gpr	$\Delta cin5$	t90/t0	1	Cy3/Cy5
	13669343_2007-11-02_0635_Nonnormalized_data.gpr	$\Delta cin5$	t90/t0	2	Cy5/Cy3
	13669349_2008-02-21_0635_Nonnormalized_data.gpr	$\Delta cin5$	t90/t0	3	Cy5/Cy3
	13724272_2008-03-20_0635_Nonnormalized_data.gpr	$\Delta cin5$	t90/t0	4	Cy3/Cy5
	13721682_2008-05-21_0635_Nonnormalized_data.gpr	$\Delta cin5$	t120/t0	1	Cy3/Cy5
	13669340_2007-11-02_0635_Nonnormalized_data.gpr	$\Delta cin5$	t120/t0	2	Cy5/Cy3
	13669347_2008-02-21_0635_Nonnormalized_data.gpr	$\Delta cin5$	t120/t0	3	Cy5/Cy3
	13724270_2008-03-20_0635_Nonnormalized_data.gpr	$\Delta cin5$	t120/t0	4	Cy3/Cy5
	13738236_2010-07-01_0635_Nonnormalized_data.gpr	$\Delta gln3$	t15/t0	2	Cy3/Cy5
	13738299_2010-07-22_0635.gpr	$\Delta gln3$	t15/t0	3	Cy5/Cy3
	13722128_2010-06-23_0635.gpr	$\Delta gln3$	t15/t0	4	Cy5/Cy3
	13738305_2010-07-02_0635_nonnormalized.gpr	$\Delta gln3$	t15/t0	5	Cy3/Cy5
	13721681_2010-06-11_0635_Nonnormalized_data.gpr	$\Delta gln3$	t30/t0	1	Cy5/Cy3
	13738234_2010-07-01_0635_Nonnormalized_data.gpr	$\Delta gln3$	t30/t0	2	Cy3/Cy5
	13722125_2010-06-23_0635.gpr	$\Delta gln3$	t30/t0	4	Cy5/Cy3
	13738304_2010-07-02_0635_Nonnormalized_data.gpr	$\Delta gln3$	t30/t0	5	Cy3/Cy5
	13721679_2010-06-11_0635_Nonnormalized_data.gpr	$\Delta gln3$	t60/t0	1	Cy5/Cy3
	13738235_2010-07-01_0635_Nonnormalized_data.gpr	$\Delta gln3$	t60/t0	2	Cy3/Cy5
	13738298_2010-07-22_0635.gpr	$\Delta gln3$	t60/t0	3	Cy3/Cy5

	13722129_2010-06-23_0635.gpr	$\Delta gln3$	t60/t0	4	Cy5/Cy3
	13721680_2010-06-11_0635_Nonnormalized_data.gpr	$\Delta gln3$	t90/t0	1	Cy5/Cy3
	13738233_2010-07-01_0635_Nonnormalized_data.gpr	$\Delta gln3$	t90/t0	2	Cy3/Cy5
	13738297_2010-07-22_rescanned_0635.gpr	$\Delta gln3$	t90/t0	3	Cy5/Cy3
	13738303_2010-07-02_0635_Nonnormalized_data.gpr	$\Delta gln3$	t90/t0	5	Cy3/Cy5
	13722124_2010-06-11_0635_Nonnormalized_data.gpr	$\Delta gln3$	t120/t0	1	Cy5/Cy3
	13738232_2010-07-01_0635_Nonnormalized_data.gpr	$\Delta gln3$	t120/t0	2	Cy3/Cy5
	13738296_2010-07-22_0635_Nonnormalized_data.gpr	$\Delta gln3$	t120/t0	4	Cy5/Cy3
	13738301_2010-07-02_0635_Nonnormalized_data.gpr	$\Delta gln3$	t120/t0	5	Cy3/Cy5
	14204845_2011-01-26_0635_Nonnormalized_data.gpr	$\Delta hmo1$	t15/t0	1	Cy5/Cy3
	14205398_2010-12-09_0635_Nonnormalized_data.gpr	$\Delta hmo1$	t15/t0	2	Cy5/Cy3
	14204560_2011-02-02_0635_Nonnormalized_data.gpr	$\Delta hmo1$	t15/t0	3	Cy3/Cy5
	14205387_2011-02-09_0635_Nonnormalized_data.gpr	$\Delta hmo1$	t15/t0	4	Cy3/Cy5
	14204839_2011-01-26_0635_Nonnormalized_data.gpr	$\Delta hmo1$	t30/t0	1	Cy5/Cy3
	14205401_2010-12-09_rescan_0635_Nonnormalized_data.gpr	$\Delta hmo1$	t30/t0	2	Cy5/Cy3
	13738295_2011-02-04_0635_Nonnormalized_data.gpr	$\Delta hmo1$	t30/t0	3	Cy3/Cy5
	14205390_2011-02-09_0635_Nonnormalized_data.gpr	$\Delta hmo1$	t30/t0	4	Cy3/Cy5
	14204836_2011-01-26_0635_Nonnormalized_data.gpr	$\Delta hmo1$	t60/t0	1	Cy5/Cy3
	14204827_2010-12-09_rescan_0635_Nonnormalized_data.gpr	$\Delta hmo1$	t60/t0	2	Cy5/Cy3
	14204562_2011-02-02_0635_Nonnormalized_data.gpr	$\Delta hmo1$	t60/t0	3	Cy3/Cy5
	14205396_2011-02-09_0635_Nonnormalized_data.gpr	$\Delta hmo1$	t60/t0	4	Cy3/Cy5
	14204833_2011-01-26_0635_Nonnormalized_data.gpr	$\Delta hmo1$	t90/t0	1	Cy5/Cy3
	14204834_2010-12-09_rescan_0635_Nonnormalized_data.gpr	$\Delta hmo1$	t90/t0	2	Cy5/Cy3
	14204561_2011-02-02_PMT640-560_0635_Nonnormalized_data.gpr	$\Delta hmo1$	t90/t0	3	Cy3/Cy5
	14204825_2011-02-09_0635_Nonnormalized_data.gpr	$\Delta hmo1$	t90/t0	4	Cy3/Cy5
	14204826_2011-01-26_0635_Nonnormalized_data.gpr	$\Delta hmo1$	t120/t0	1	Cy5/Cy3
	14205402_2010-12-09_0635_Nonnormalized_data.gpr	$\Delta hmo1$	t120/t0	2	Cy5/Cy3
	14204558_2011-02-02_0635_Nonnormalized_data.gpr	$\Delta hmo1$	t120/t0	3	Cy3/Cy5
	14205393_2011-02-09_0635_Nonnormalized_data.gpr	$\Delta hmo1$	t120/t0	4	Cy3/Cy5
	13738314_2010-07-16_0635_Nonnormalized_data.gpr	$\Delta zap1$	t15/t0	2	Cy5/Cy3
	14205400_2010-10-14_0635_Nonnormalized_data.gpr	$\Delta zap1$	t15/t0	3	Cy3/Cy5
	13722120_2010-06-30_0635_Nonnormalized_data.gpr	$\Delta zap1$	t15/t0	4	Cy5/Cy3
	13738240_2010-07-23_0635_Nonnormalized_data.gpr	$\Delta zap1$	t15/t0	5	Cy3/Cy5
	13738315_2010-07-16_0635_Nonnormalized_data.gpr	$\Delta zap1$	t30/t0	2	Cy5/Cy3
	14205397_2010-10-14_0635_Nonnormalized_data.gpr	$\Delta zap1$	t30/t0	3	Cy3/Cy5
	13722119_2010-06-30_0635_Nonnormalized_data.gpr	$\Delta zap1$	t30/t0	4	Cy5/Cy3
	13738237_2010-07-23_0635_Nonnormalized_data.gpr	$\Delta zap1$	t30/t0	5	Cy3/Cy5
	13738311_2010-07-16_0635_Nonnormalized_data.gpr	$\Delta zap1$	t60/t0	2	Cy5/Cy3
	14205394_2010-10-14_0635_Nonnormalized_data.gpr	$\Delta zap1$	t60/t0	3	Cy3/Cy5
	13722122_2010-06-30_second_scan_0635_Nonnormalized_data.gpr	$\Delta zap1$	t60/t0	4	Cy5/Cy3
	13738239_2010-07-23_0635_Nonnormalized_data.gpr	$\Delta zap1$	t60/t0	5	Cy3/Cy5
	13738294_2010-07-16_0635_Nonnormalized_data.gpr	$\Delta zap1$	t90/t0	2	Cy5/Cy3

	14205388_2010-10-14_0635_Nonnormalized_data.gpr	$\Delta zapI$	t90/t0	3	Cy3/Cy5
	13722123_2010-06-30_0635_Nonnormalized_data.gpr	$\Delta zapI$	t90/t0	4	Cy5/Cy3
	13738241_2010-07-23_0635_Nonnormalized_data.gpr	$\Delta zapI$	t90/t0	5	Cy3/Cy5
	13738312_2010-07-16_0635_Nonnormalized_data.gpr	$\Delta zapI$	t120/t0	2	Cy5/Cy3
	14205395_2010-10-14_0635_Nonnormalized_data.gpr	$\Delta zapI$	t120/t0	3	Cy3/Cy5
	13722121_2010-06-30_0635_Nonnormalized_data.gpr	$\Delta zapI$	t120/t0	4	Cy5/Cy3
	13738238_2010-07-23_0635_Nonnormalized_data.gpr	$\Delta zapI$	t120/t0	5	Cy3/Cy5

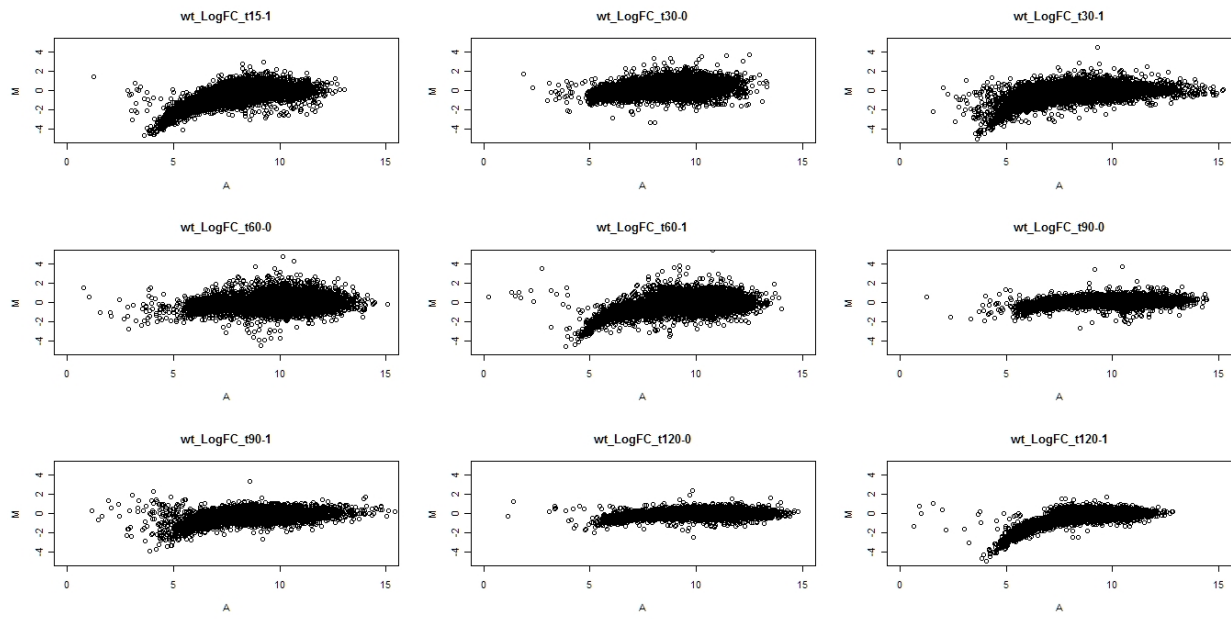


Fig. S1. MA plots before normalization of the log fold change ($M = \log_2(R/G)$ where R is the Cy5 dye and G is the Cy3 dye) versus the total intensity ($A = \log_2(R*G)$ where R is the Cy5 dye and G is the Cy3 dye) for each spot on GCAT microarrays measuring gene expression in the wild type 15, 30, 60, 90, and 120 minutes into the cold shock and recovery experiment.

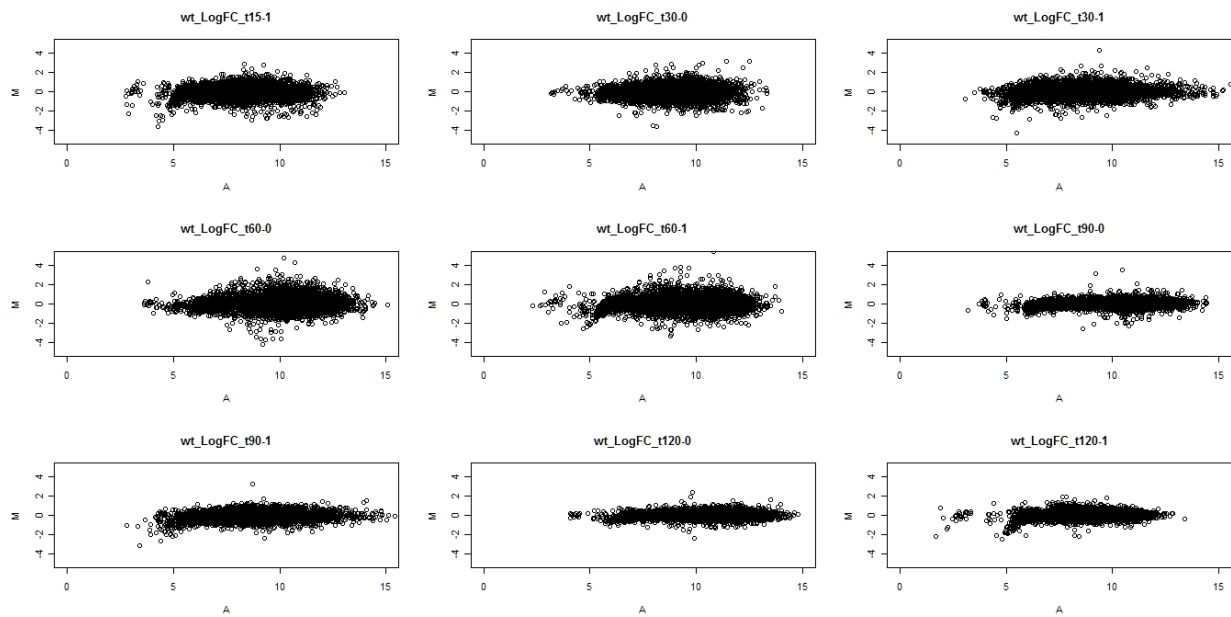


Fig. S2. MA plots after within array normalization of the log fold change ($M = \log_2(R/G)$ where R is the Cy5 dye and G is the Cy3 dye) versus the total intensity ($A = \log_2(R*G)$ where R is the Cy5 dye and G is the Cy3 dye) for each spot on GCAT microarrays measuring gene expression in the wild type 15, 30, 60, 90, and 120 minutes into the cold shock and recovery experiment.

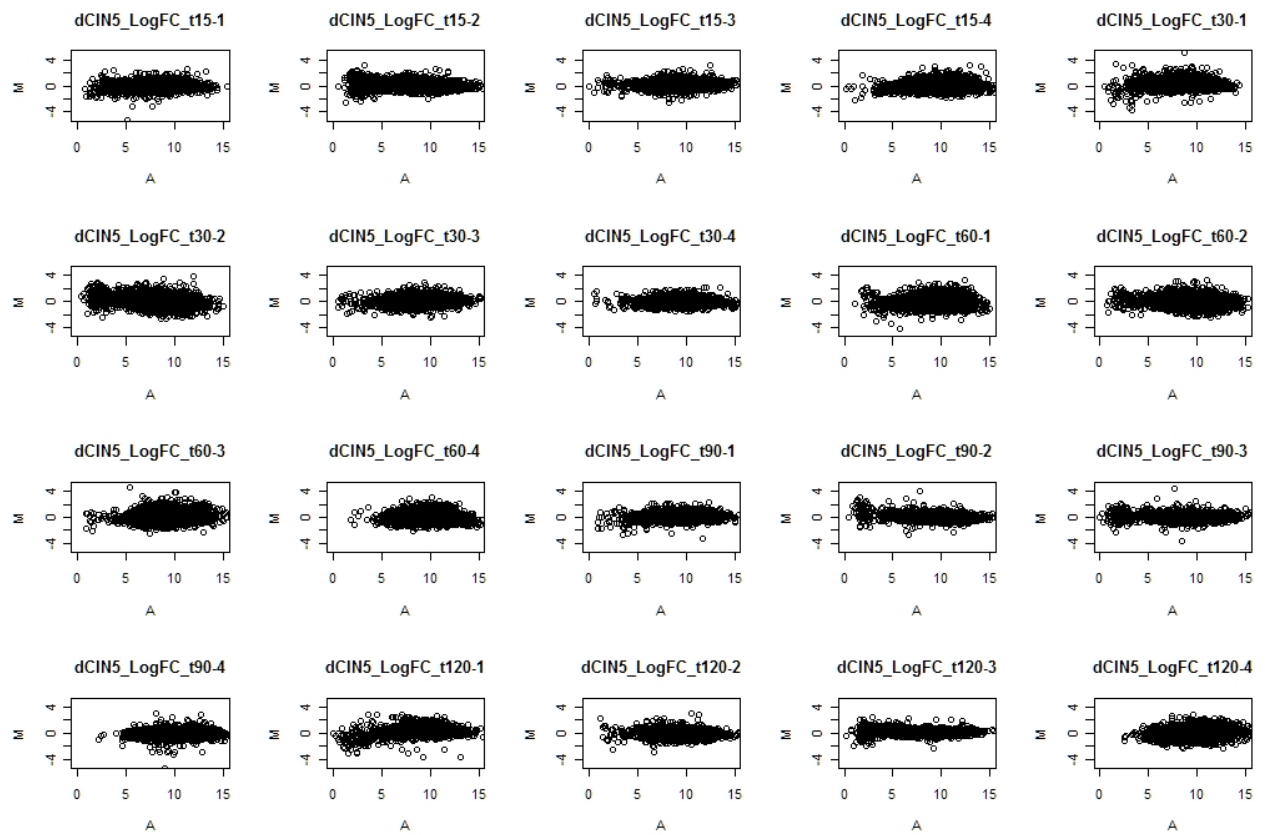


Fig. S3. MA plots before normalization of the log fold change $M = \log_2(R/G)$ where R is the Cy5 dye and G is the Cy3 dye) versus the total intensity ($A = \log_2(R*G)$ where R is the Cy5 dye and G is the Cy3 dye) for each spot on microarrays measuring gene expression in the $\Delta cin5$ strain 15, 30, 60, 90, and 120 minutes into the cold shock and recovery experiment.

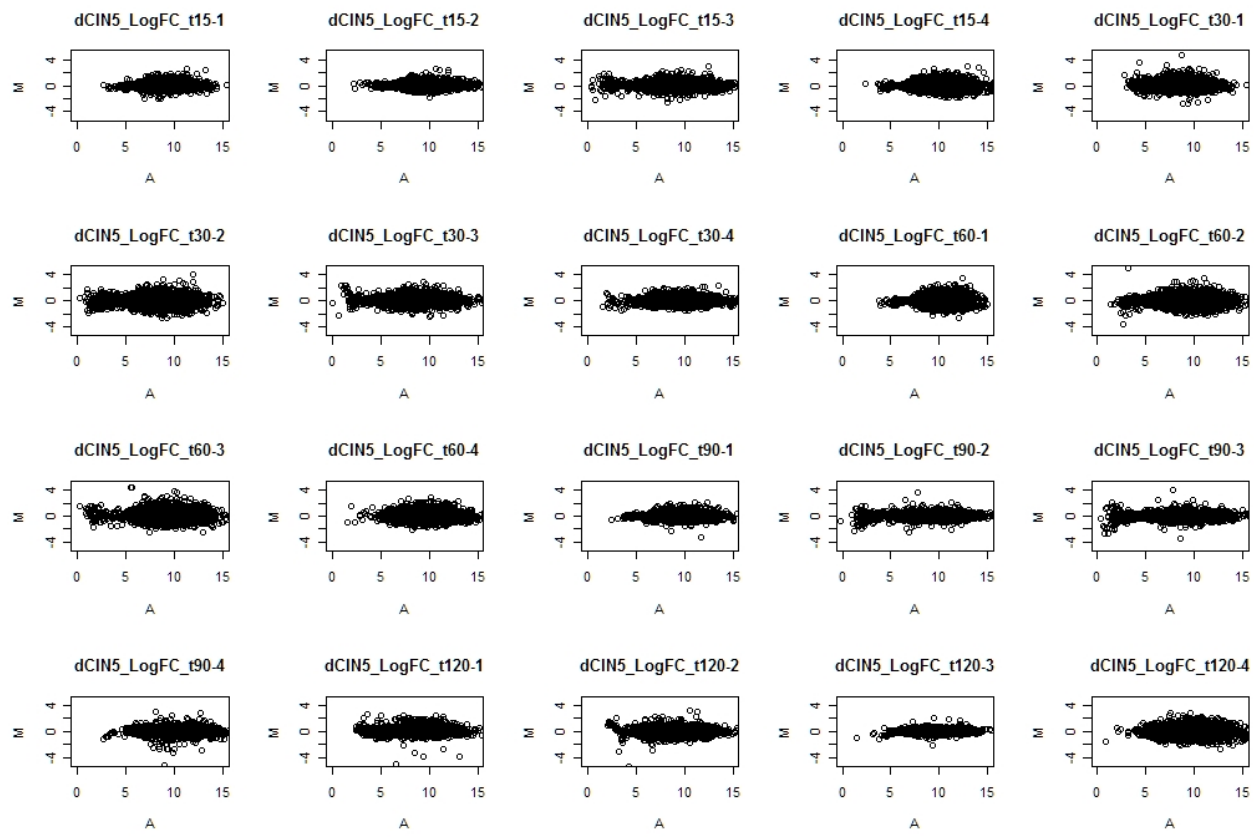


Fig. S4. MA plots after within array normalization of the log fold change ($M = \log_2(R/G)$ where R is the Cy5 dye and G is the Cy3 dye) versus the total intensity ($A = \log_2(R^*G)$ where R is the Cy5 dye and G is the Cy3 dye) for each spot on microarrays measuring gene expression in the $\Delta cin5$ strain 15, 30, 60, 90, and 120 minutes into the cold shock and recovery experiment.

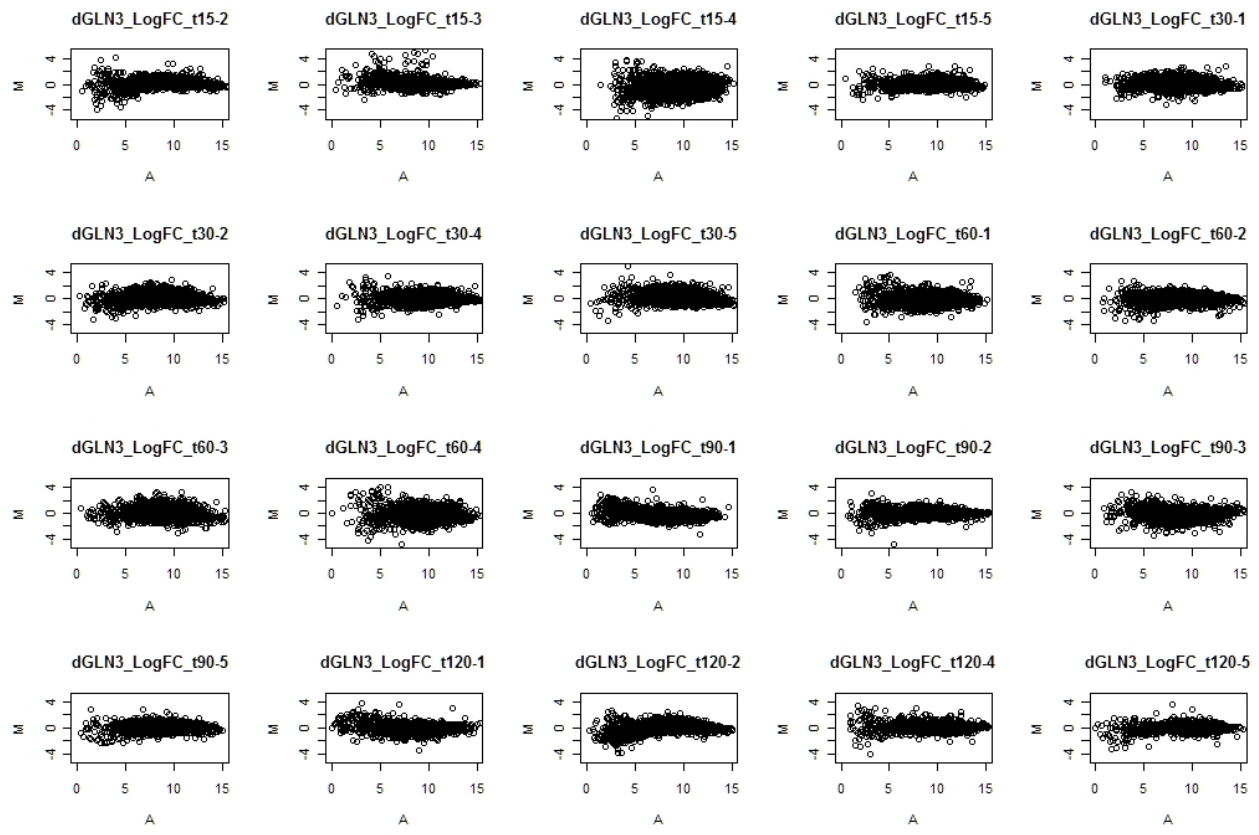


Fig. S5. MA plots before normalization of the log fold change ($M = \log_2(R/G)$ where R is the Cy5 dye and G is the Cy3 dye) versus the total intensity ($A = \log_2(R^*G)$ where R is the Cy5 dye and G is the Cy3 dye) for each spot on microarrays measuring gene expression in the $\Delta gln3$ strain 15, 30, 60, 90, and 120 minutes into the cold shock and recovery experiment.

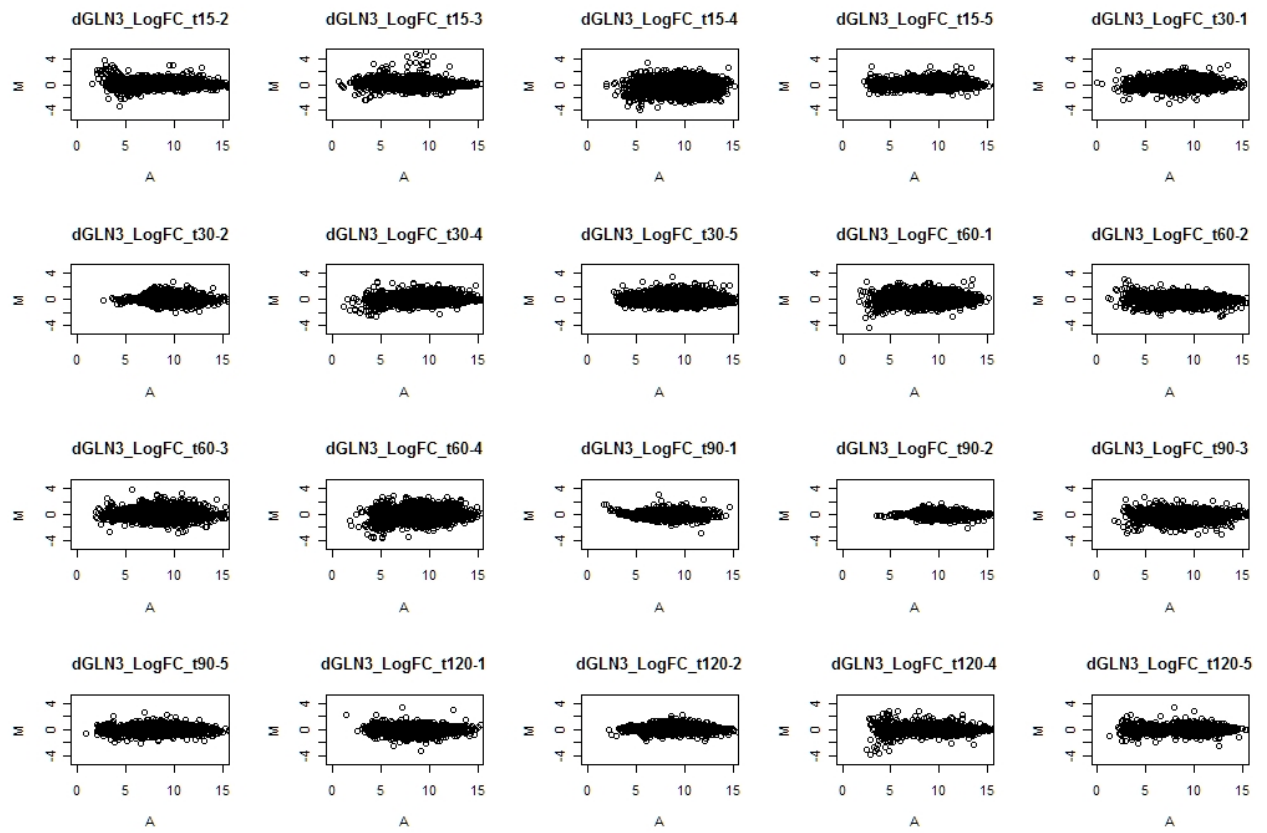


Fig. S6. MA plots after within array normalization of the log fold change ($M = \log_2(R/G)$ where R is the Cy5 dye and G is the Cy3 dye) versus the total intensity ($A = \log_2(R*G)$ where R is the Cy5 dye and G is the Cy3 dye) for each spot on microarrays measuring gene expression in the $\Delta gln3$ strain 15, 30, 60, 90, and 120 minutes into the cold shock and recovery experiment.

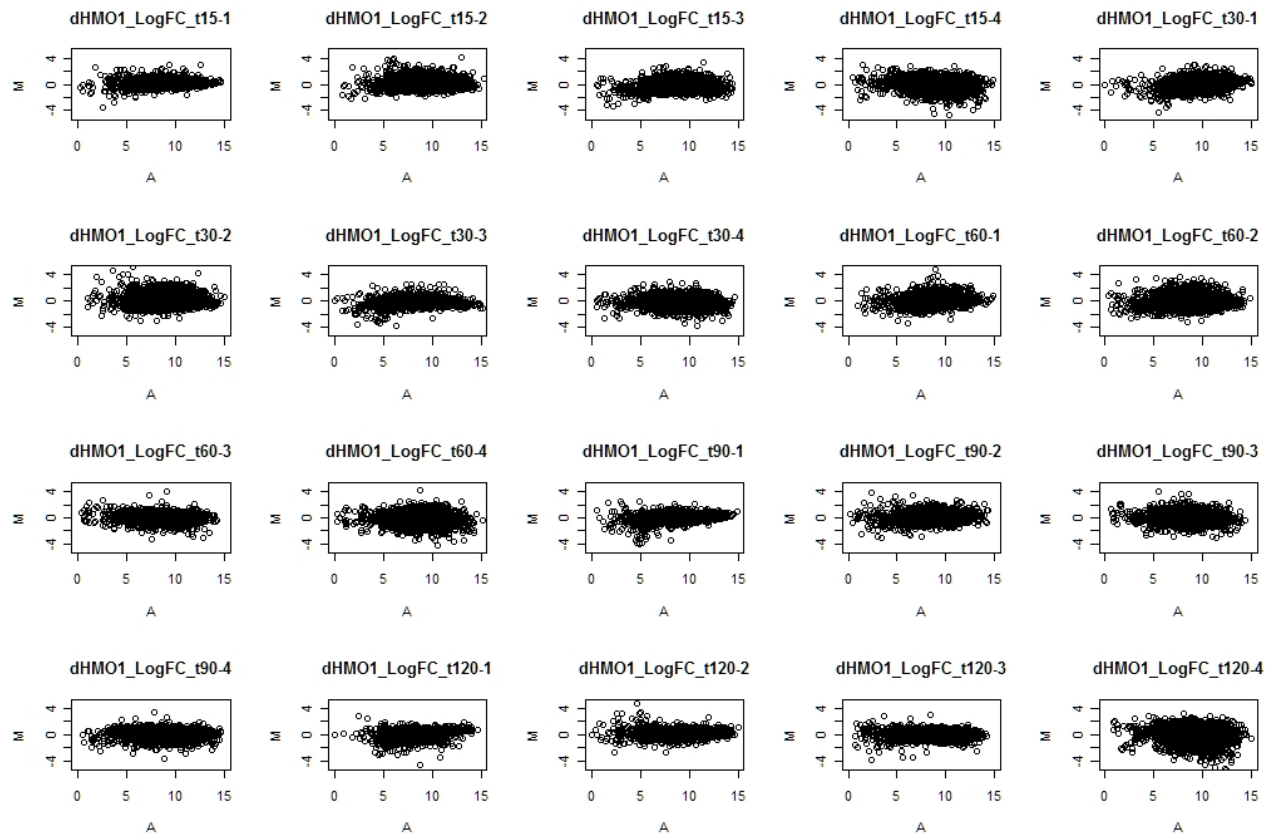


Fig. S7. MA plots before normalization of the log fold change ($M = \log_2(R/G)$ where R is the Cy5 dye and G is the Cy3 dye) versus the total intensity ($A = \log_2(R^*G)$ where R is the Cy5 dye and G is the Cy3 dye) for each spot on microarrays measuring gene expression in the *Δhmo1* strain 15, 30, 60, 90, and 120 minutes into the cold shock and recovery experiment.

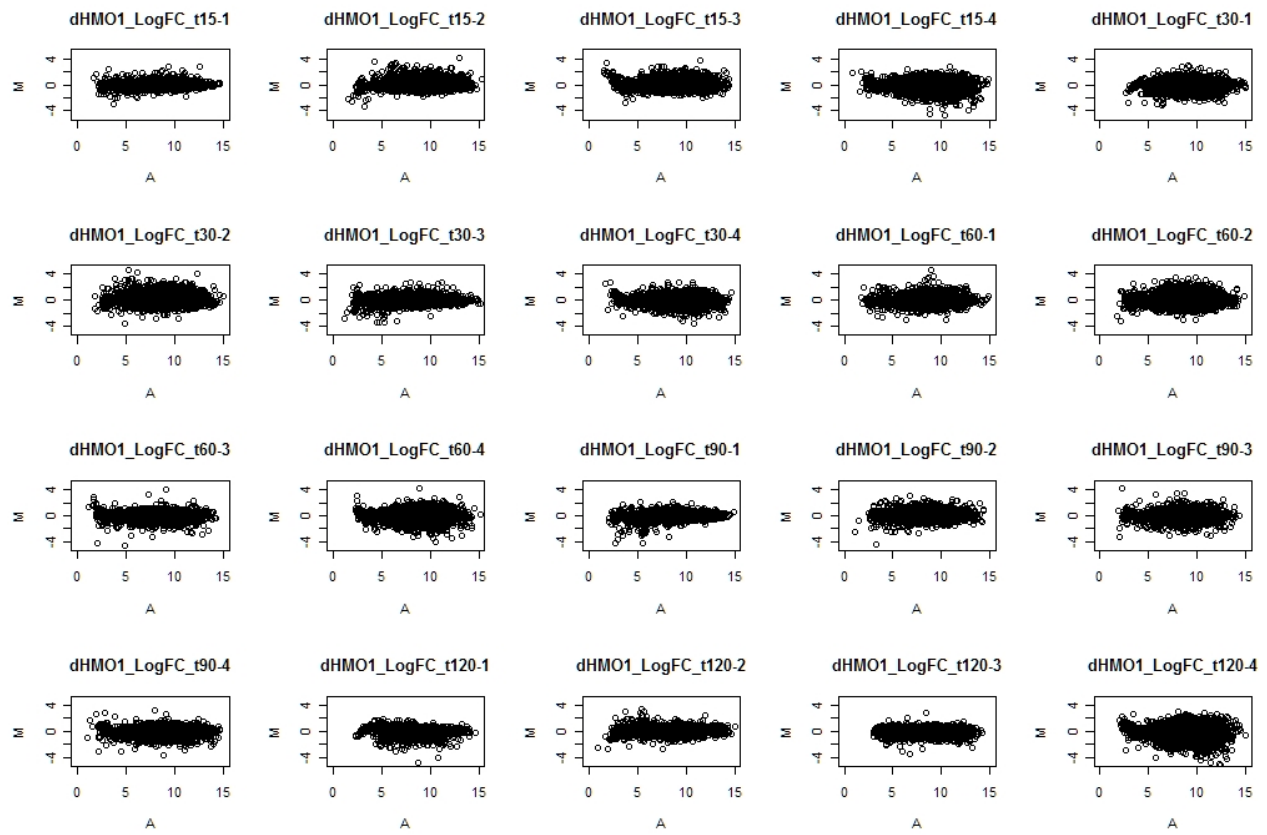


Fig. S8. MA plots after within array normalization of the log fold change ($M = \log_2(R/G)$ where R is the Cy5 dye and G is the Cy3 dye) versus the total intensity ($A = \log_2(R^*G)$ where R is the Cy5 dye and G is the Cy3 dye) for each spot on microarrays measuring gene expression in the $\Delta hmo1$ strain 15, 30, 60, 90, and 120 minutes into the cold shock and recovery experiment.

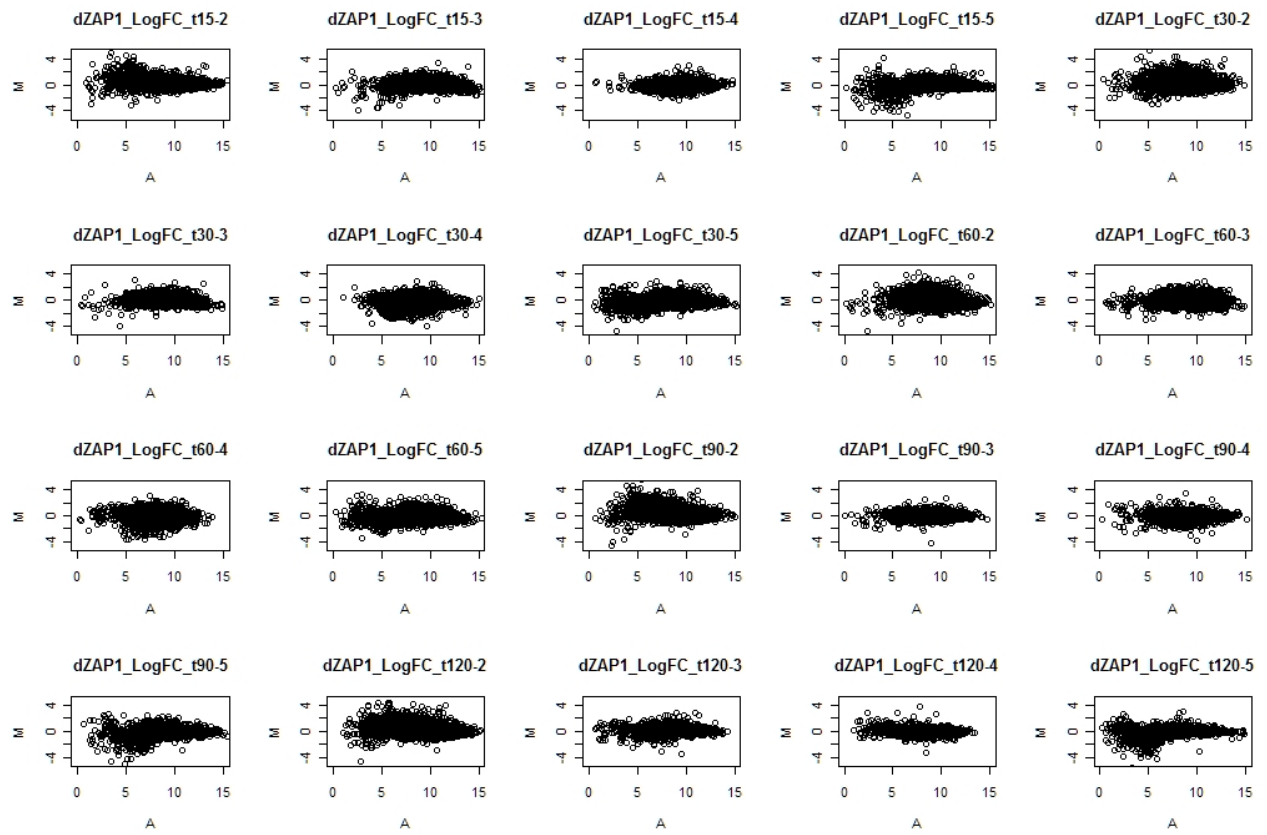


Fig. S9. MA plots before normalization of the log fold change ($M = \log_2(R/G)$ where R is the Cy5 dye and G is the Cy3 dye) versus the total intensity ($A = \log_2(R^*G)$ where R is the Cy5 dye and G is the Cy3 dye) for each spot on microarrays measuring gene expression in the $\Delta zap1$ strain 15, 30, 60, 90, and 120 minutes into the cold shock and recovery experiment.

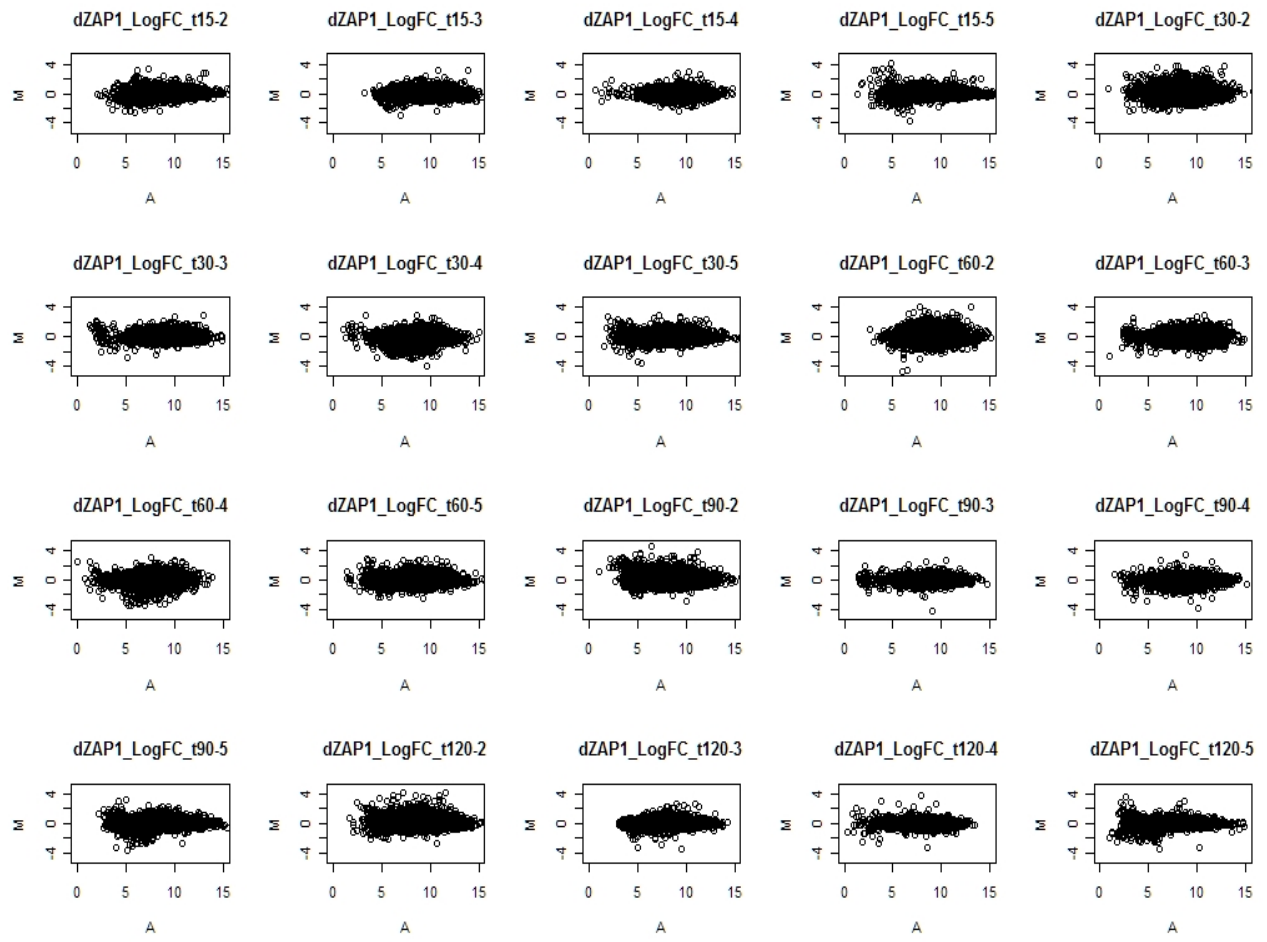


Fig. S10. MA plots after within array normalization of the log fold change ($M = \log_2(R/G)$ where R is the Cy5 dye and G is the Cy3 dye) versus the total intensity ($A = \log_2(R^*G)$ where R is the Cy5 dye and G is the Cy3 dye) for each spot on microarrays measuring gene expression in the $\Delta zap1$ strain 15, 30, 60, 90, and 120 minutes into the cold shock and recovery experiment.

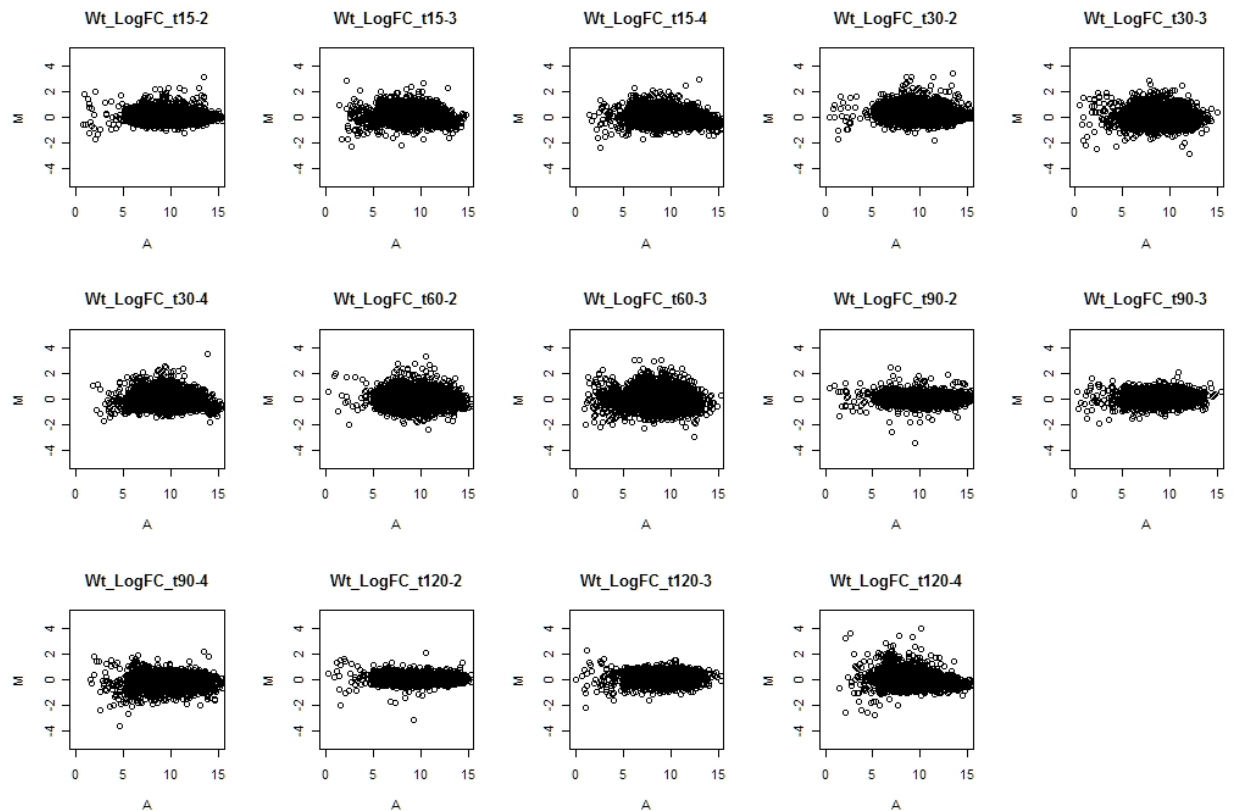


Fig. S11. MA plots before normalization of the log fold change ($M = \log_2(R/G)$ where R is the Cy5 dye and G is the Cy3 dye) versus the total intensity ($A = \log_2(R^*G)$ where R is the Cy5 dye and G is the Cy3 dye) for each spot on “Ontario” microarrays measuring gene expression in the wild type strain 15, 30, 60, 90, and 120 minutes into the cold shock and recovery experiment.

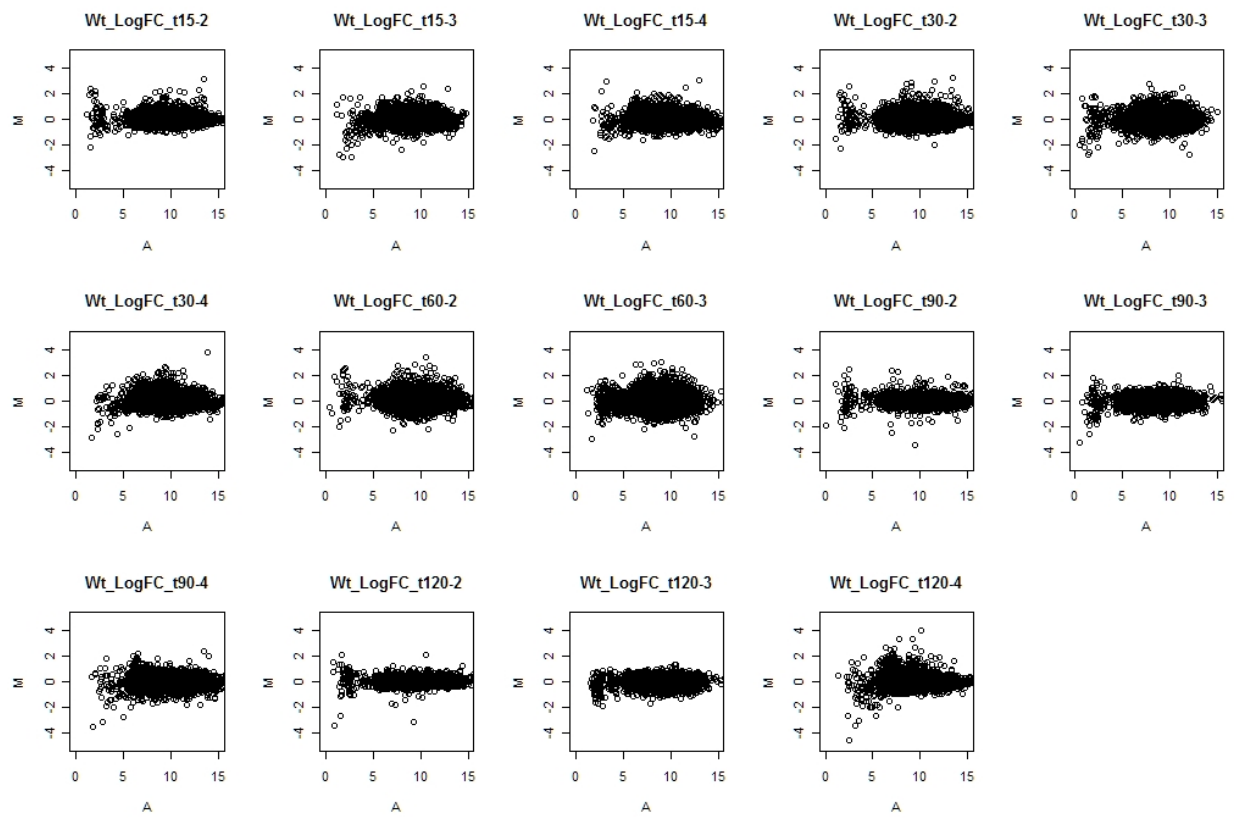


Fig. S12. MA plots after within array normalization of the log fold change ($M = \log_2(R/G)$ where R is the Cy5 dye and G is the Cy3 dye) versus the total intensity ($A = \log_2(R^*G)$ where R is the Cy5 dye and G is the Cy3 dye) for each spot on “Ontario” microarrays measuring gene expression in the wild type strain 15, 30, 60, 90, and 120 minutes into the cold shock and recovery experiment.

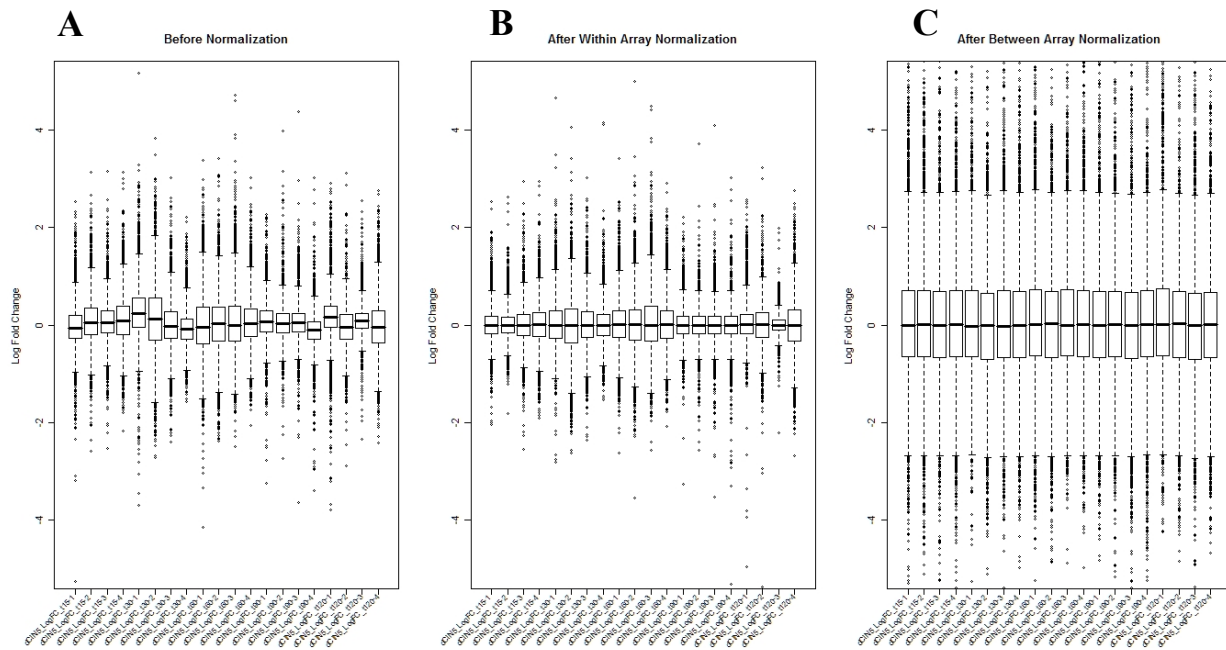


Fig. S13. The effects of within array and between array normalization on the log fold change of spots on the DNA microarrays collected for the $\Delta cin5$ strain. **(A)** Before normalization. **(B)** After within array normalization by loess. **(C)** After between array normalization using MAD scaling. In plots A, B, and C, the box plots represent the following sequence of $\Delta cin5$ strain data: t_{15} flask 1, t_{15} flask 2, t_{15} flask 3, t_{15} flask 4, t_{30} flask 1, t_{30} flask 2, t_{30} flask 3, t_{30} flask 4, t_{60} flask 1, t_{60} flask 2, t_{60} flask 3, t_{60} flask 4, t_{90} flask 1, t_{90} flask 2, t_{90} flask 3, t_{90} flask 4, t_{120} flask 1, t_{120} flask 2, t_{120} flask 3, and t_{120} flask 4.

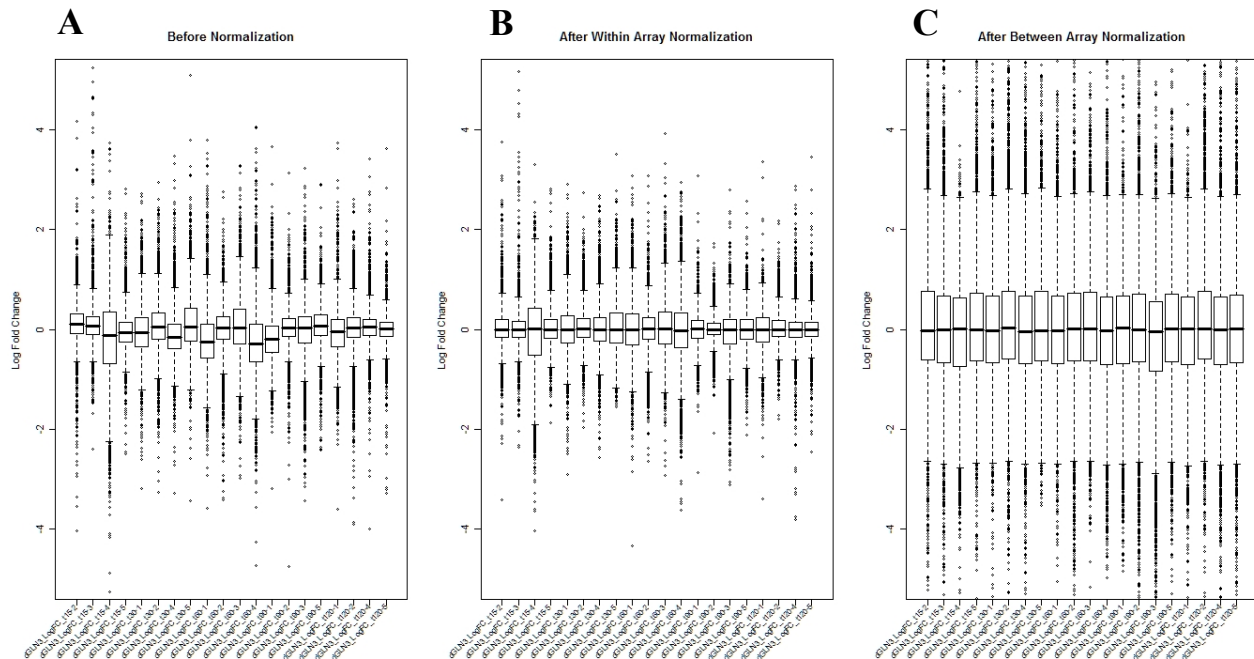


Fig. S14. The effects of within array and between array normalization on the log fold change of spots on the DNA microarrays collected for the $\Delta gln3$ strain. **(A)** Before normalization. **(B)** After within array normalization by loess. **(C)** After between array normalization using MAD scaling. In plots A, B, and C, the box plots represent the following sequence of $\Delta gln3$ strain data: t_{15} flask 2, t_{15} flask 3, t_{15} flask 4, t_{15} flask 5, t_{30} flask 1, t_{30} flask 2, t_{30} flask 3, t_{30} flask 4, t_{30} flask 5, t_{60} flask 1, t_{60} flask 2, t_{60} flask 3, t_{60} flask 4, t_{90} flask 1, t_{90} flask 2, t_{90} flask 3, t_{90} flask 5, t_{120} flask 1, t_{120} flask 2, t_{120} flask 4, and t_{120} flask 5.

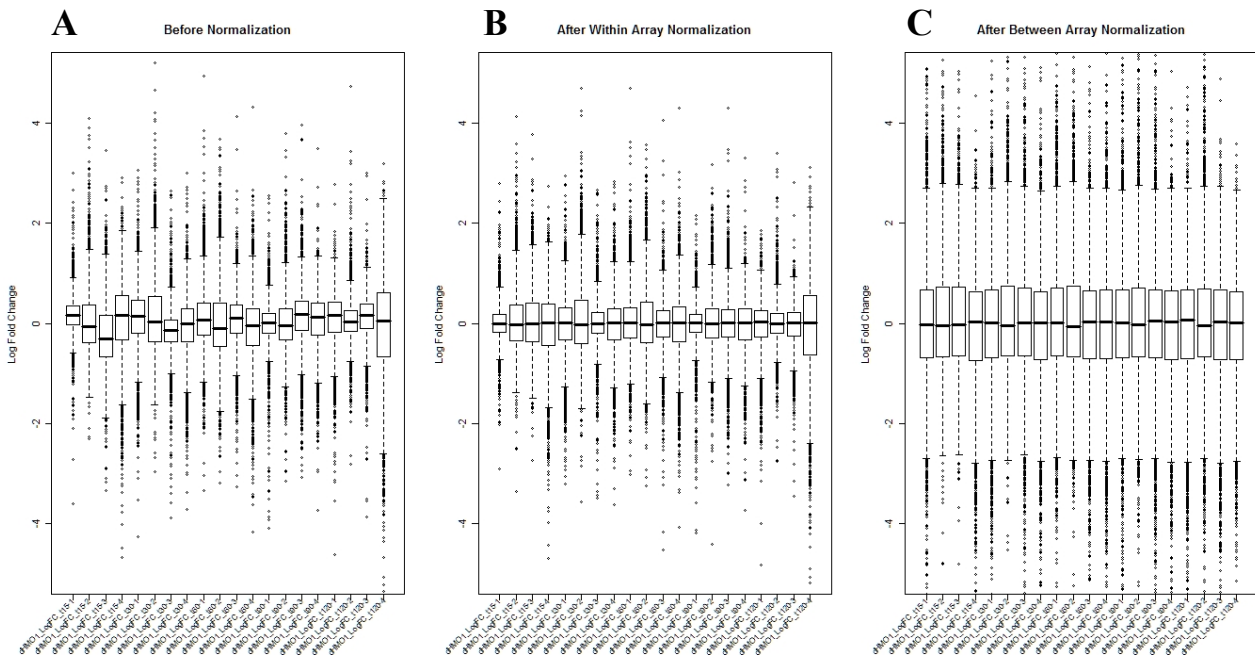


Fig. S15. The effects of within array and between array normalization on the log fold change of spots on the DNA microarrays collected for the $\Delta hmo1$ strain. **(A)** Before normalization. **(B)** After within array normalization by loess. **(C)** After between array normalization using MAD scaling. In plots **A**, **B**, and **C**, the box plots represent the following sequence of $\Delta hmo1$ strain data: t_{15} flask 1, t_{15} flask 2, t_{15} flask 3, t_{15} flask 4, t_{30} flask 1, t_{30} flask 2, t_{30} flask 3, t_{30} flask 4, t_{60} flask 1, t_{60} flask 2, t_{60} flask 3, t_{60} flask 4, t_{90} flask 1, t_{90} flask 2, t_{90} flask 3, t_{90} flask 4, t_{120} flask 1, t_{120} flask 2, t_{120} flask 3, and t_{120} flask 4

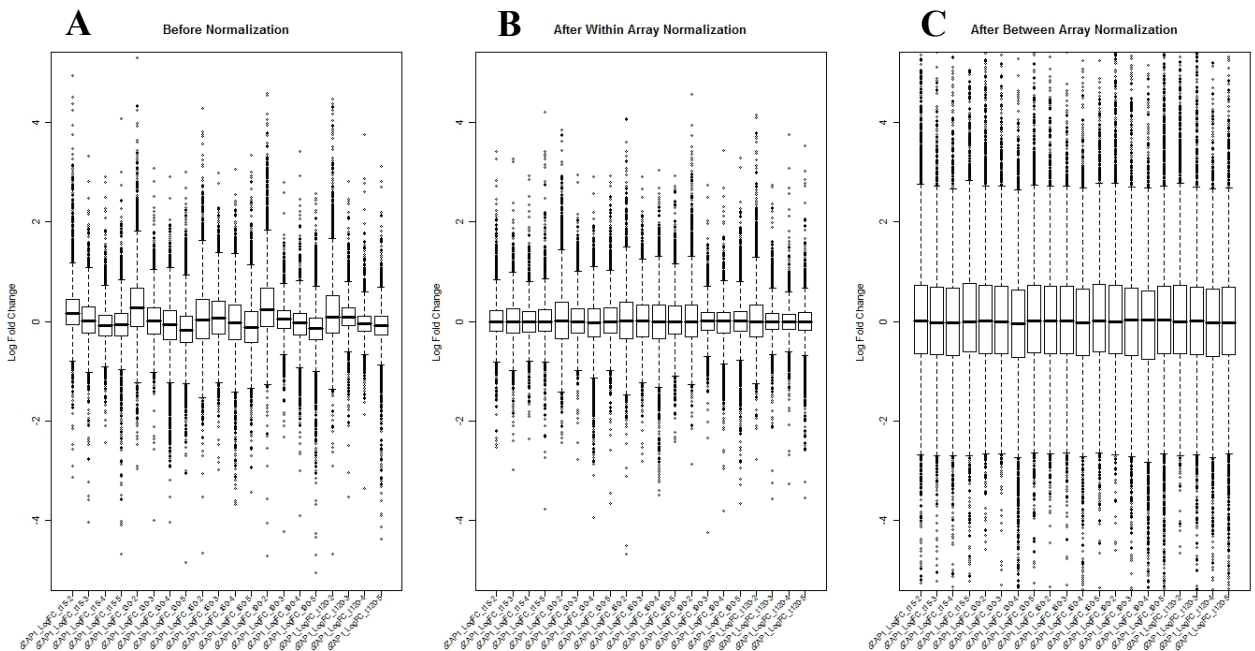


Fig. S16. The effects of within array and between array normalization on the log fold change of spots on the DNA microarrays collected for the $\Delta zap1$ strain. **(A)** Before normalization. **(B)** After within array normalization by loess. **(C)** After between array normalization using MAD scaling. In plots **A**, **B**, and **C**, the box plots represent the following sequence of $\Delta gln3$ strain data: t_{15} flask 2, t_{15} flask 3, t_{15} flask 4, t_{15} flask 5, t_{30} flask 2, t_{30} flask 3, t_{30} flask 4, t_{30} flask 5, t_{60} flask 2, t_{60} flask 3, t_{60} flask 4, t_{60} flask 5, t_{90} flask 2, t_{90} flask 3, t_{90} flask 4, t_{90} flask 5, t_{120} flask 2, t_{120} flask 3, t_{120} flask 4, and t_{120} flask 5.

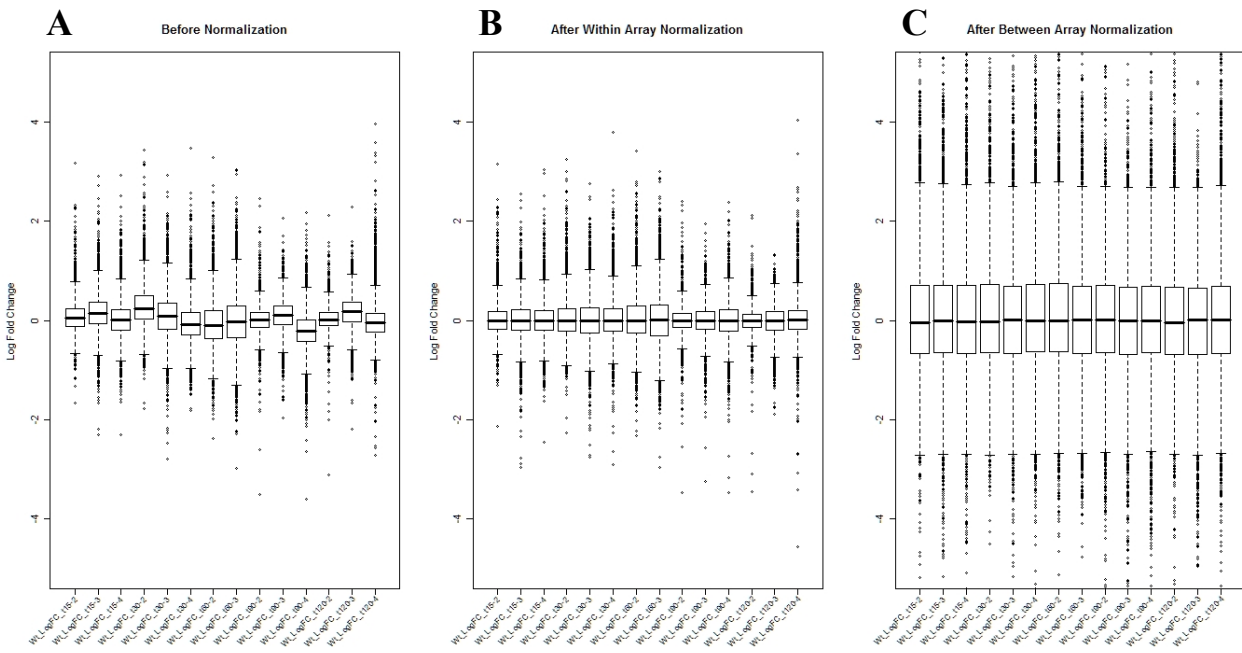


Fig. S17. The effects of within array and between array normalization on the log fold change of spots on the DNA microarrays collected for the wild type strain. **(A)** Before normalization. **(B)** After within array normalization by loess. **(C)** After between array normalization using MAD scaling. In plots A, B, and C, the box plots represent the following sequence of wild type strain data: t_{15} flask 2, t_{15} flask 3, t_{15} flask 4, t_{30} flask 2, t_{30} flask 3, t_{30} flask 4, t_{60} flask 2, t_{60} flask 3, t_{90} flask 2, t_{90} flask 3, t_{90} flask 4, t_{120} flask 2, t_{120} flask 3, and t_{120} flask 4.

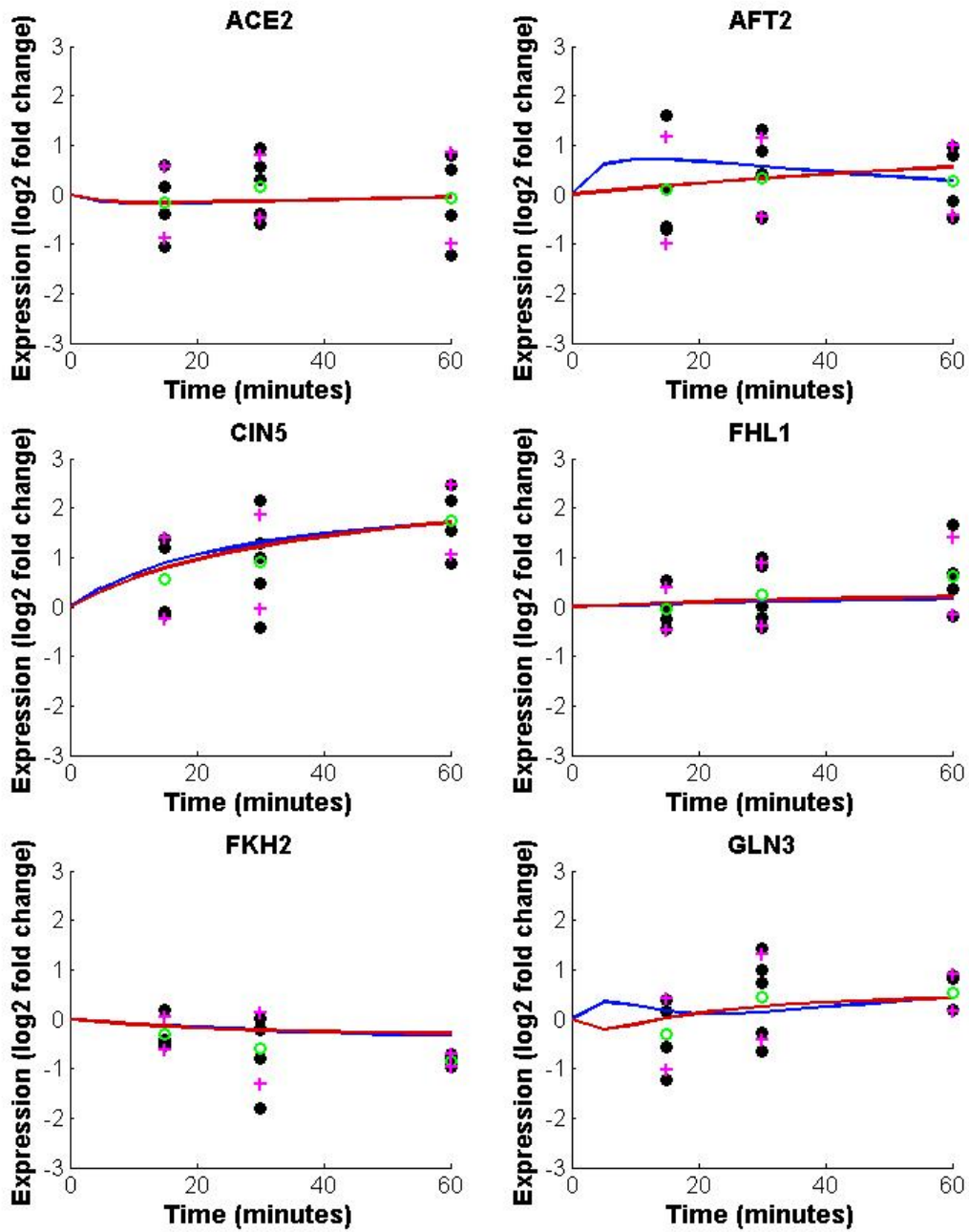


Fig. S18a. The wild type forward simulations for *ACE2*, *AFT2*, *CIN5*, *FHL1*, *FKH2*, and *GLN3*. The models fitted by both the sigmoid function (blue line) and Michaelis-Menten function (red line) are shown. The green circles designate the average log fold change for each time point in the cold shock experiment. The magenta pluses designate ± 1 standard deviation in the log fold change for each time point in the cold shock experiment.

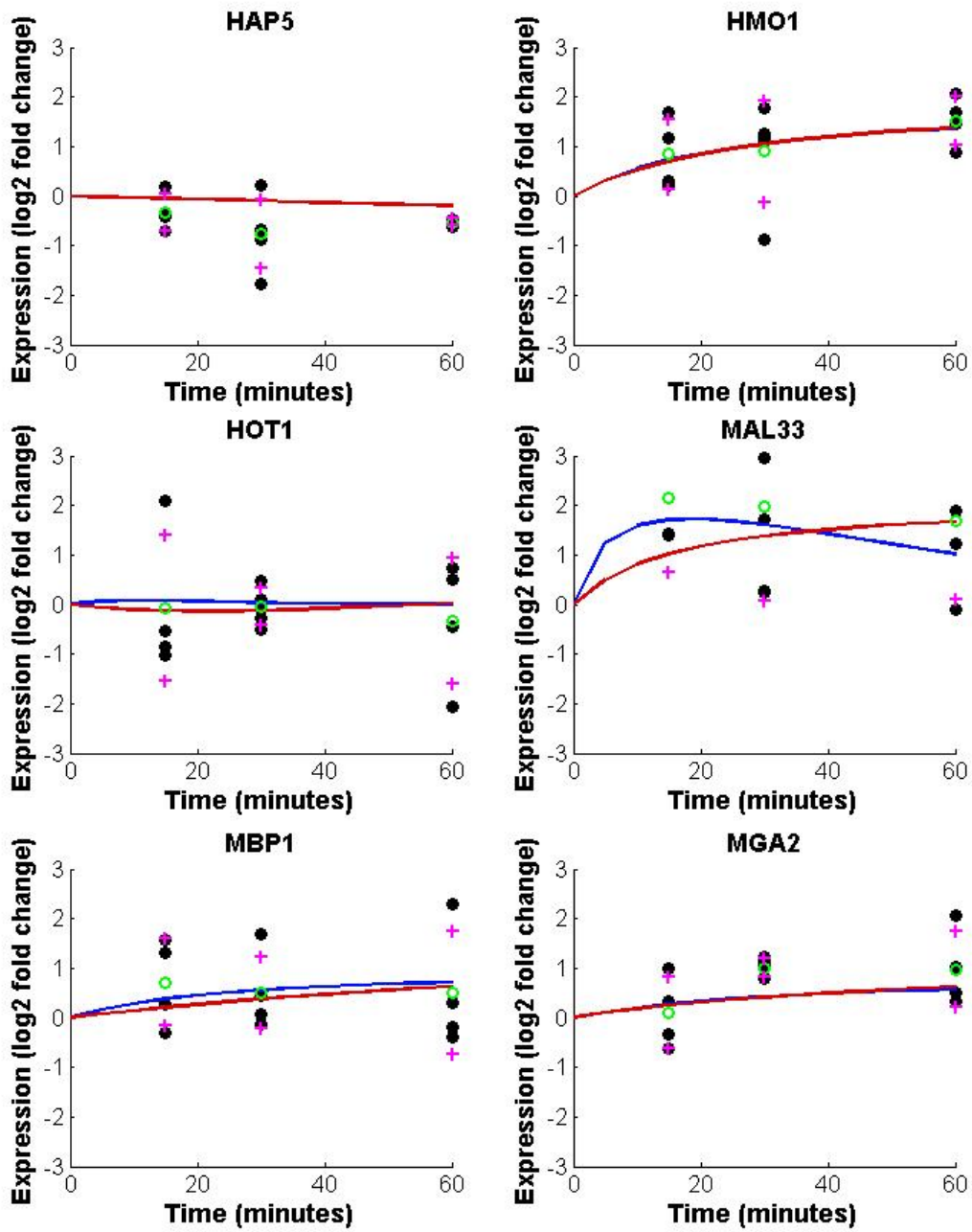


Fig. S18b. The wild type forward simulations for *HAP5*, *HMO1*, *HOT1*, *MAL33*, *MBP1*, and *MGA2*. The models fitted by both the sigmoid function (blue line) and Michaelis-Menten function (red line) are shown. The green circles designate the average log fold change for each time point in the cold shock experiment. The magenta pluses designate ± 1 standard deviation in the log fold change for each time point in the cold shock experiment.

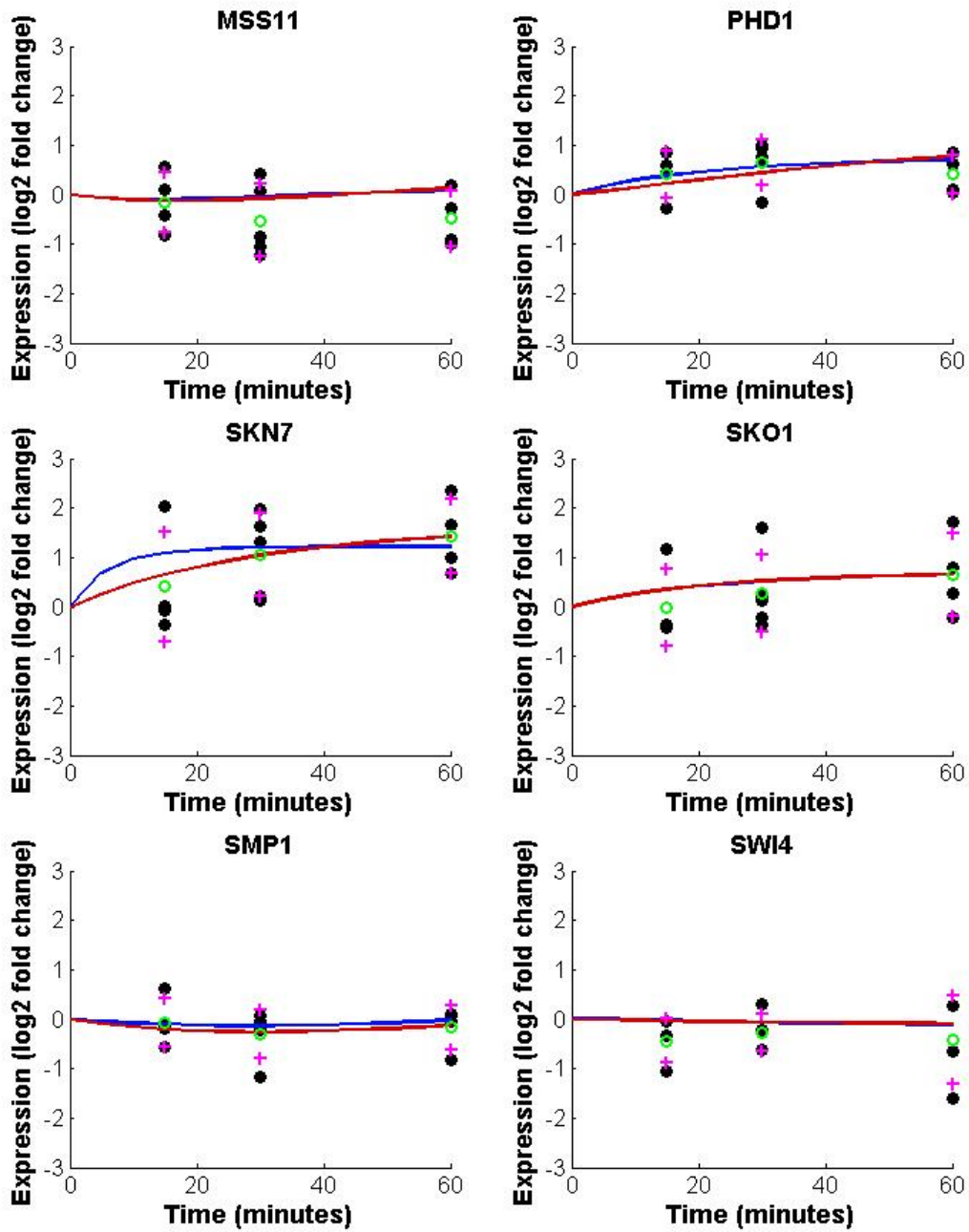


Fig. S18c. The wild type forward simulations for *MSS11*, *PHD1*, *SKN7*, *SKO1*, and *SWI4*. The models fitted by both the sigmoid function (blue line) and Michaelis-Menten function (red line) are shown. The green circles designate the average log fold change for each time point in the cold shock experiment. The magenta pluses designate ± 1 standard deviation in the log fold change for each time point in the cold shock experiment.

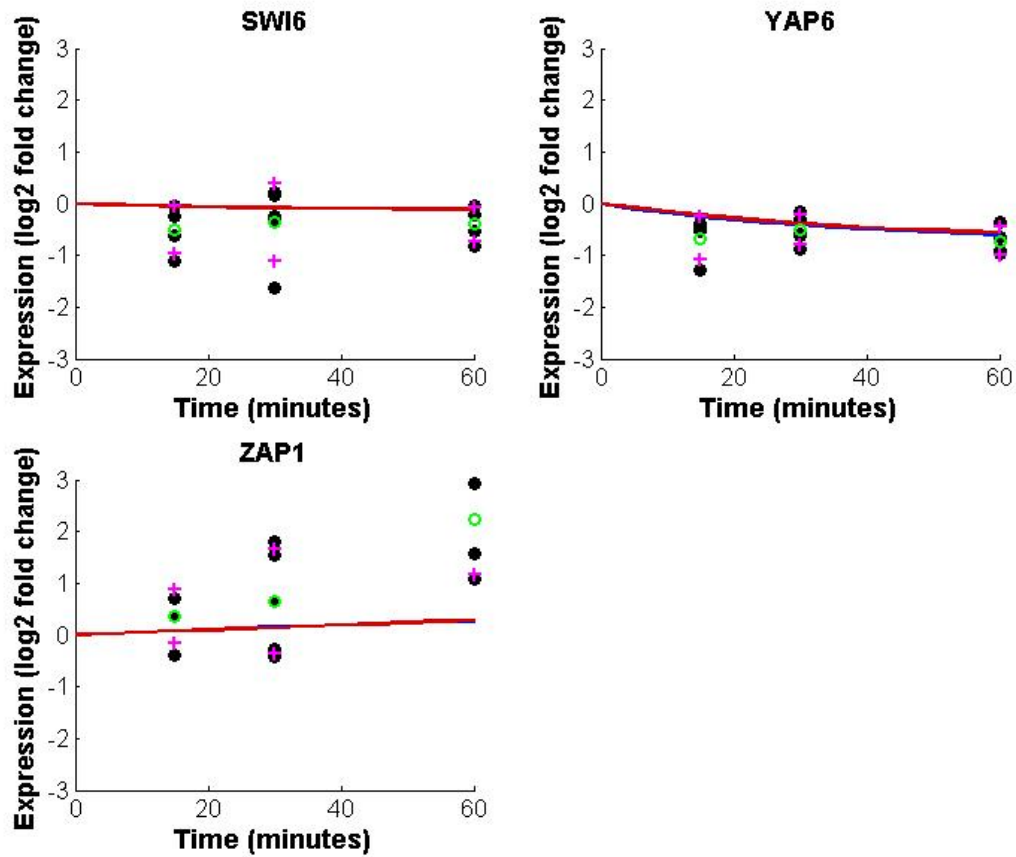


Fig. S18d. The wild type forward simulations for *SWI6*, *YAP6*, and *ZAP1*. The models fitted by both the sigmoid function (blue line) and Michaelis-Menten function (red line) are shown. The green circles designate the average log fold change for each time point in the cold shock experiment. The magenta pluses designate ± 1 standard deviation in the log fold change for each time point in the cold shock experiment.

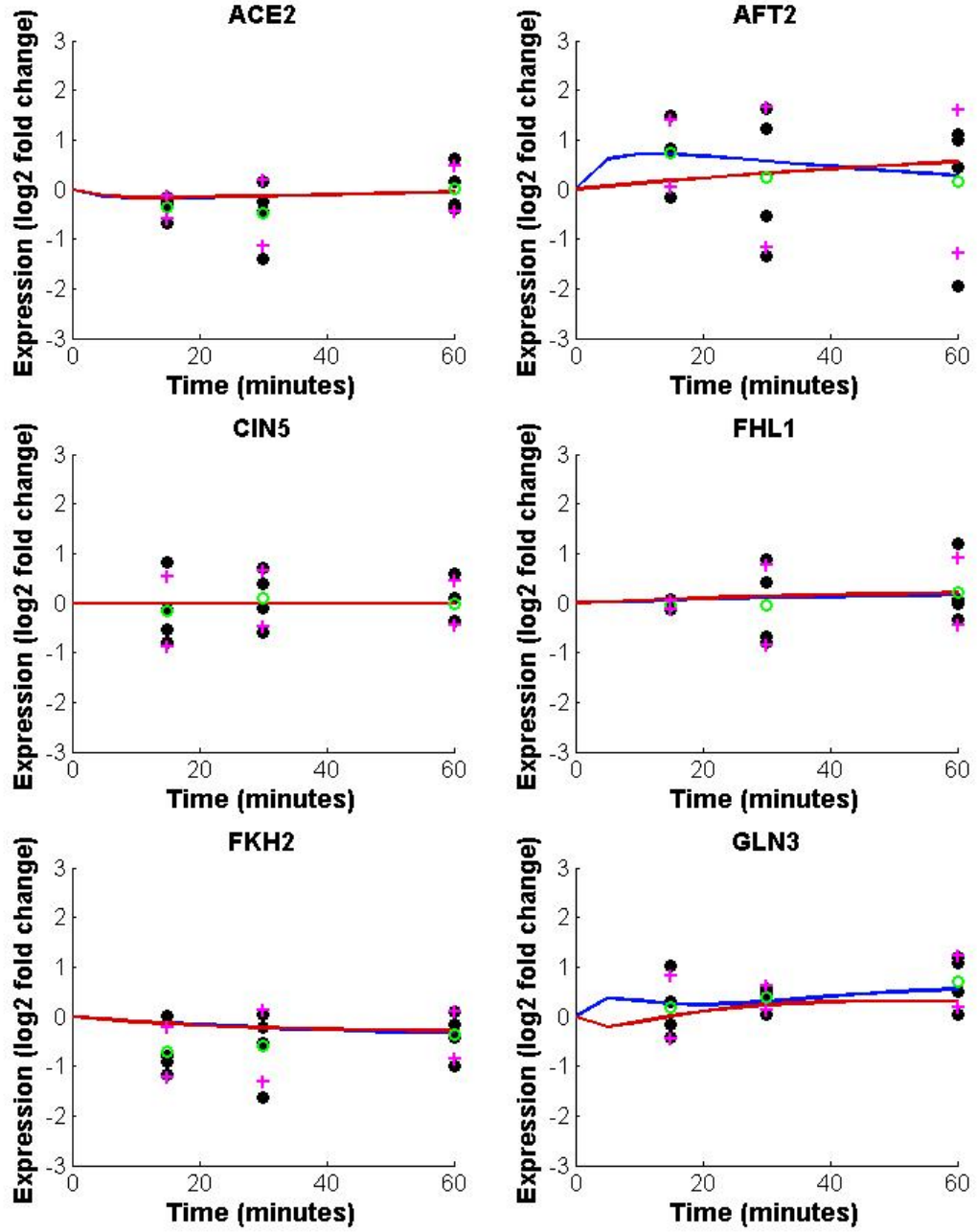


Fig. S19a. The $\Delta cin5$ forward simulations for *ACE2*, *AFT2*, *CIN5*, *FHL1*, *FKH2*, and *GLN3*. The models fitted by both the sigmoid function (blue line) and Michaelis-Menten function (red line) are shown. The green circles designate the average log fold change for each time point in the cold shock experiment. The magenta pluses designate ± 1 standard deviation in the log fold change for each time point in the cold shock experiment.

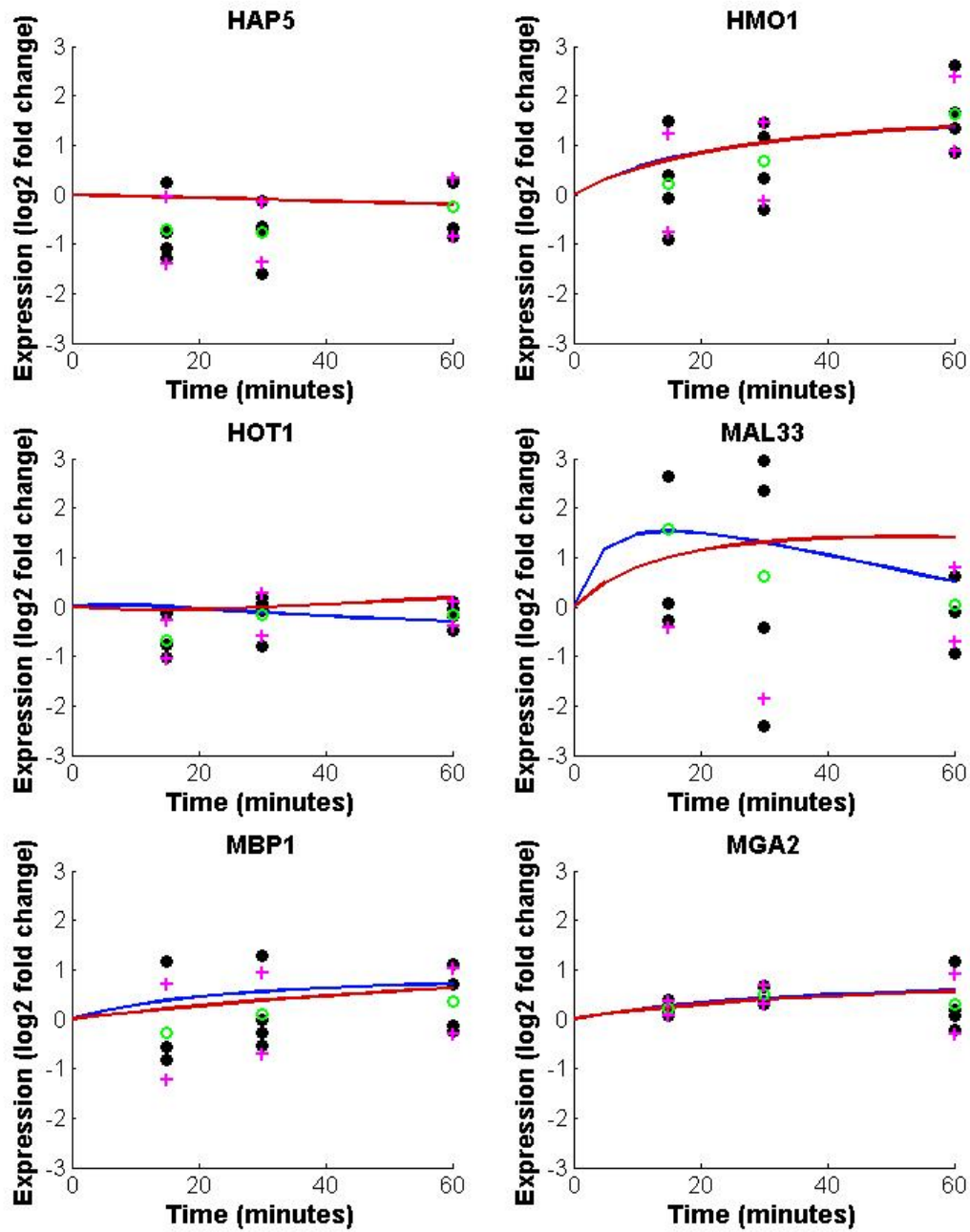


Fig. S19b. The $\Delta cin5$ forward simulations for *HAP5*, *HMO1*, *HOT1*, *MAL33*, *MBP1*, and *MGA2*. The models fitted by both the sigmoid function (blue line) and Michaelis-Menten function (red line) are shown. The green circles designate the average log fold change for each time point in the cold shock experiment. The magenta pluses designate ± 1 standard deviation in the log fold change for each time point in the cold shock experiment.

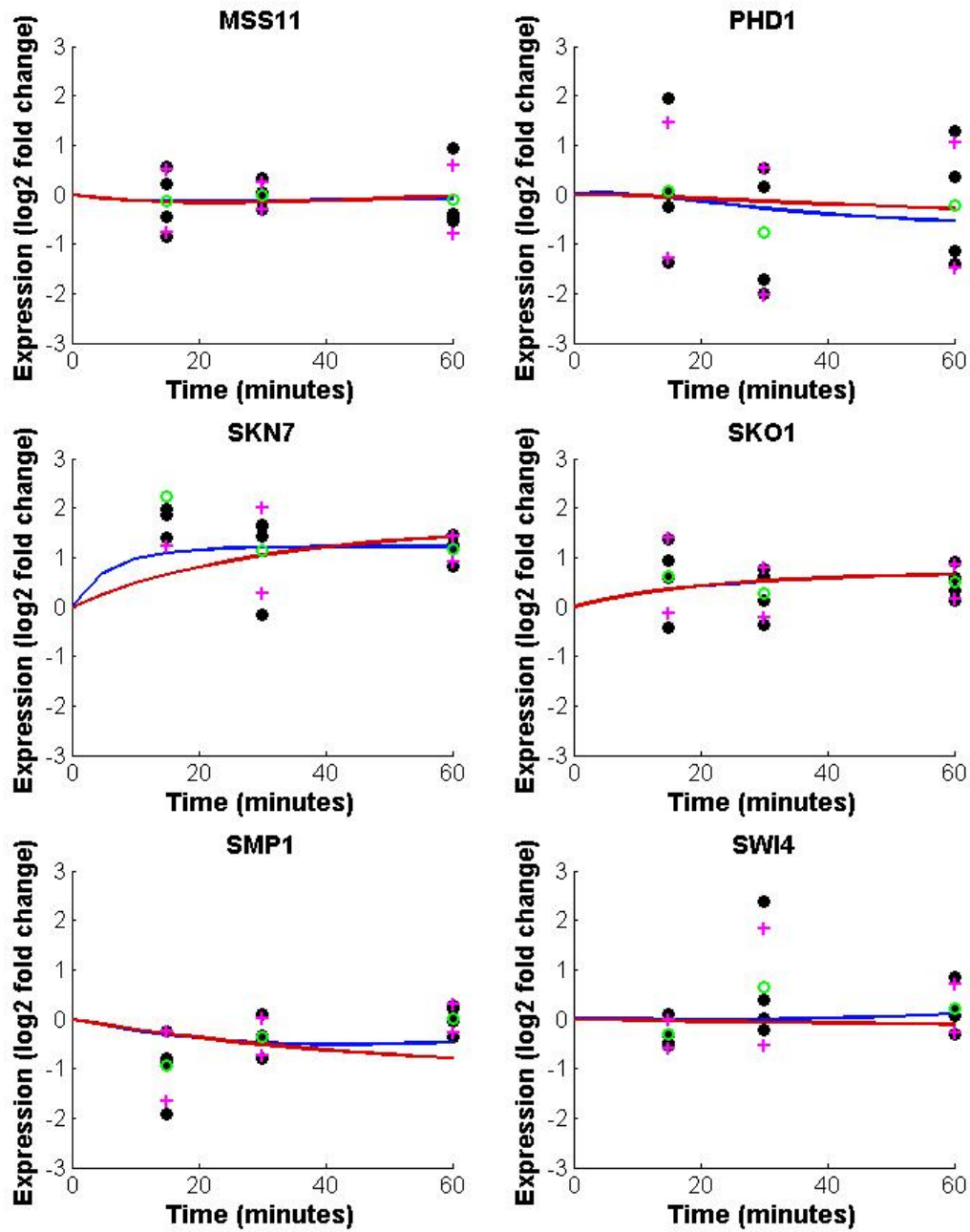


Fig. S19c. The $\Delta cin5$ forward simulations for *MSS11*, *PHD1*, *SKN7*, *SKO1*, and *SWI4*. The models fitted by both the sigmoid function (blue line) and Michaelis-Menten function (red line) are shown. The green circles designate the average log fold change for each time point in the cold shock experiment. The magenta pluses designate ± 1 standard deviation in the log fold change for each time point in the cold shock experiment.

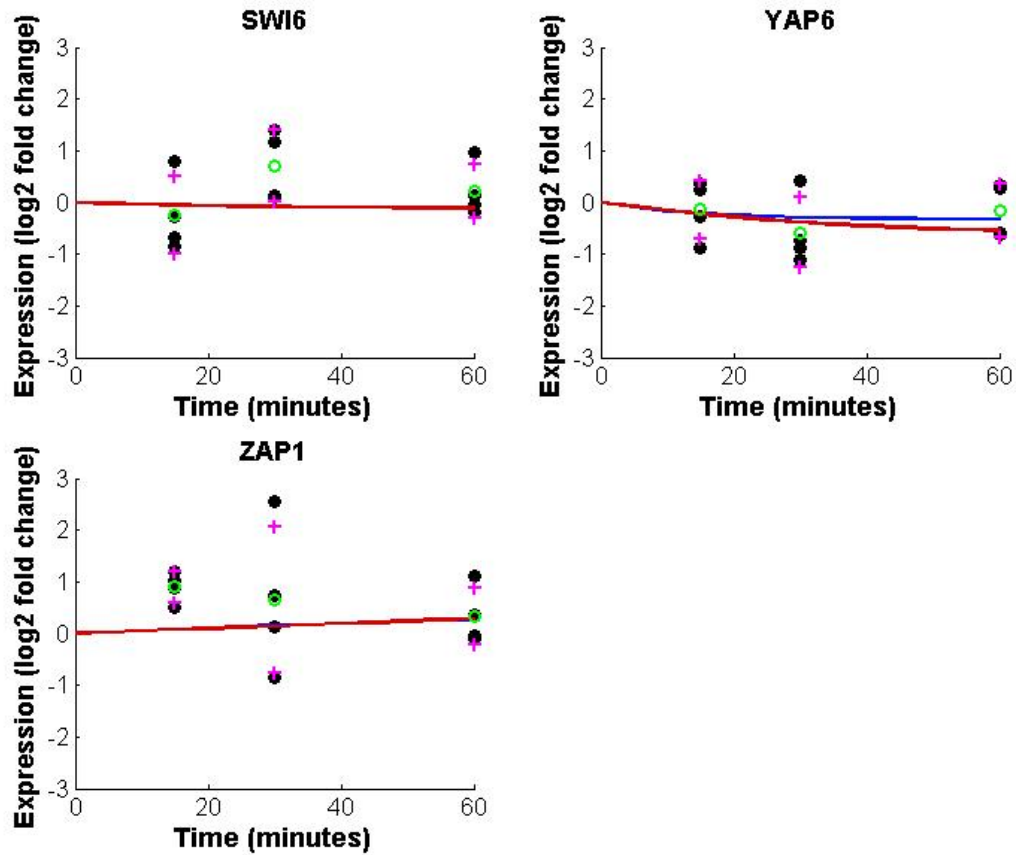


Fig. S19d. The $\Delta cin5$ forward simulations for *SWI6*, *YAP6*, and *ZAP1*. The models fitted by both the sigmoid function (blue line) and Michaelis-Menten function (red line) are shown. The green circles designate the average log fold change for each time point in the cold shock experiment. The magenta pluses designate ± 1 standard deviation in the log fold change for each time point in the cold shock experiment.

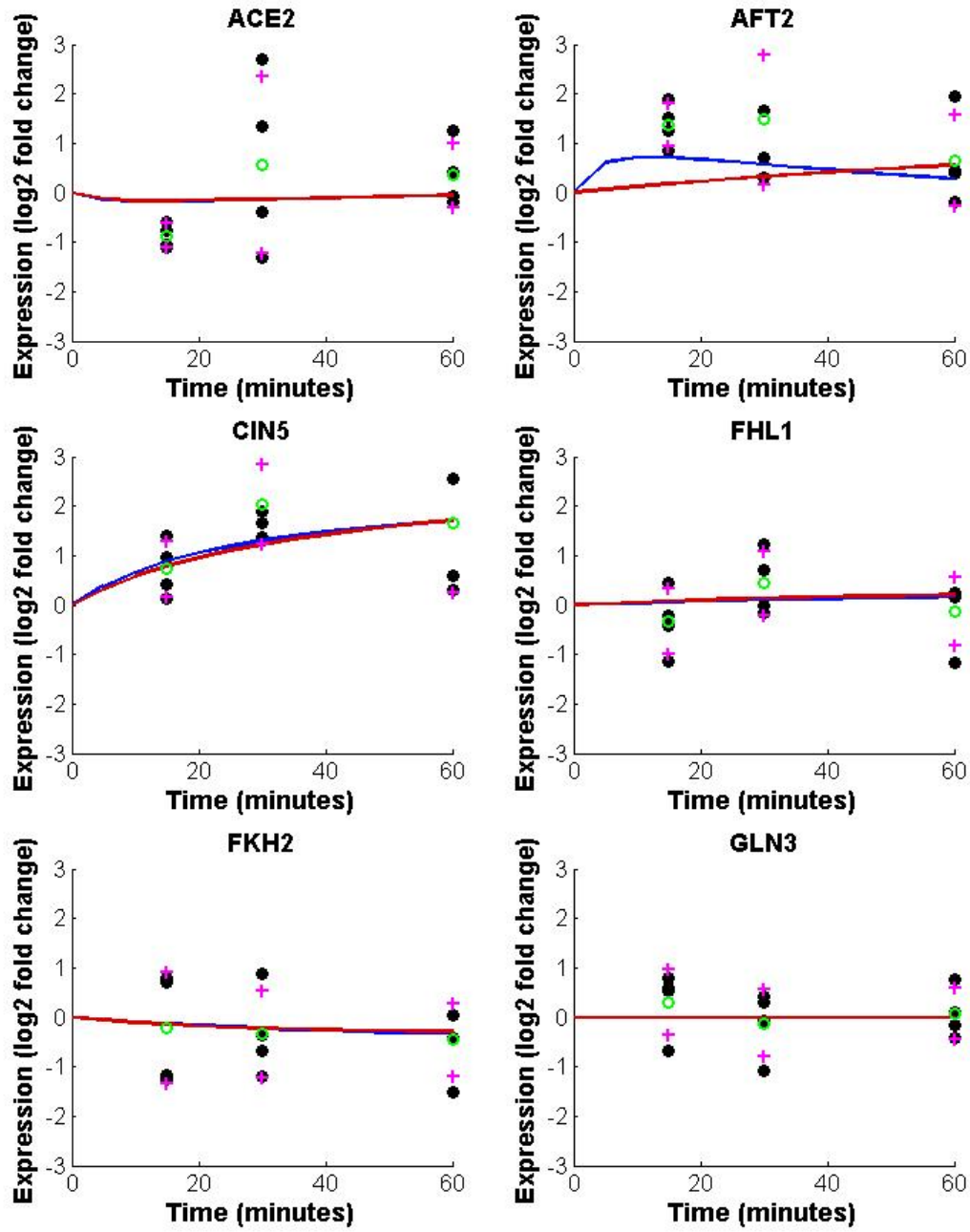


Fig. S20a. The $\Delta gln3$ forward simulations for *ACE2*, *AFT2*, *CIN5*, *FHL1*, *FKH2*, and *GLN3*. The models fitted by both the sigmoid function (blue line) and Michaelis-Menten function (red line) are shown. The green circles designate the average log fold change for each time point in the cold shock experiment. The magenta pluses designate ± 1 standard deviation in the log fold change for each time point in the cold shock experiment.

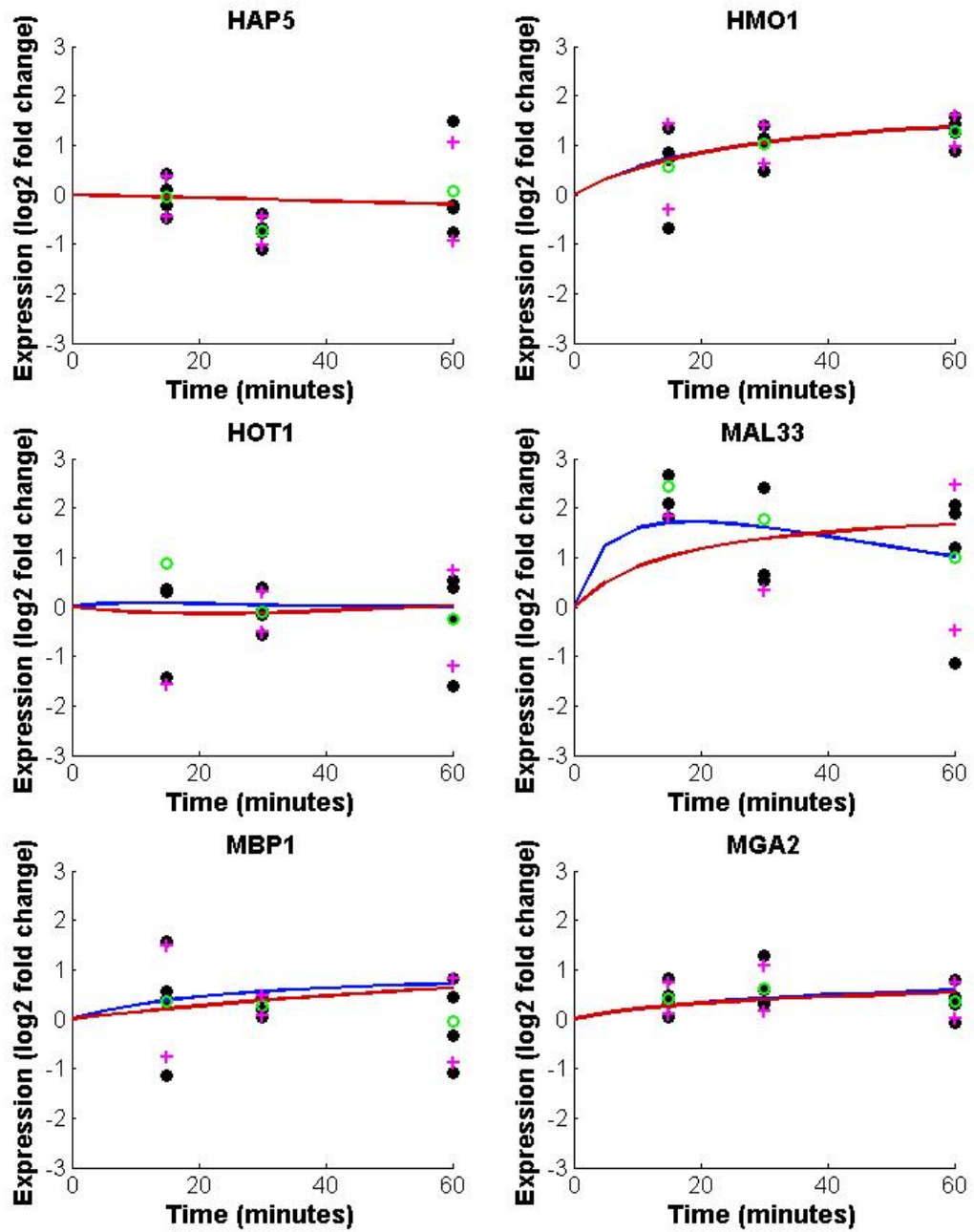


Fig. S20b. The $\Delta gln3$ forward simulations for *HAP5*, *HMO1*, *HOT1*, *MAL33*, *MBP1*, and *MGA2*. The models fitted by both the sigmoid function (blue line) and Michaelis-Menten function (red line) are shown. The green circles designate the average log fold change for each time point in the cold shock experiment. The magenta pluses designate ± 1 standard deviation in the log fold change for each time point in the cold shock experiment.

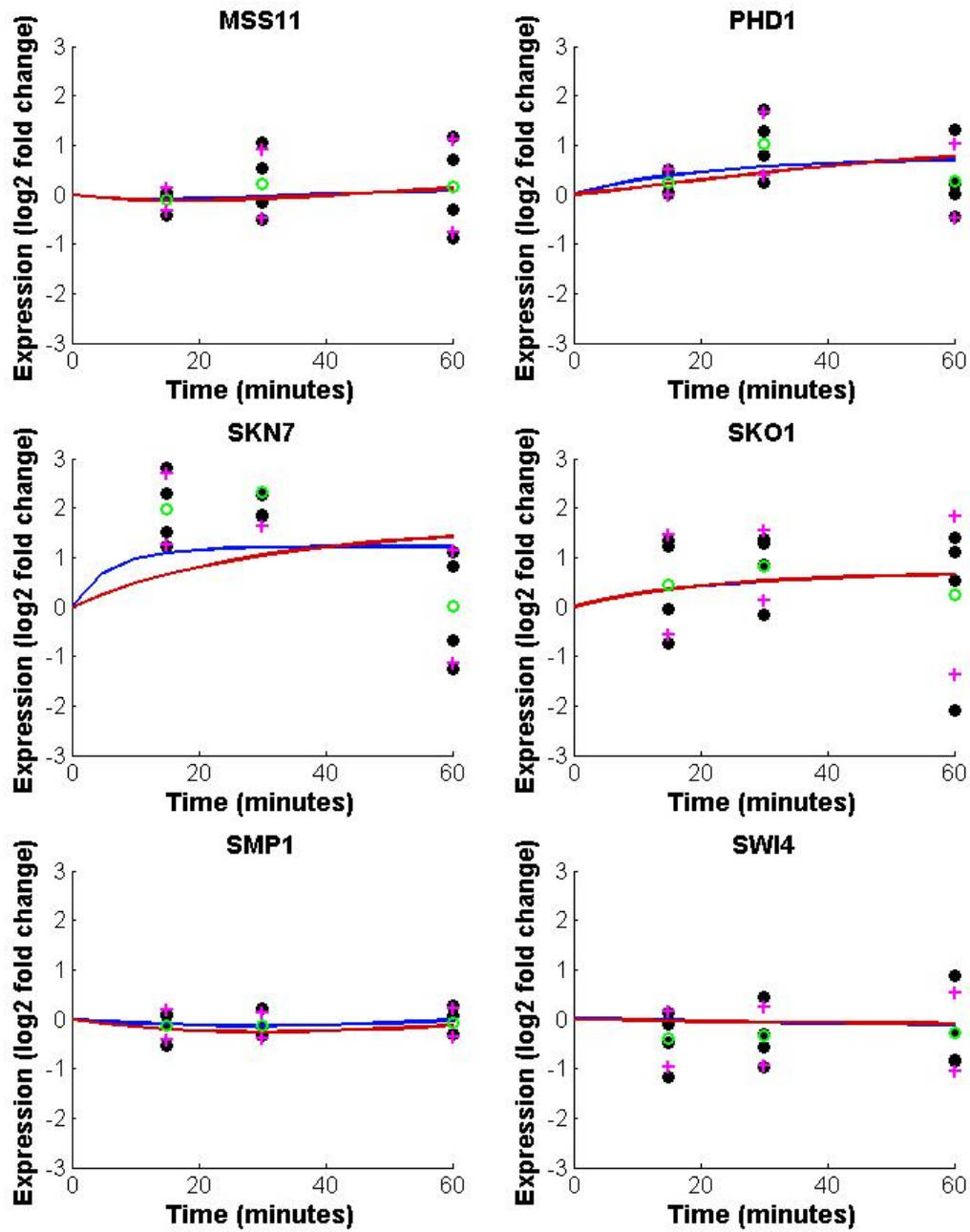


Fig. S20c. The $\Delta gln3$ forward simulations for *MSS11*, *PHD1*, *SKN7*, *SKO1*, and *SWI4*. The models fitted by both the sigmoid function (blue line) and Michaelis-Menten function (red line) are shown. The green circles designate the average log fold change for each time point in the cold shock experiment. The magenta pluses designate ± 1 standard deviation in the log fold change for each time point in the cold shock experiment.

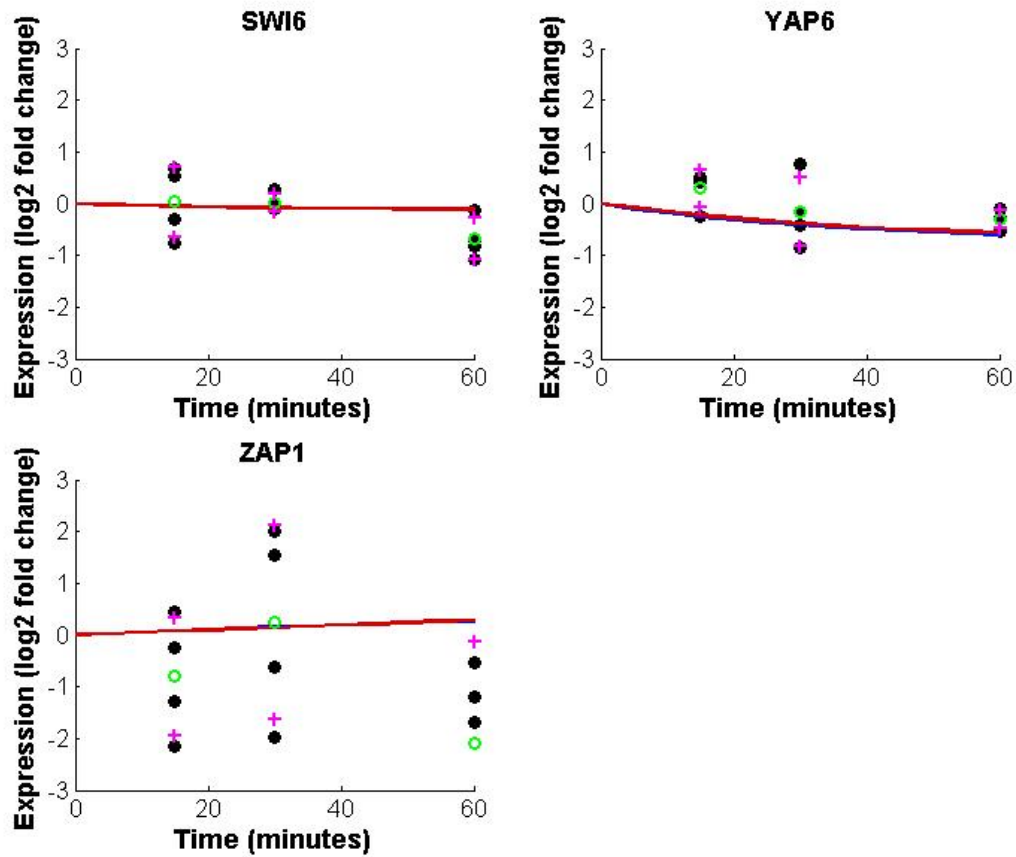


Fig. S20d. The $\Delta gln3$ forward simulations for *SWI6*, *YAP6*, and *ZAP1*. The models fitted by both the sigmoid function (blue line) and Michaelis-Menten function (red line) are shown. The green circles designate the average log fold change for each time point in the cold shock experiment. The magenta pluses designate ± 1 standard deviation in the log fold change for each time point in the cold shock experiment.

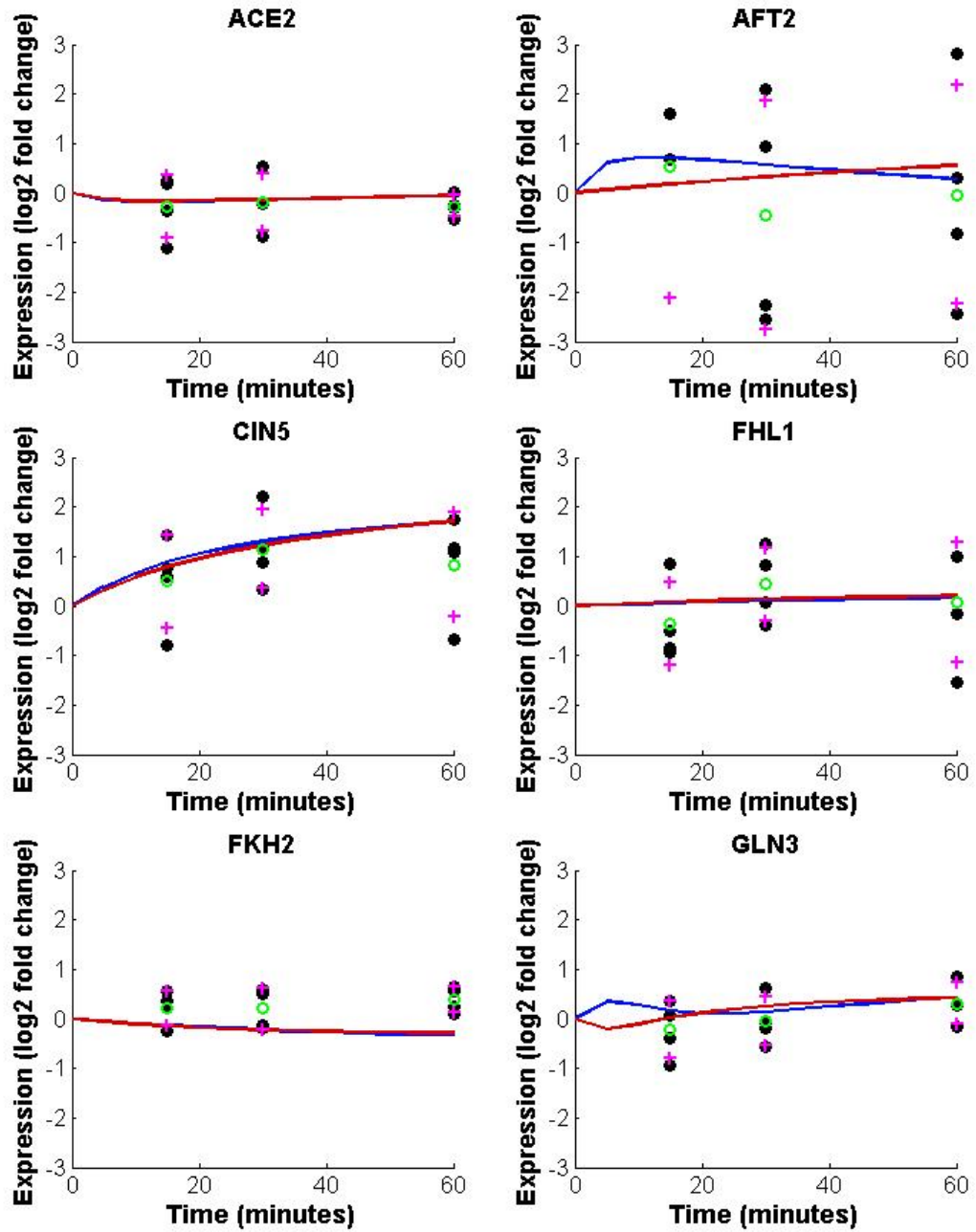


Fig. S21a. The $\Delta hmoI$ forward simulations for *ACE2*, *AFT2*, *CIN5*, *FHL1*, *FKH2*, and *GLN3*. The models fitted by both the sigmoid function (blue line) and Michaelis-Menten function (red line) are shown. The green circles designate the average log fold change for each time point in the cold shock experiment. The magenta pluses designate ± 1 standard deviation in the log fold change for each time point in the cold shock experiment.

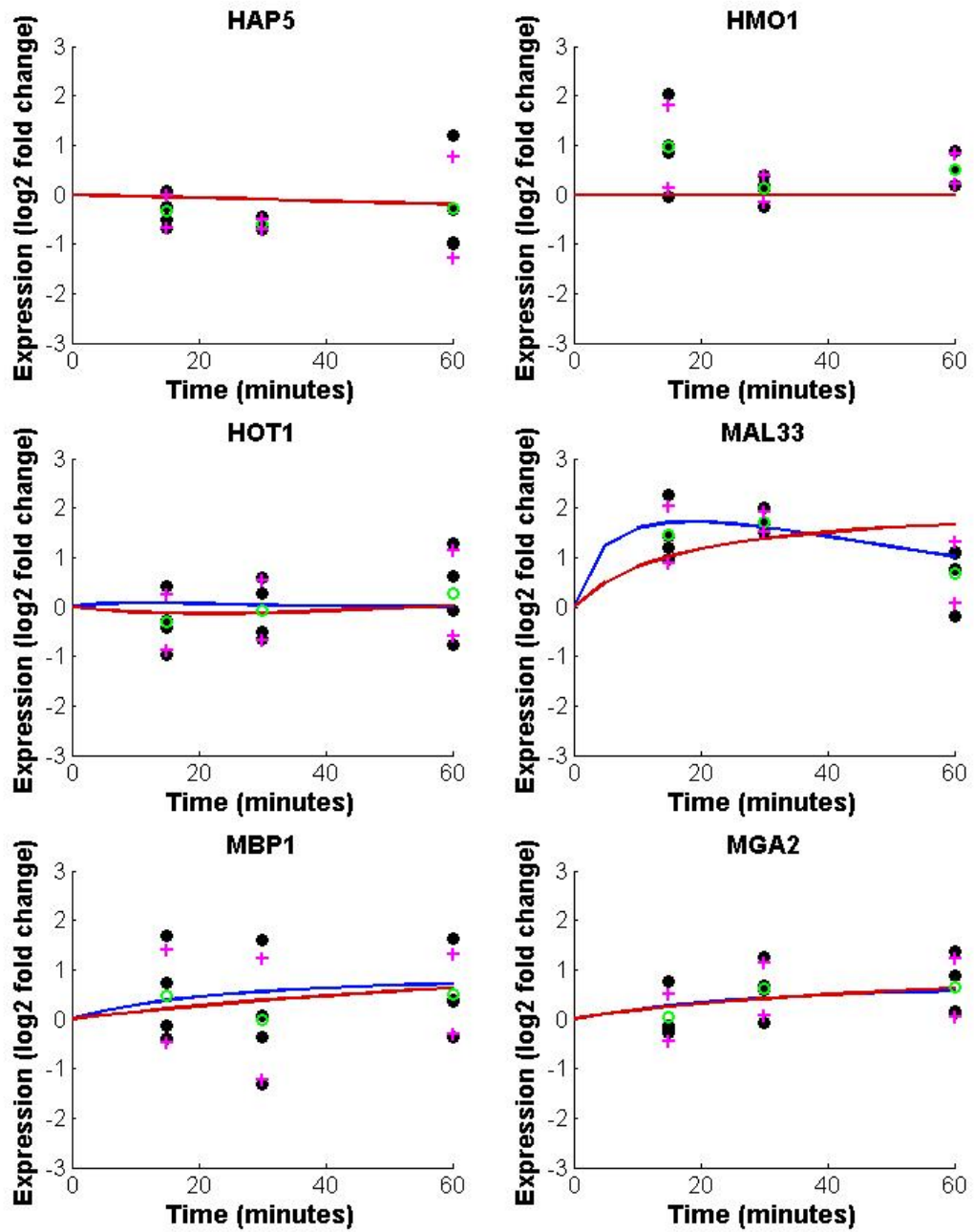


Fig. S21b. The $\Delta hmo1$ forward simulations for *HAP5*, *HMO1*, *HOT1*, *MAL33*, *MBP1*, and *MGA2*. The models fitted by both the sigmoid function (blue line) and Michaelis-Menten function (red line) are shown. The green circles designate the average log fold change for each time point in the cold shock experiment. The magenta pluses designate ± 1 standard deviation in the log fold change for each time point in the cold shock experiment.

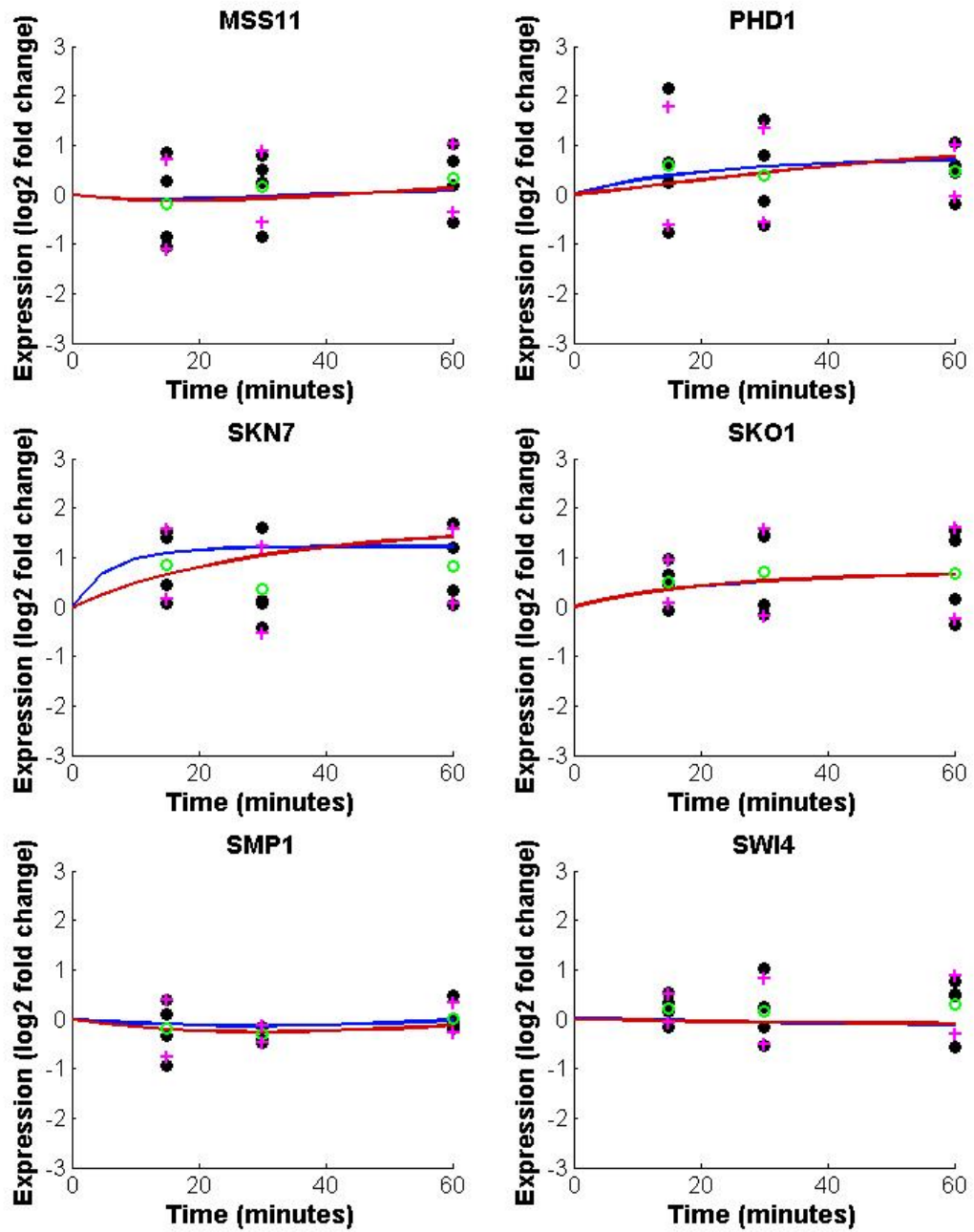


Fig. S21c. The $\Delta hmo1$ forward simulations for *MSS11*, *PHD1*, *SKN7*, *SKO1*, and *SWI4*. The models fitted by both the sigmoid function (blue line) and Michaelis-Menten function (red line) are shown. The green circles designate the average log fold change for each time point in the cold shock experiment. The magenta pluses designate ± 1 standard deviation in the log fold change for each time point in the cold shock experiment.

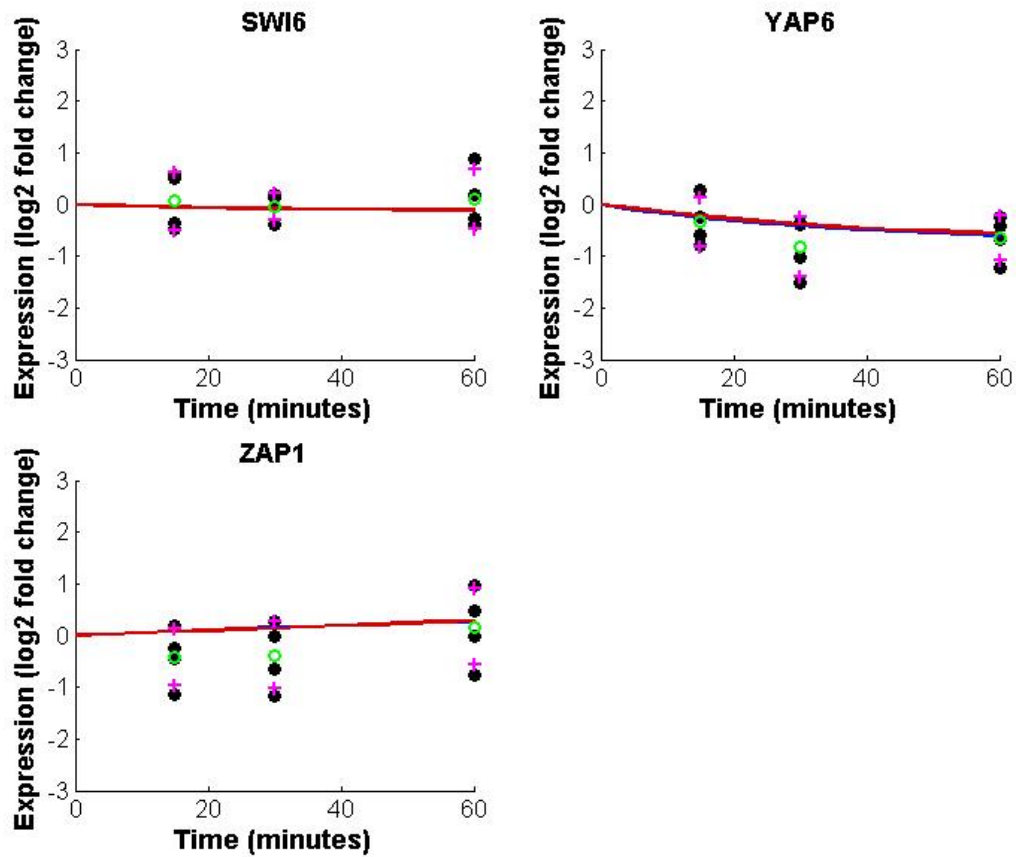


Fig. S21d. The $\Delta hmo1$ forward simulations for *SWI6*, *YAP6*, and *ZAP1*. The models fitted by both the sigmoid function (blue line) and Michaelis-Menten function (red line) are shown. The green circles designate the average log fold change for each time point in the cold shock experiment. The magenta pluses designate ± 1 standard deviation in the log fold change for each time point in the cold shock experiment.

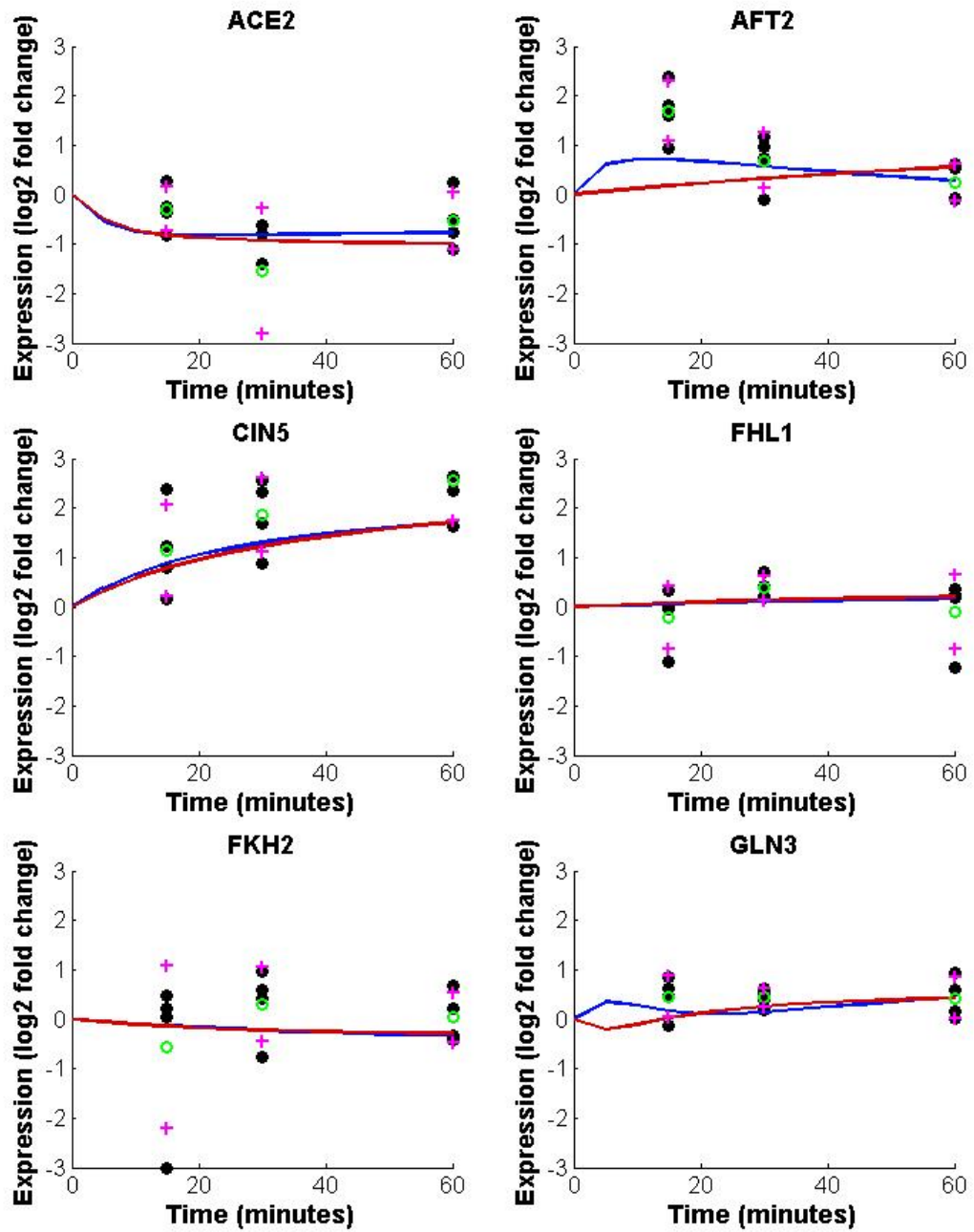


Fig. S22a. The $\Delta zap1$ forward simulations for *ACE2*, *AFT2*, *CIN5*, *FHL1*, *FKH2*, and *GLN3*. The models fitted by both the sigmoid function (blue line) and Michaelis-Menten function (red line) are shown. The green circles designate the average log fold change for each time point in the cold shock experiment. The magenta pluses designate ± 1 standard deviation in the log fold change for each time point in the cold shock experiment.

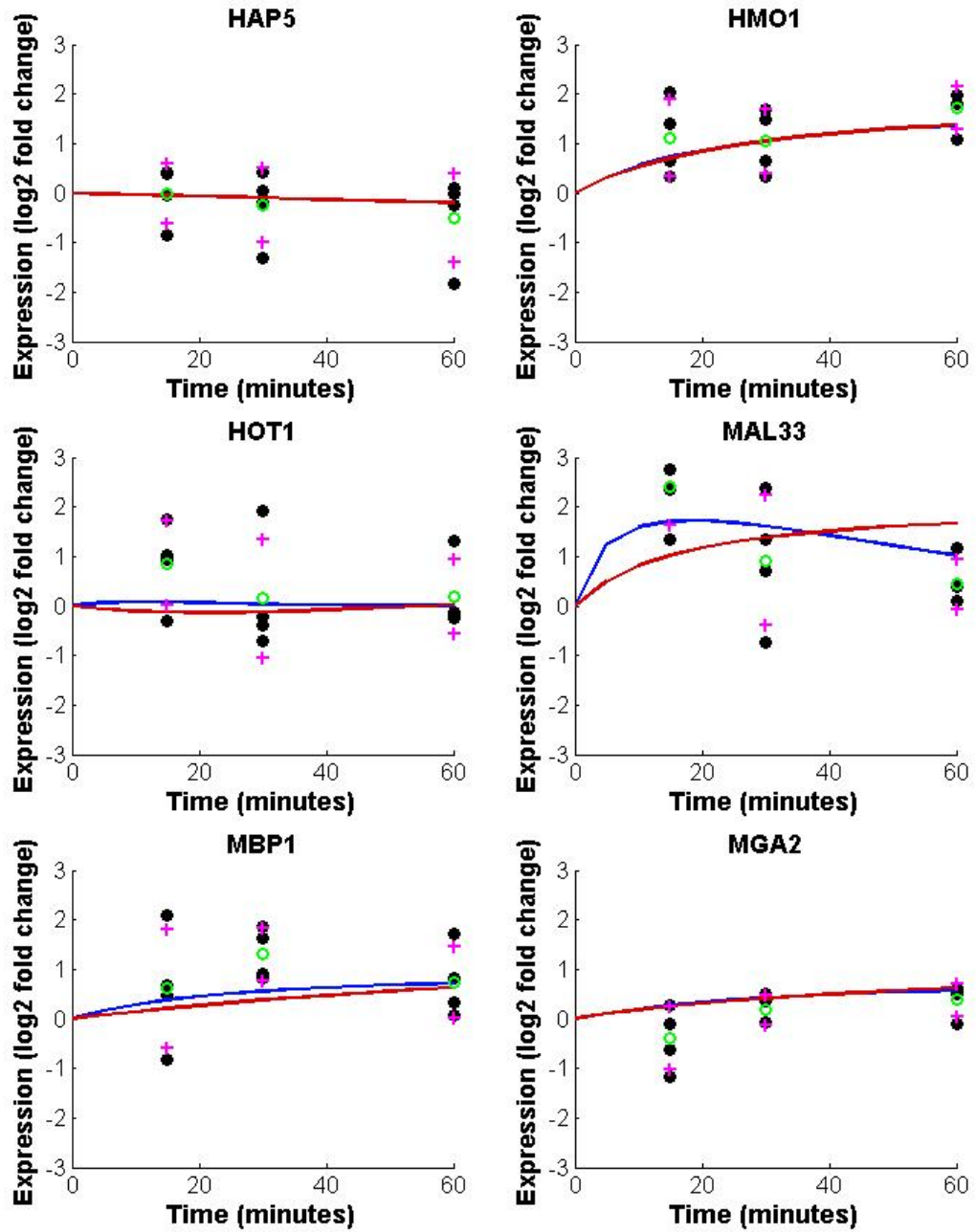


Fig. S22b. The $\Delta zap1$ forward simulations for *HAP5*, *HMO1*, *HOT1*, *MAL33*, *MBP1*, and *MGA2*. The models fitted by both the sigmoid function (blue line) and Michaelis-Menten function (red line) are shown. The green circles designate the average log fold change for each time point in the cold shock experiment. The magenta pluses designate ± 1 standard deviation in the log fold change for each time point in the cold shock experiment.

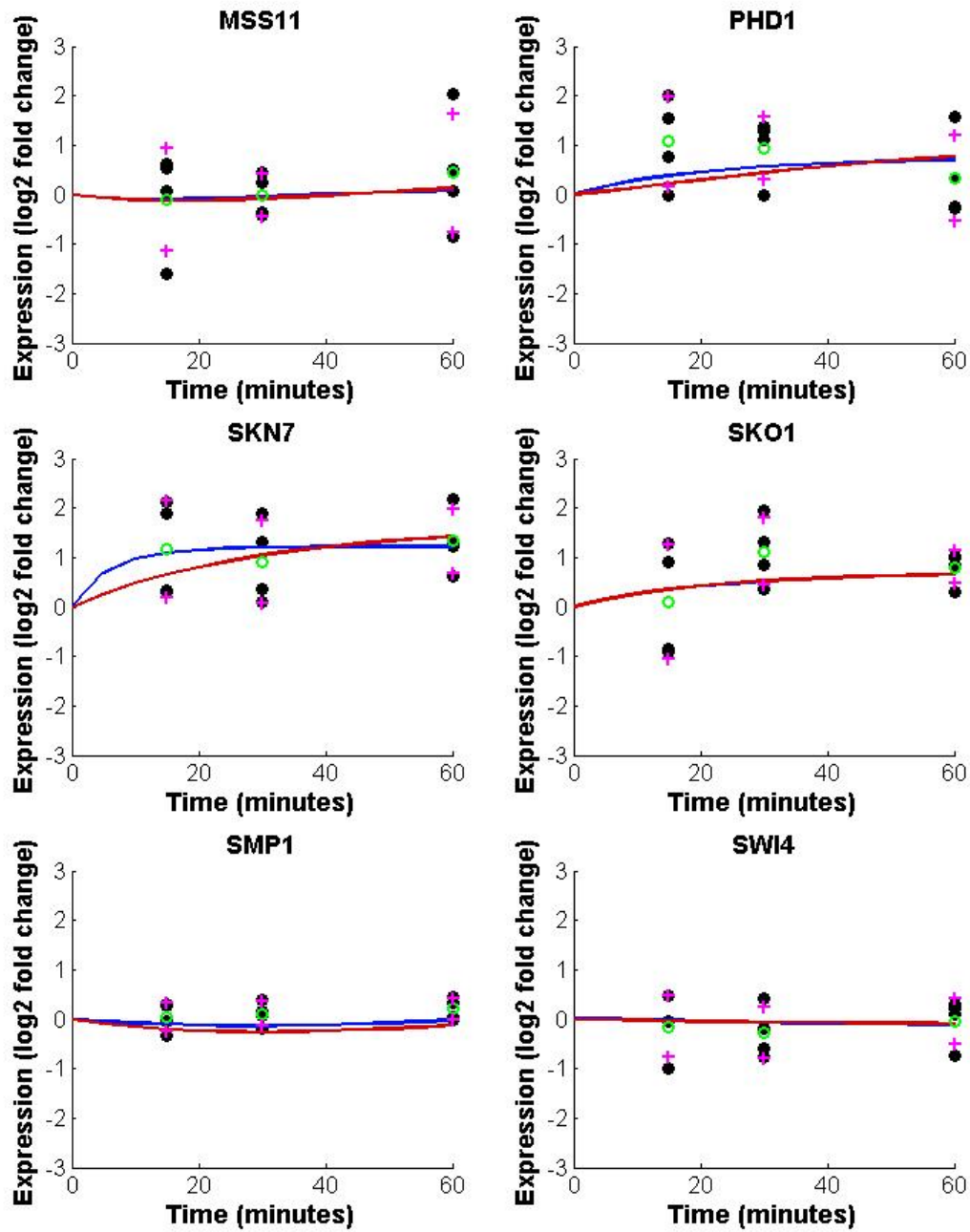


Fig. S22c. The $\Delta zap1$ forward simulations for *MSS11*, *PHD1*, *SKN7*, *SKO1*, and *SWI4*. The models fitted by both the sigmoid function (blue line) and Michaelis-Menten function (red line) are shown. The green circles designate the average log fold change for each time point in the cold shock experiment. The magenta pluses designate ± 1 standard deviation in the log fold change for each time point in the cold shock experiment.

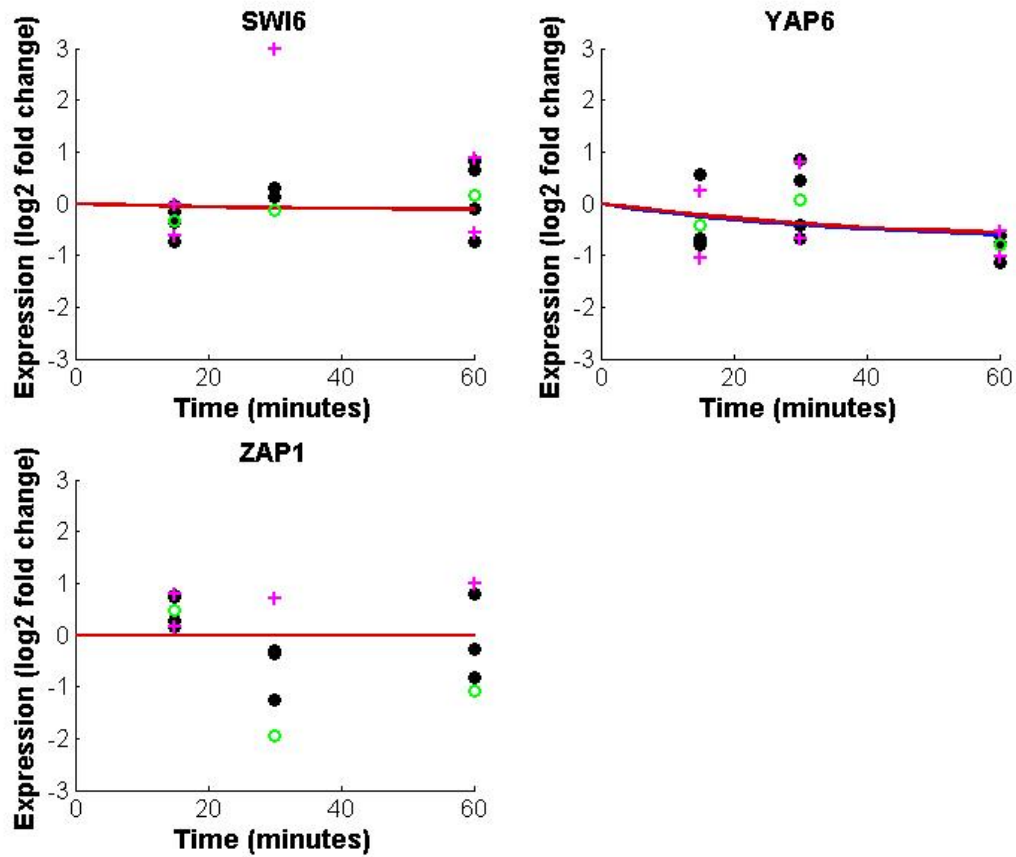


Fig. S22d. The $\Delta zap1$ forward simulations for *SWI6*, *YAP6*, and *ZAP1*. The models fitted by both the sigmoid function (blue line) and Michaelis-Menten function (red line) are shown. The green circles designate the average log fold change for each time point in the cold shock experiment. The magenta pluses designate ± 1 standard deviation in the log fold change for each time point in the cold shock experiment.

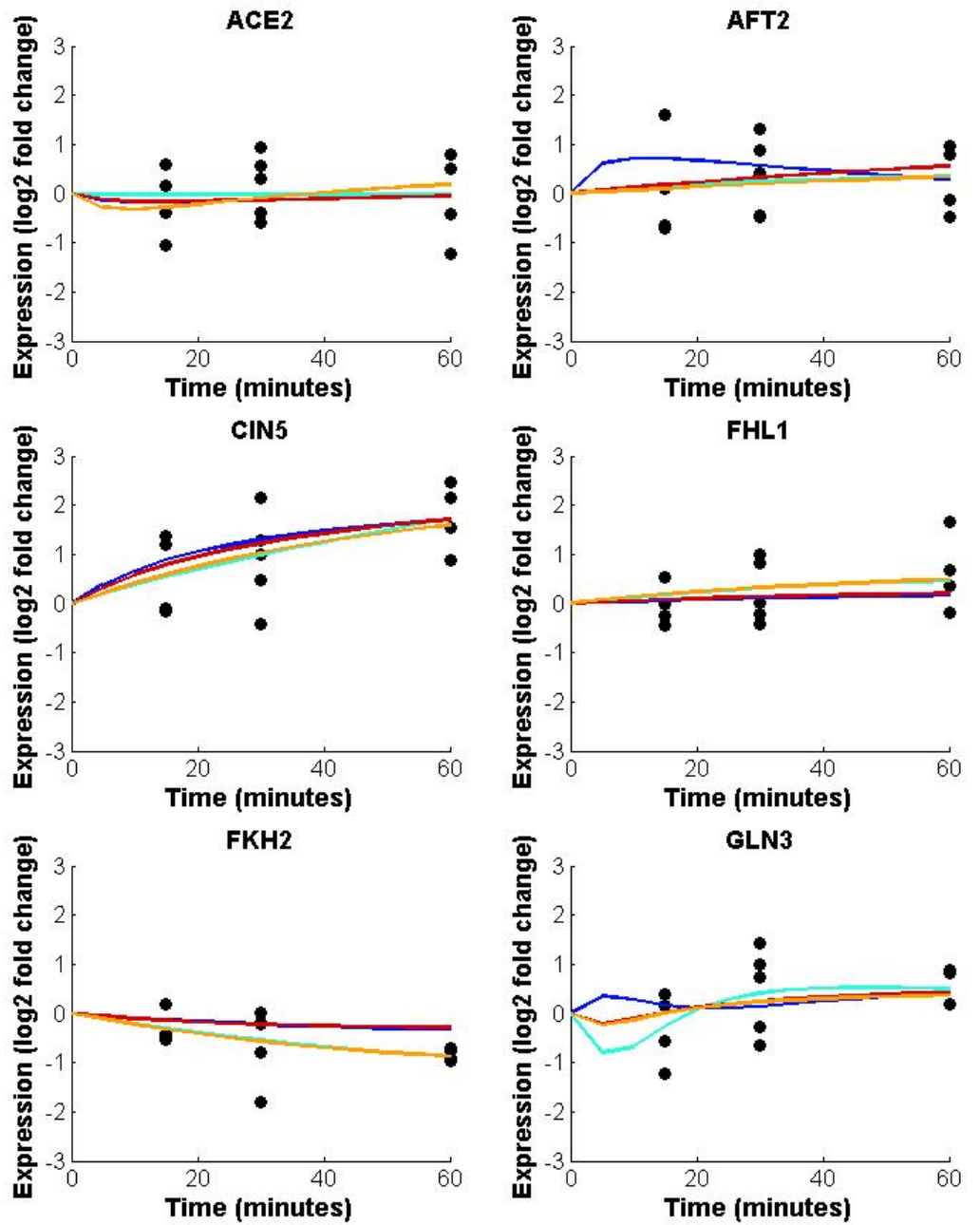


Fig. S23a. The wild type forward simulations for *ACE2*, *AFT2*, *CIN5*, *FHL1*, *FKH2*, and *GLN3* based on Michaelis-Menten kinetics and the sigmoid function. The models were fit using data for all strains (*) and for individual strains (**) in the simulation.

- wt Data
- Sigmoid Model*
- Sigmoid Model**
- Michaelis-Menten Model*
- Michaelis-Menten Model**

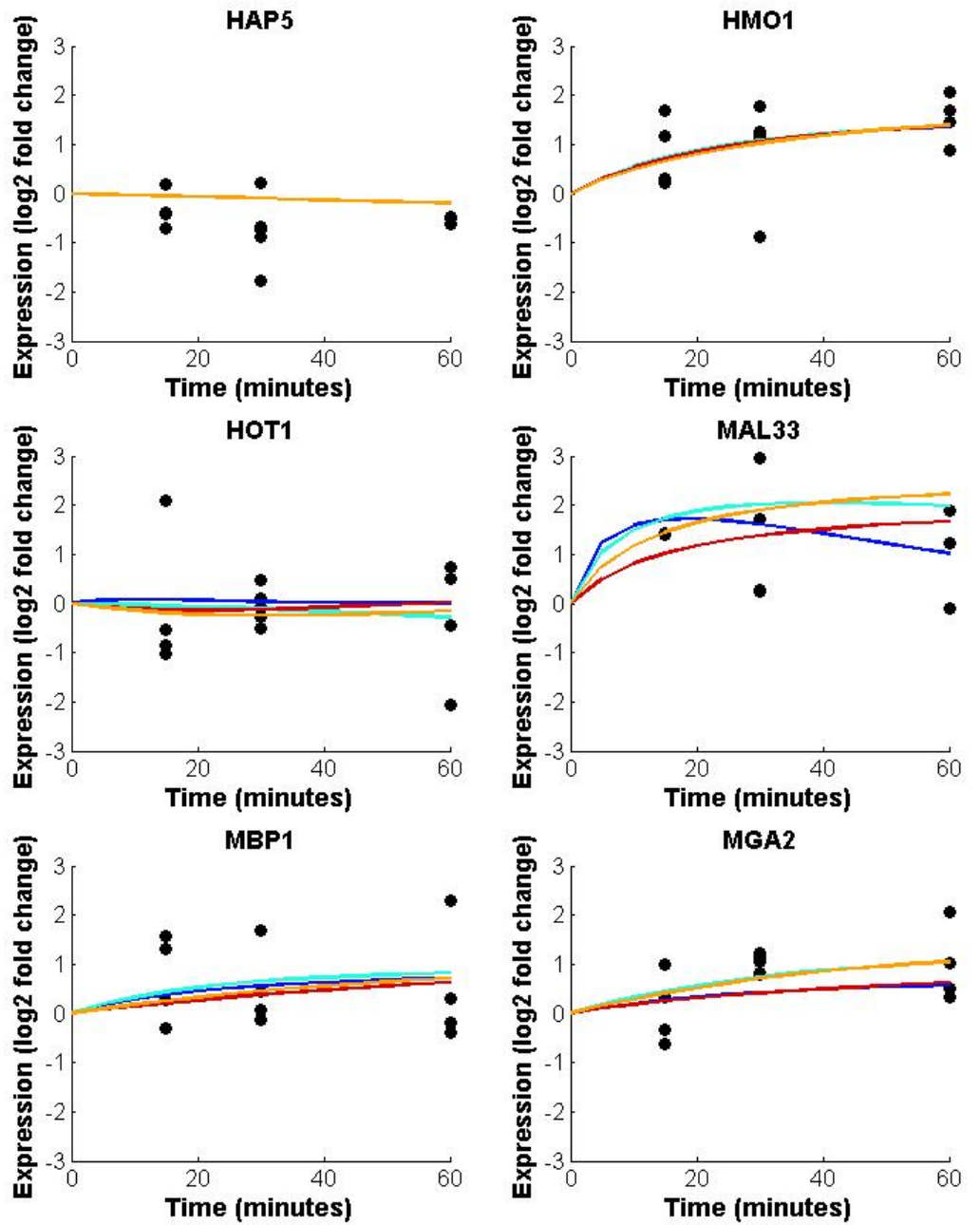


Fig. S23b. The wild type forward simulations for *HAP5*, *HMO1*, *HOT1*, *MAL33*, *MBP1*, and *MGA2* based on Michaelis-Menten kinetics and the sigmoid function. The models were fit using data for all strains (*) and for individual strains (**) in the simulation.

- wt Data
- Sigmoid Model*
- Sigmoid Model**
- Michaelis-Menten Model*
- Michaelis-Menten Model**

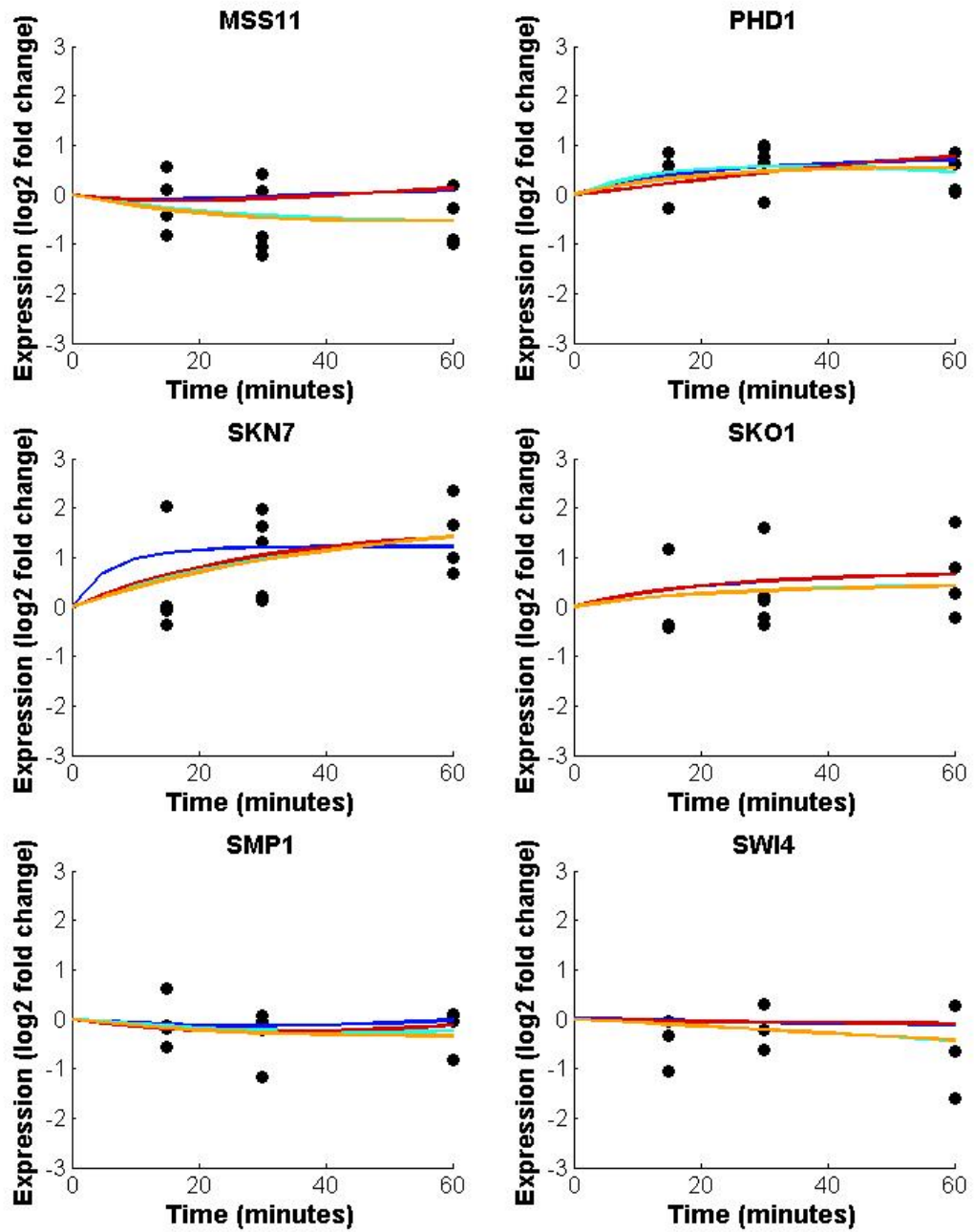


Fig. S23c. The wild type forward simulations for *MSS11*, *PHD1*, *SKN7*, *SKO1*, and *SWI4* based on Michaelis-Menten kinetics and the sigmoid function. The models were fit using data for all strains (*) and for individual strains (**) in the simulation.

- wt Data
- Sigmoid Model*
- Sigmoid Model**
- Michaelis-Menten Model*
- Michaelis-Menten Model**

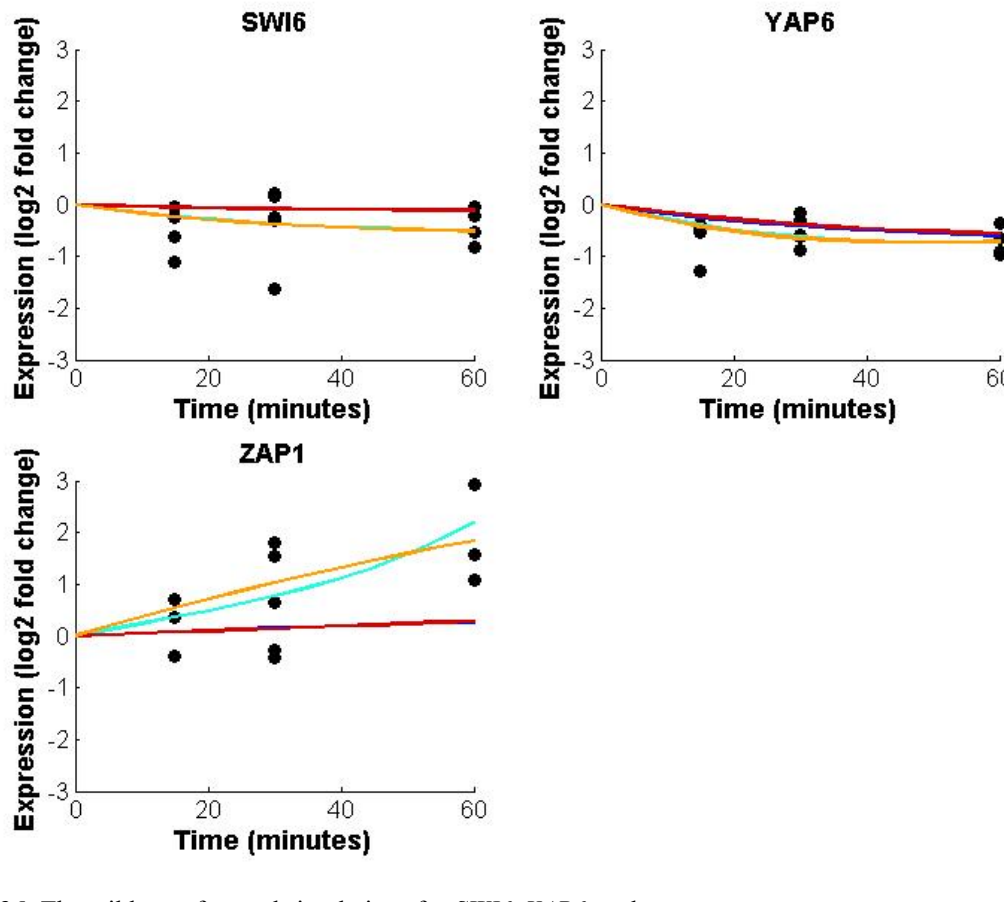


Fig. S23d. The wild type forward simulations for *SWI6*, *YAP6*, and *ZAP1* based on Michaelis-Menten kinetics and the sigmoid function. The models were fit using data for all strains (*) and for individual strains (**) in the simulation.

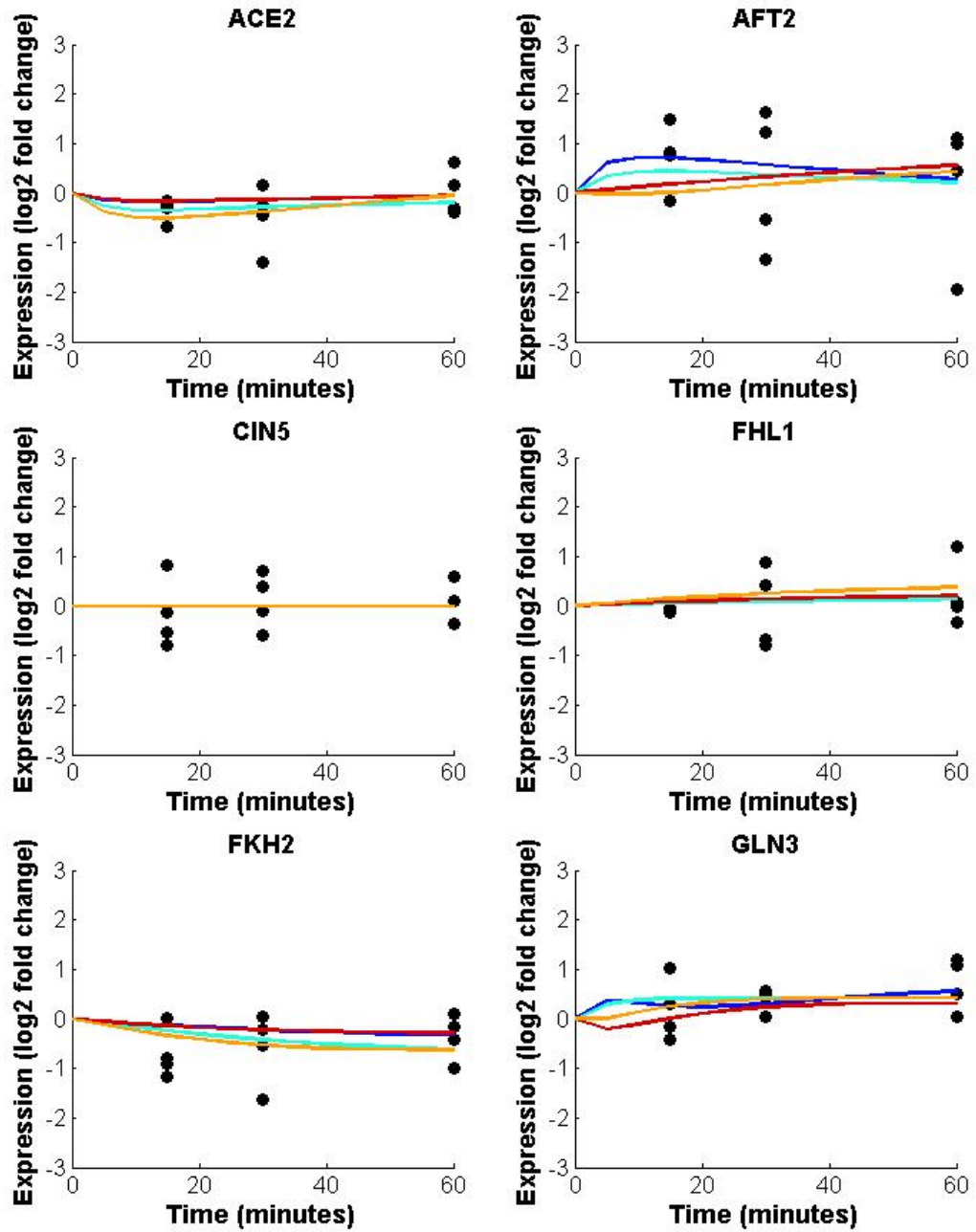


Fig. S24a. The $\Delta cin5$ forward simulations for *ACE2*, *AFT2*, *CIN5*, *FHL1*, *FKH2*, and *GLN3* based on Michaelis-Menten kinetics and the sigmoid function. The models were fit using data for all strains (*) and for individual strains (**) in the simulation.

- $\Delta cin5$ Data
- Sigmoid Model*
- Sigmoid Model**
- Michaelis-Menten Model*
- Michaelis-Menten Model**

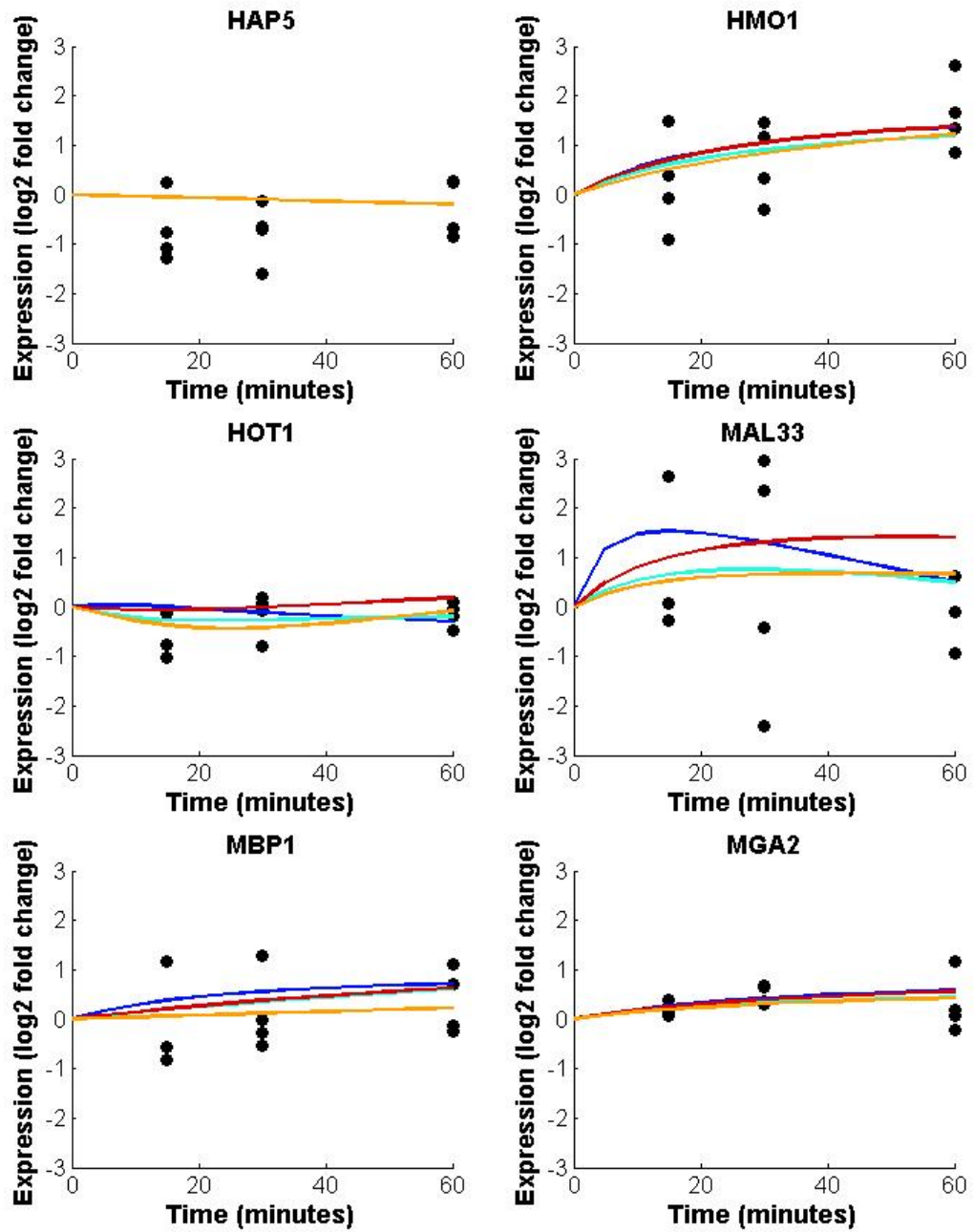


Fig. S24b. The $\Delta cin5$ forward simulations for *HAP5*, *HMO1*, *HOT1*, *MAL33*, *MBP1*, and *MGA2* based on Michaelis-Menten kinetics and the sigmoid function. The models were fit using data for all strains (*) and for individual strains (**) in the simulation.

- | | |
|---|--------------------------|
| ● | $\Delta cin5$ Data |
| — | Sigmoid Model* |
| — | Sigmoid Model** |
| — | Michaelis-Menten Model* |
| — | Michaelis-Menten Model** |

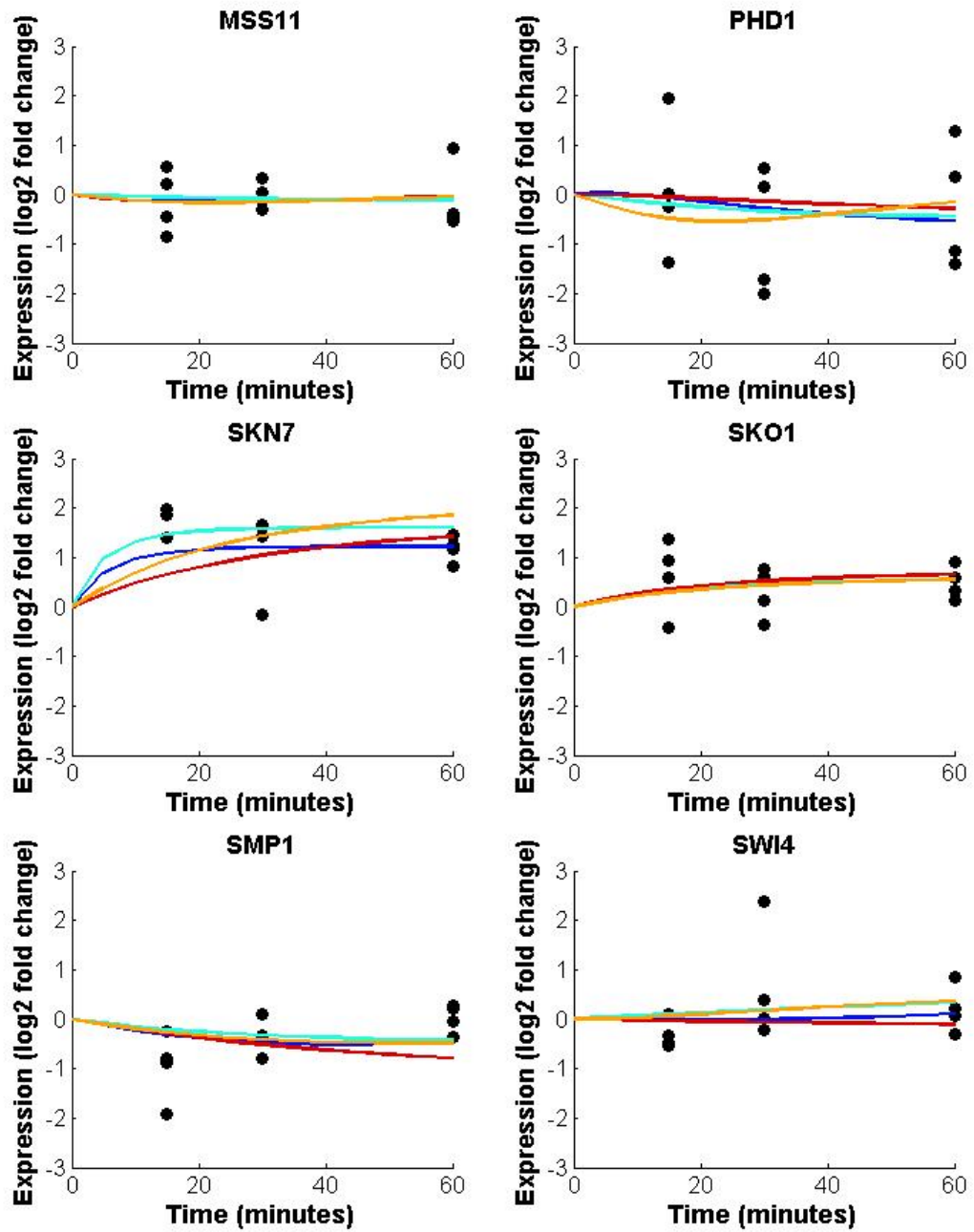


Fig. S24c. The $\Delta cin5$ forward simulations for *MSS11*, *PHD1*, *SKN7*, *SKO1*, and *SWI4* based on Michaelis-Menten kinetics and the sigmoid function. The models were fit using data for all strains (*) and for individual strains (**) in the simulation.

- $\Delta cin5$ Data
- Sigmoid Model*
- Sigmoid Model**
- Michaelis-Menten Model*
- Michaelis-Menten Model**

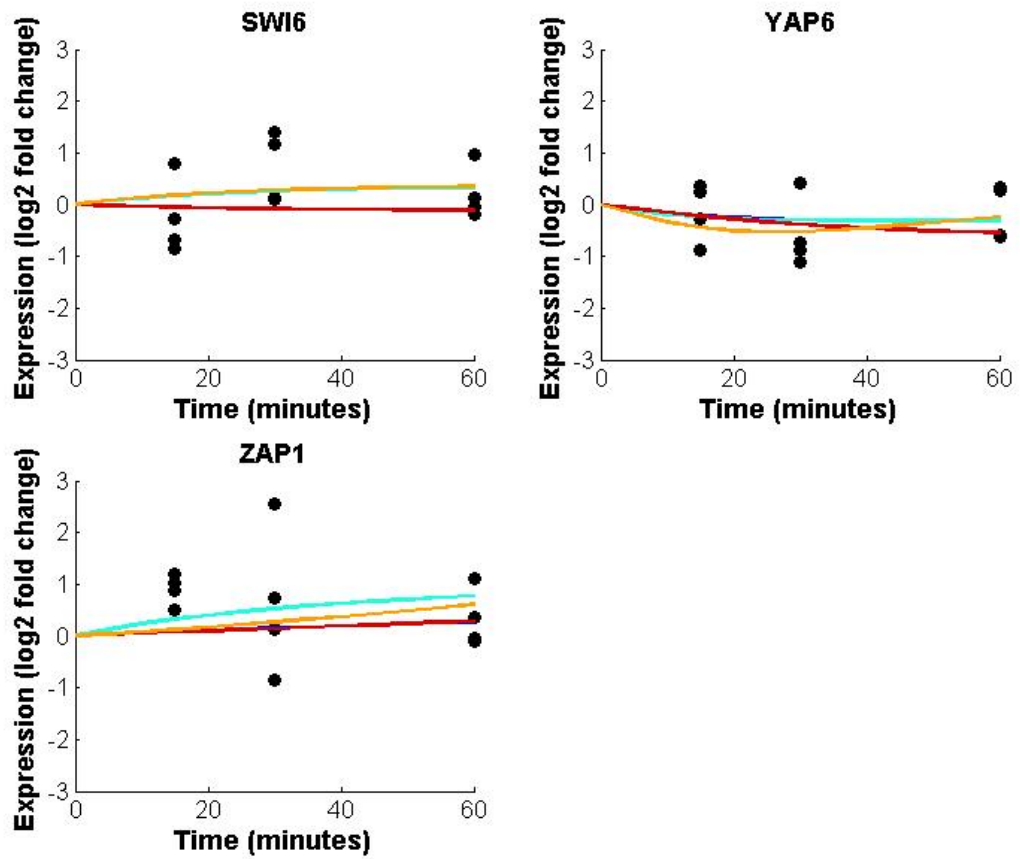


Fig. S24d. The $\Delta cin5$ forward simulations for *SWI6*, *YAP6*, and *ZAP1* based on Michaelis-Menten kinetics and the sigmoid function. The models were fit using data for all strains (*) and for individual strains (**) in the simulation.

- $\Delta cin5$ Data
- Sigmoid Model*
- Sigmoid Model**
- Michaelis-Menten Model*
- Michaelis-Menten Model**

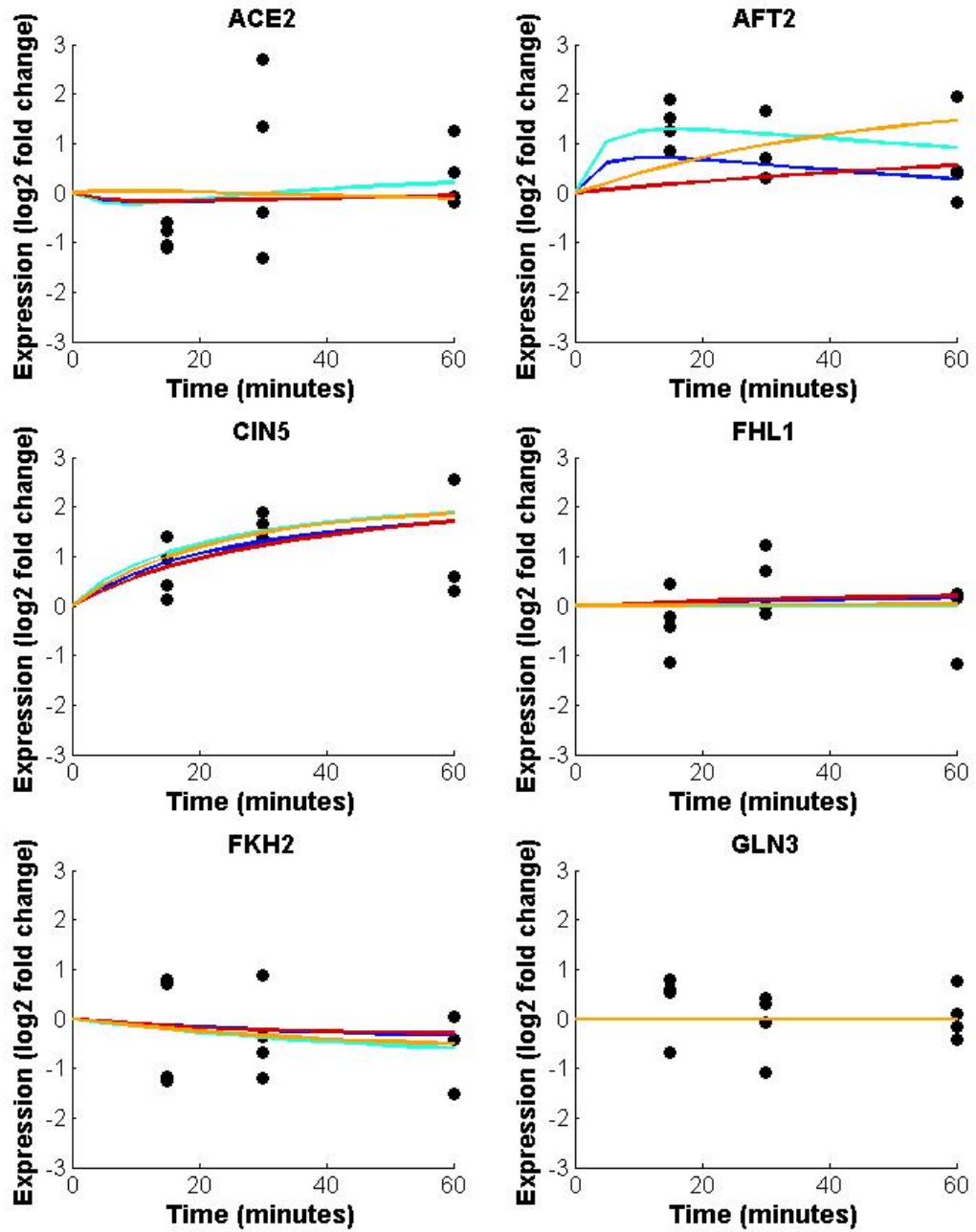


Fig. S25a. The $\Delta gln3$ forward simulations for *ACE2*, *AFT2*, *CIN5*, *FHL1*, *FKH2*, and *GLN3* based on Michaelis-Menten kinetics and the sigmoid function. The models were fit using data for all strains (*) and for individual strains (**) in the simulation.

- $\Delta gln3$ Data
- Sigmoid Model*
- Sigmoid Model**
- Michaelis-Menten Model*
- Michaelis-Menten Model**

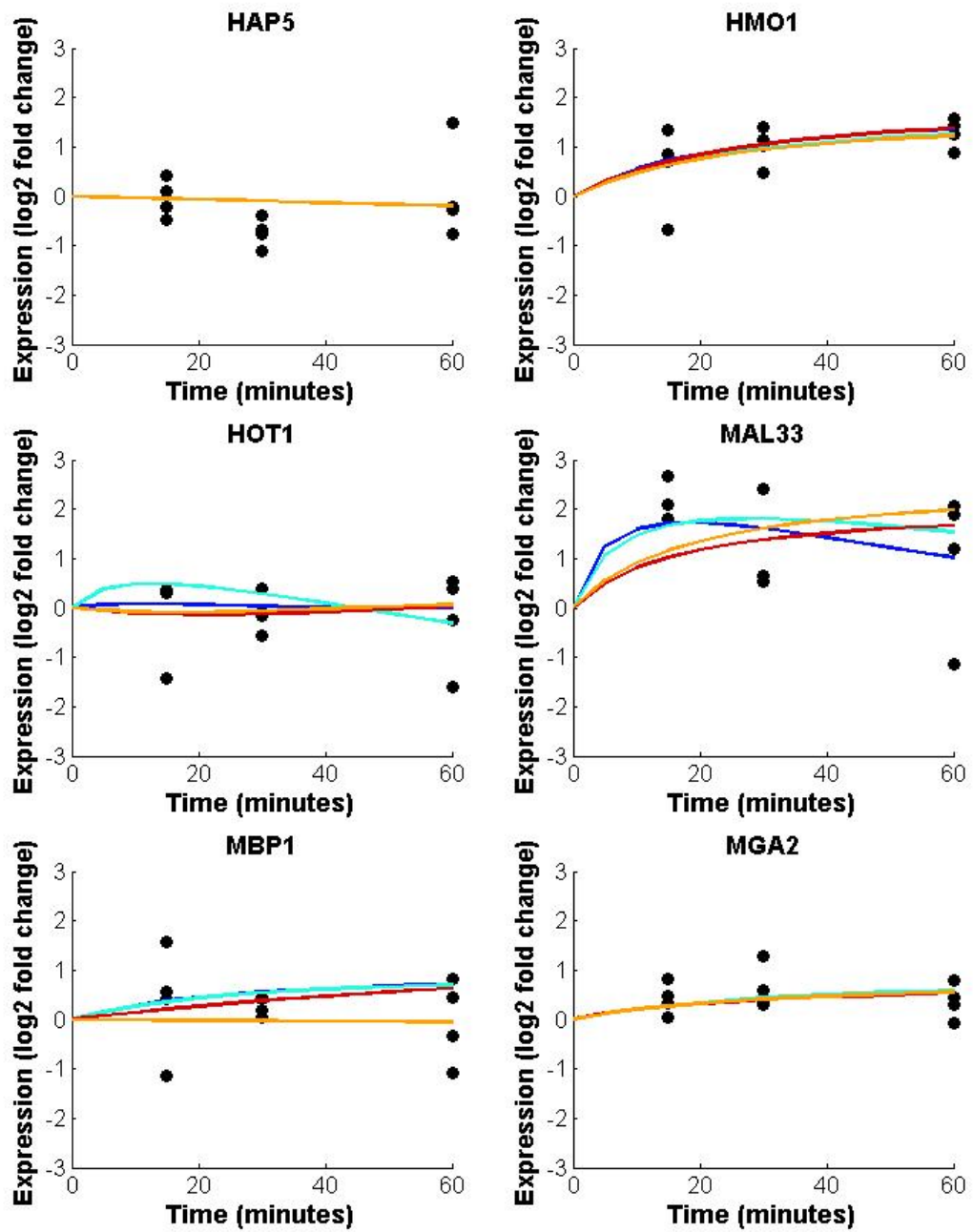


Fig. S25b. The $\Delta gln3$ forward simulations for *HAP5*, *HMO1*, *HOT1*, *MAL33*, *MBP1*, and *MGA2* based on Michaelis-Menten kinetics and the sigmoid function. The models were fit using data for all strains (*) and for individual strains (**) in the simulation.

- $\Delta gln3$ Data
- Sigmoid Model*
- Sigmoid Model**
- Michaelis-Menten Model*
- Michaelis-Menten Model**

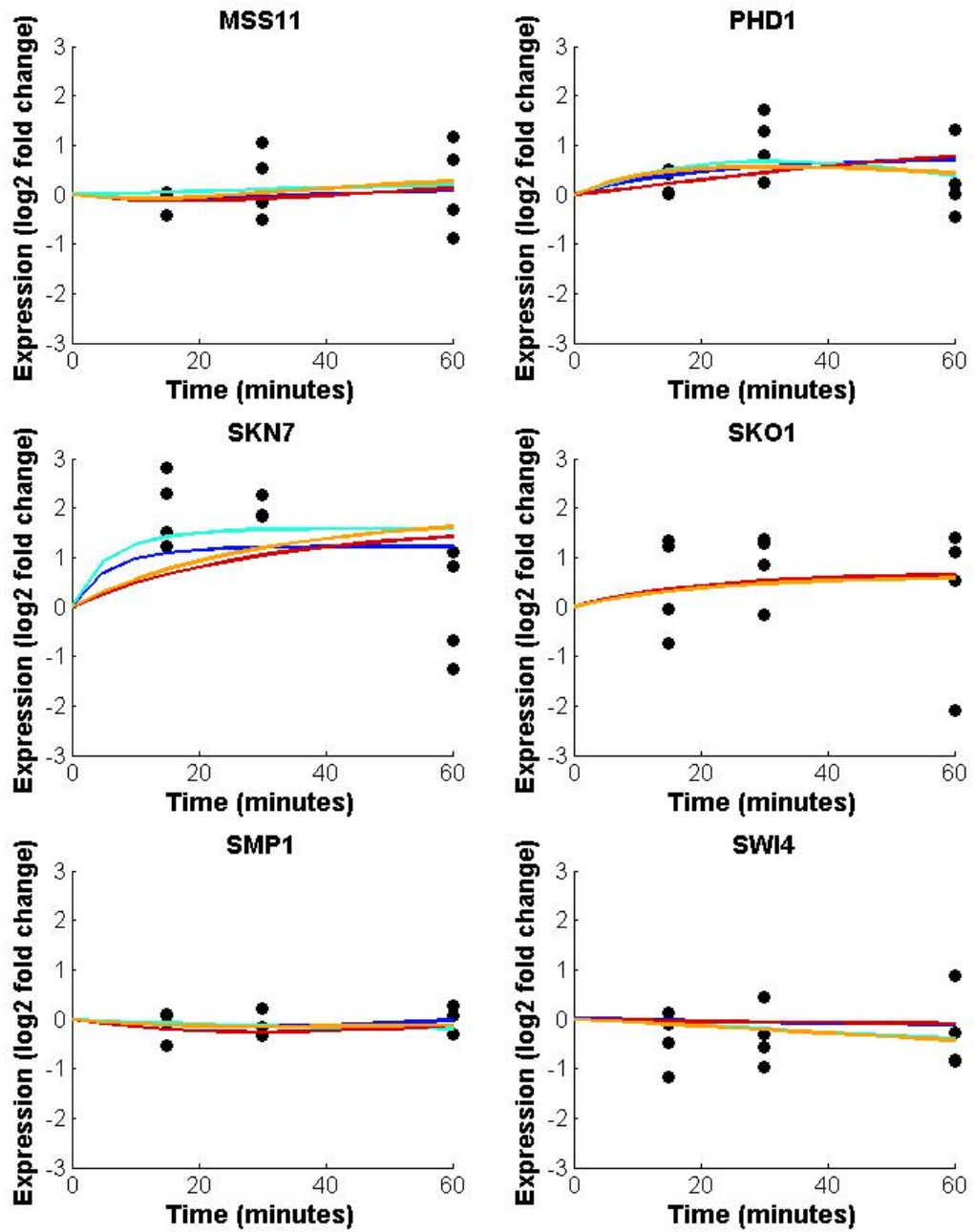


Fig. S25c. The $\Delta gln3$ forward simulations for *MSS11*, *PHD1*, *SKN7*, *SKO1*, and *SWI4* based on Michaelis-Menten kinetics and the sigmoid function. The models were fit using data for all strains (*) and for individual strains (**) in the simulation.

- $\Delta gln3$ Data
- Sigmoid Model*
- Sigmoid Model**
- Michaelis-Menten Model*
- Michaelis-Menten Model**

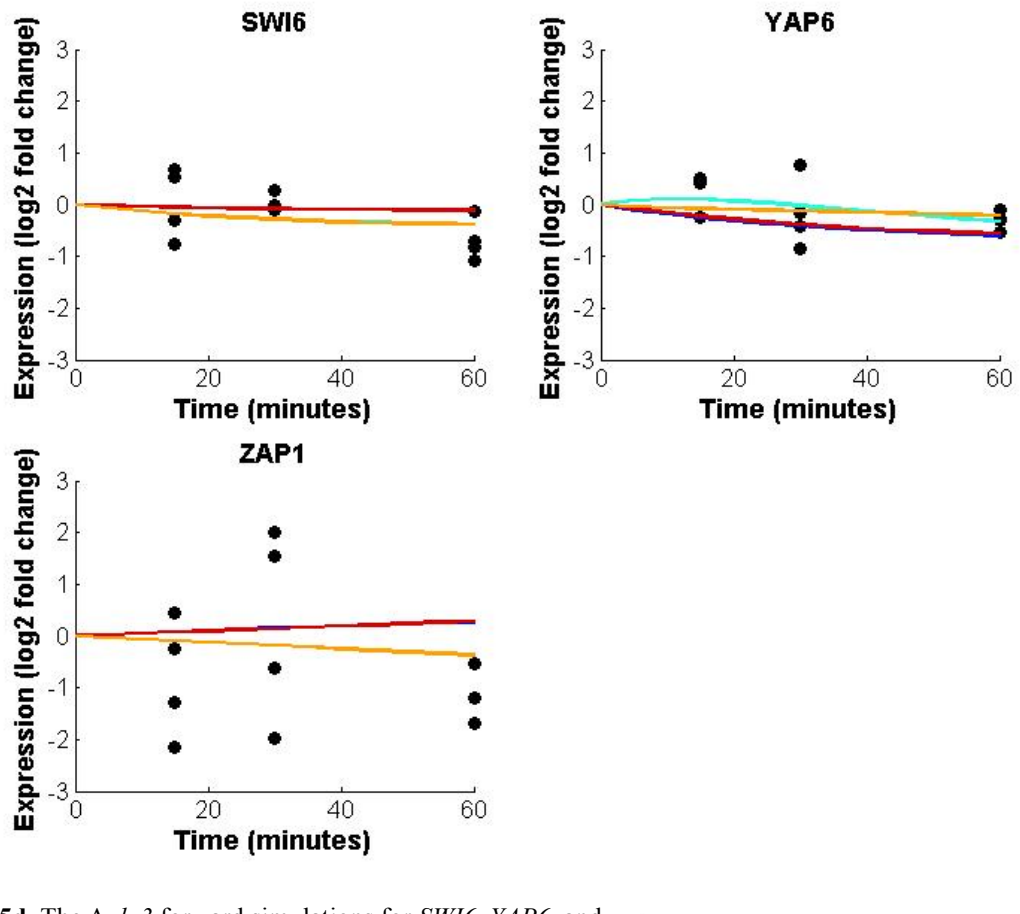


Fig. S25d. The $\Delta gln3$ forward simulations for *SWI6*, *YAP6*, and *ZAP1* based on Michaelis-Menten kinetics and the sigmoid function. The models were fit using data for all strains (*) and for individual strains (**) in the simulation.

- $\Delta gln3$ Data
- Sigmoid Model*
- Sigmoid Model**
- Michaelis-Menten Model*
- Michaelis-Menten Model**

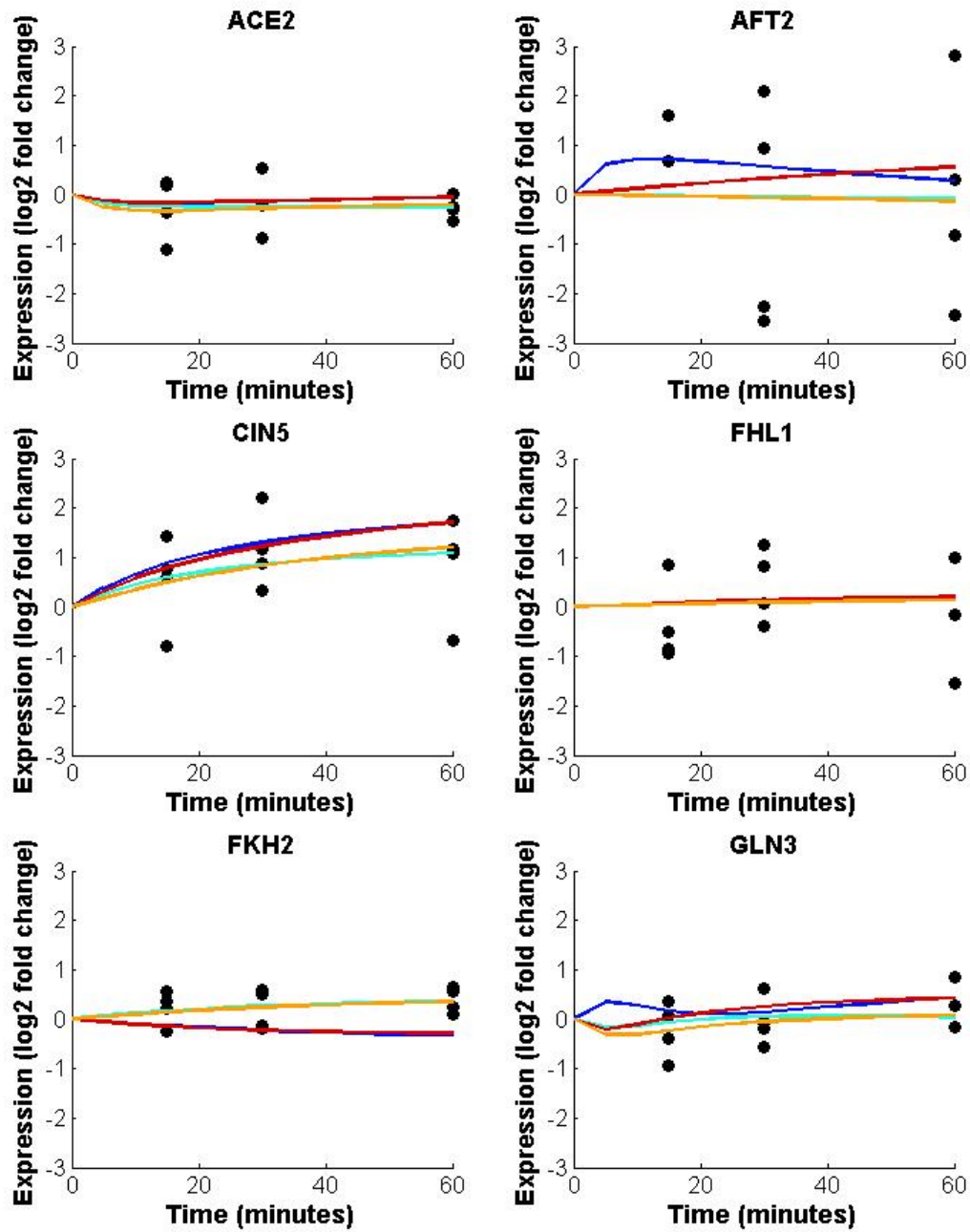


Fig. S26a. The $\Delta hmo1$ forward simulations for *ACE2*, *AFT2*, *CIN5*, *FHL1*, *FKH2*, and *GLN3* based on Michaelis-Menten kinetics and the sigmoid function. The models were fit using data for all strains (*) and for individual strains (**) in the simulation.

- $\Delta hmo1$ Data
- Sigmoid Model*
- Sigmoid Model**
- Michaelis-Menten Model*
- Michaelis-Menten Model**

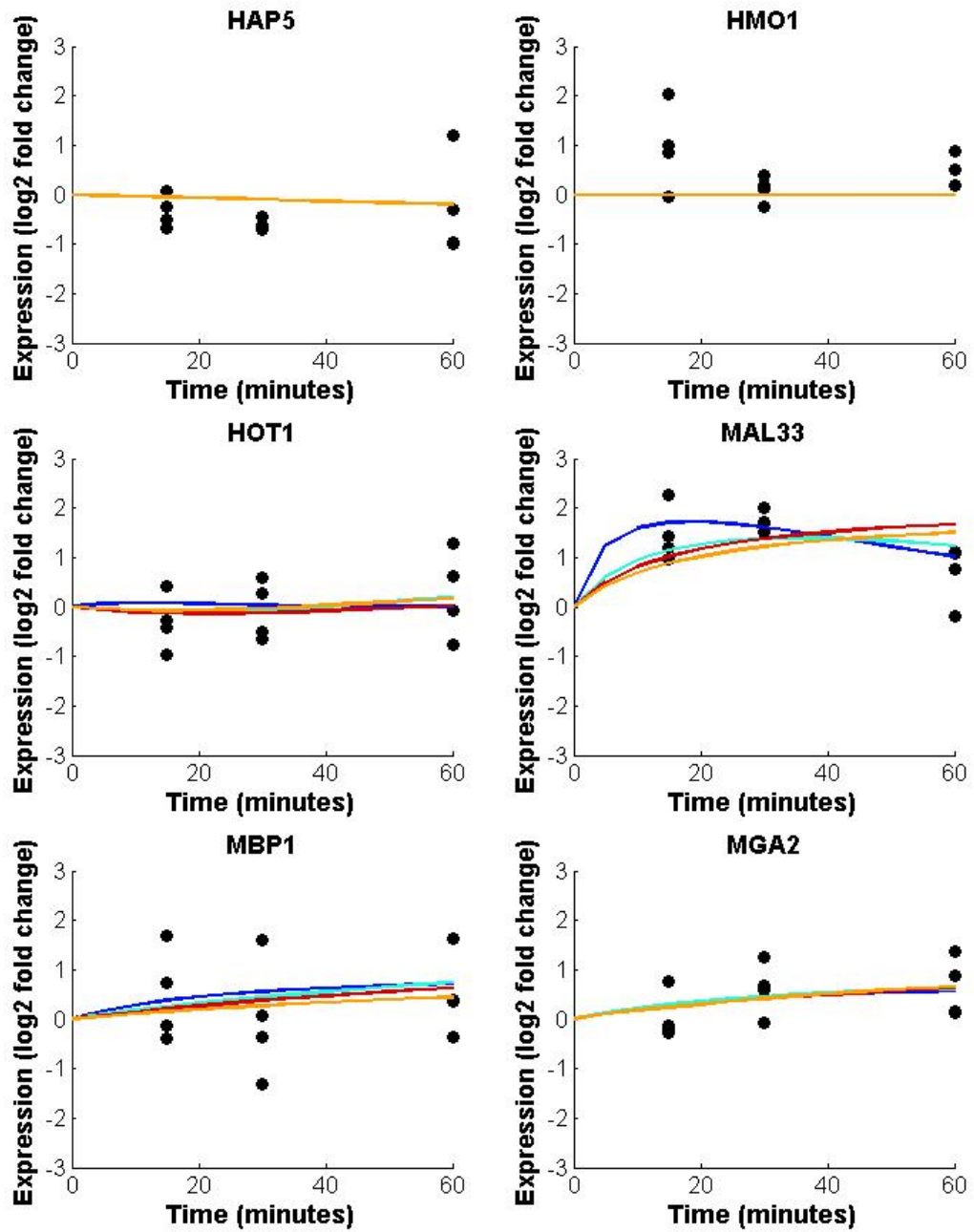


Fig. S26b. The $\Delta dhmo1$ forward simulations for *HAP5*, *HMO1*, *HOT1*, *MAL33*, *MBP1*, and *MGA2* based on Michaelis-Menten kinetics and the sigmoid function. The models were fit using data for all strains (*) and for individual strains (**) in the simulation.

- | | |
|---|--------------------------|
| ● | $\Delta dhmo1$ Data |
| — | Sigmoid Model* |
| — | Sigmoid Model** |
| — | Michaelis-Menten Model* |
| — | Michaelis-Menten Model** |

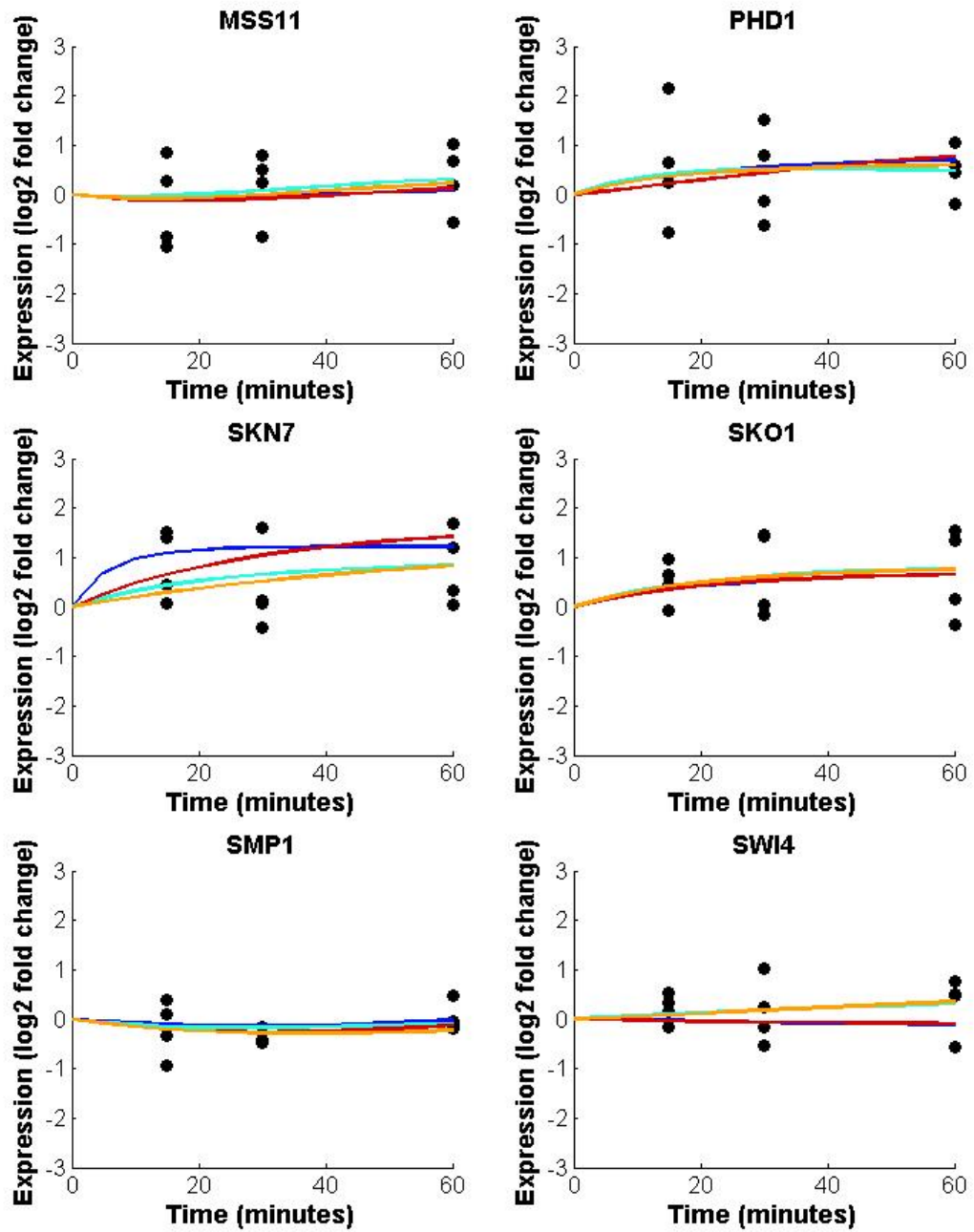
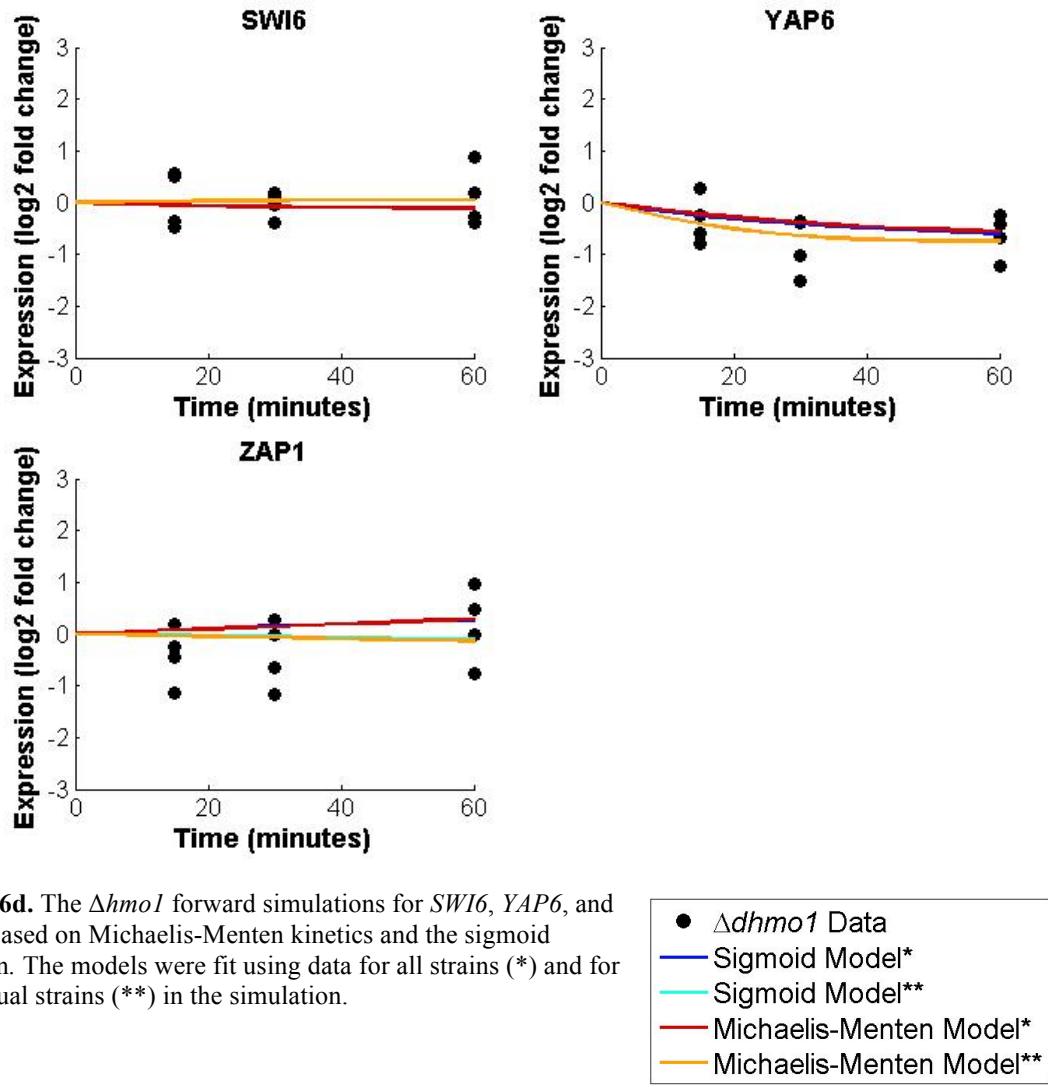


Fig. S26c. The $\Delta dhmo1$ forward simulations for *MSS11*, *PHD1*, *SKN7*, *SKO1*, and *SWI4* based on Michaelis-Menten kinetics and the sigmoid function. The models were fit using data for all strains (*) and for individual strains (**) in the simulation.

- $\Delta dhmo1$ Data
- Sigmoid Model*
- Sigmoid Model**
- Michaelis-Menten Model*
- Michaelis-Menten Model**



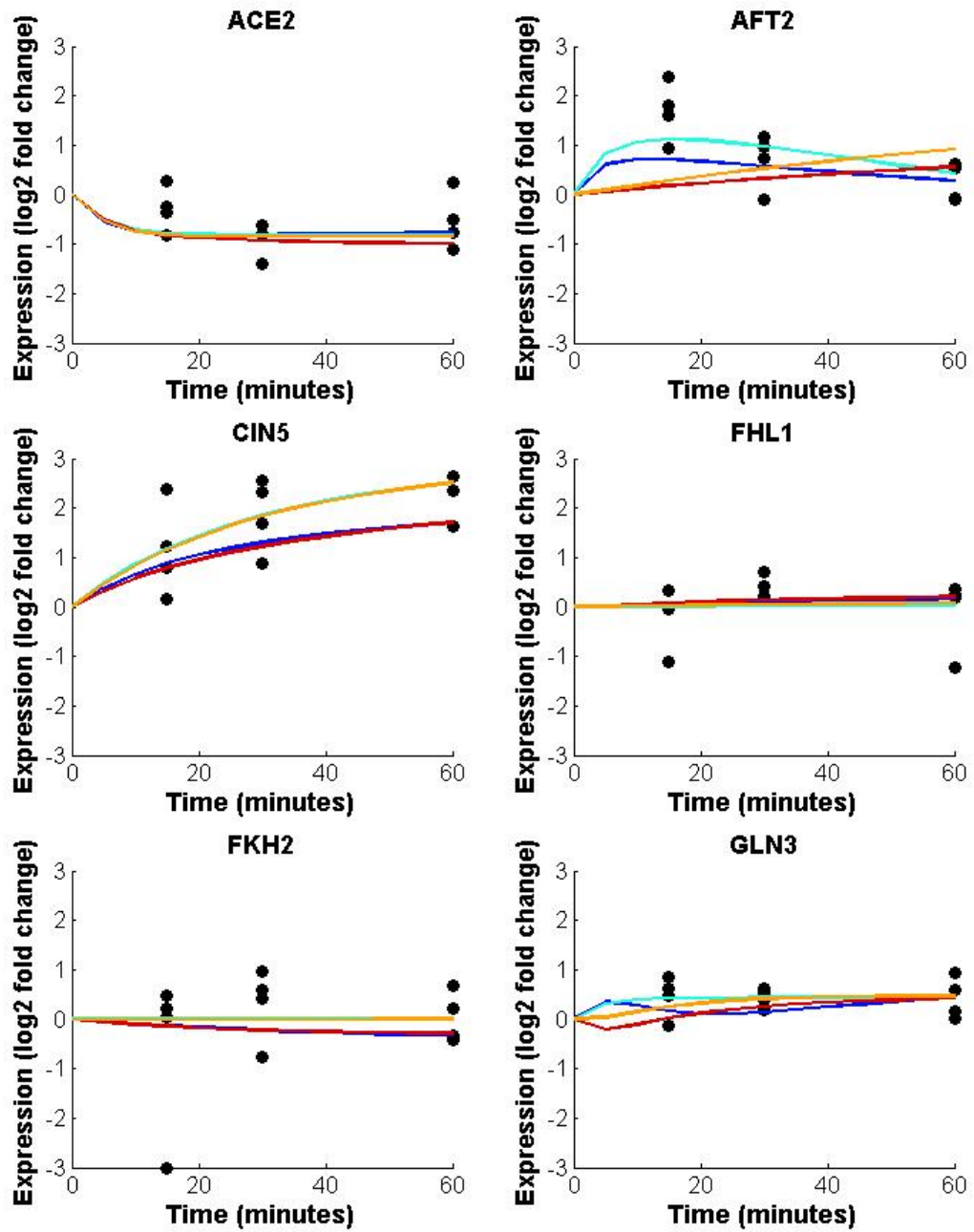


Fig. S27a. The $\Delta zap1$ forward simulations for *ACE2*, *AFT2*, *CIN5*, *FHL1*, *FKH2*, and *GLN3* based on Michaelis-Menten kinetics and the sigmoid function. The models were fit using data for all strains (*) and for individual strains (**) in the simulation.

- $\Delta zap1$ Data
- Sigmoid Model*
- Sigmoid Model**
- Michaelis-Menten Model*
- Michaelis-Menten Model**

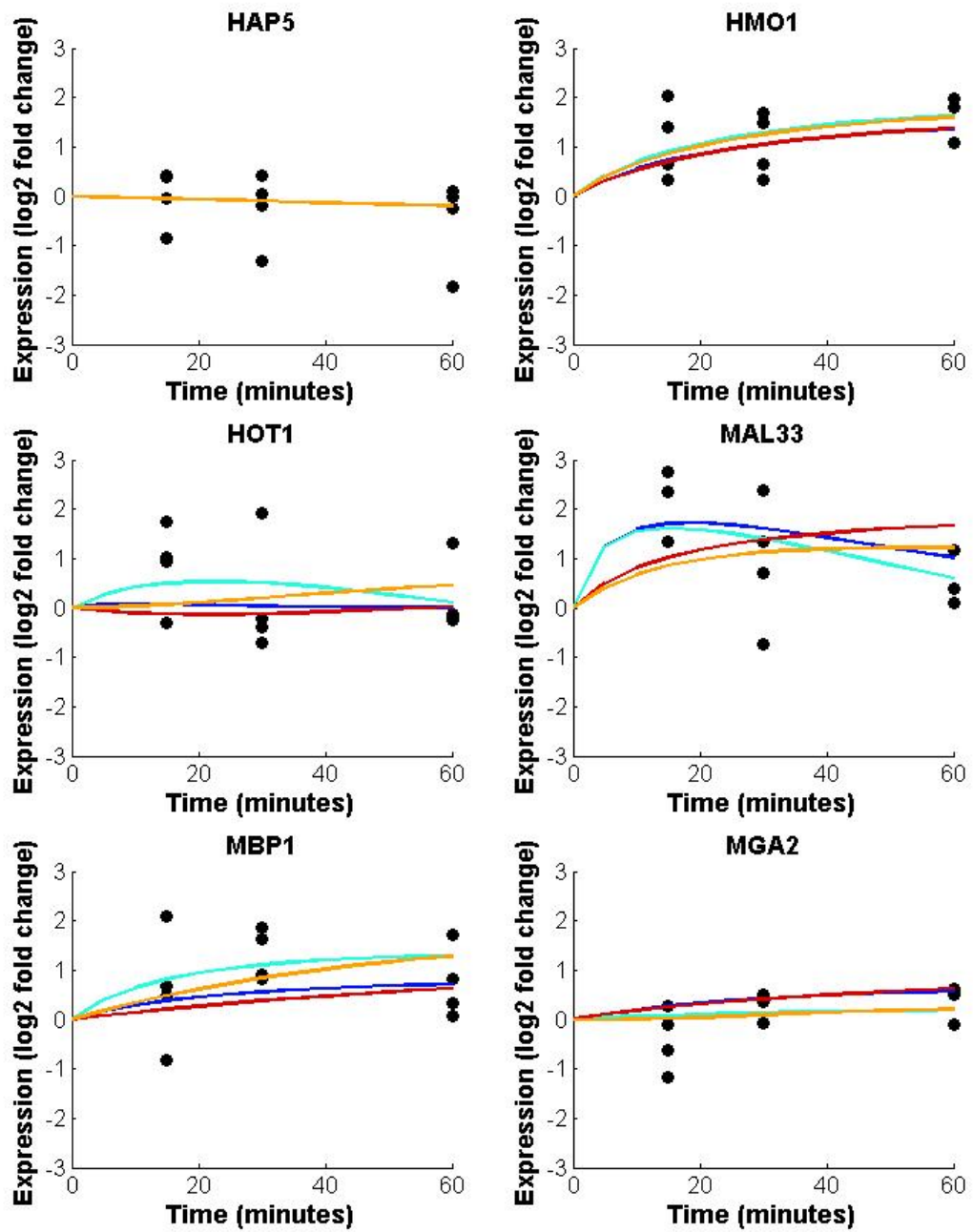


Fig. S27b. The $\Delta zap1$ forward simulations for *HAP5*, *HMO1*, *HOT1*, *MAL33*, *MBP1*, and *MGA2* based on Michaelis-Menten kinetics and the sigmoid function. The models were fit using data for all strains (*) and for individual strains (**) in the simulation.

- $\Delta zap1$ Data
- Sigmoid Model*
- Sigmoid Model**
- Michaelis-Menten Model*
- Michaelis-Menten Model**

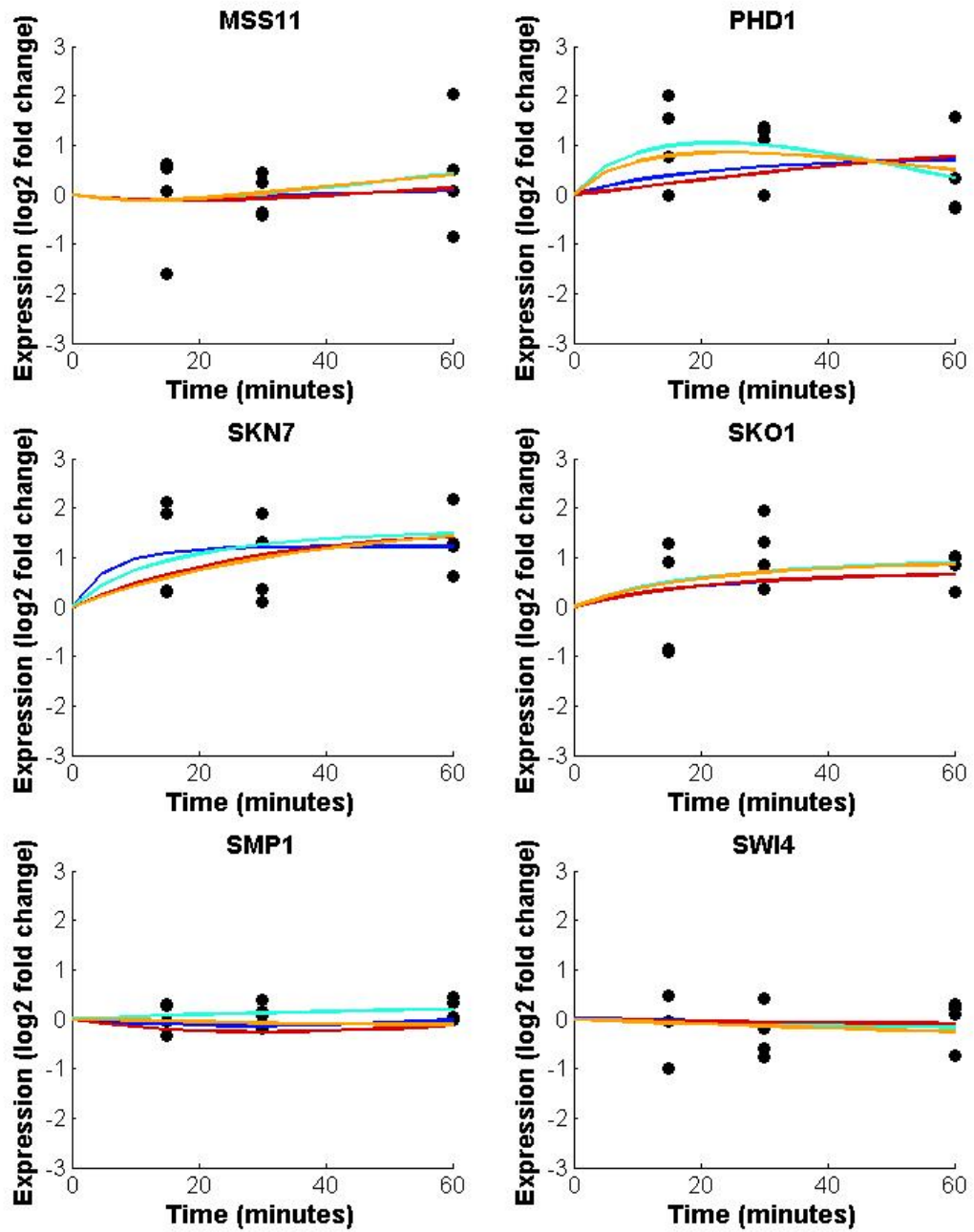


Fig. S27c. The $\Delta zap1$ forward simulations for *MSS11*, *PHD1*, *SKN7*, *SKO1*, and *SWI4* based on Michaelis-Menten kinetics and the sigmoid function. The models were fit using data for all strains (*) and for individual strains (**) in the simulation.

- $\Delta zap1$ Data
- Sigmoid Model*
- Sigmoid Model**
- Michaelis-Menten Model*
- Michaelis-Menten Model**

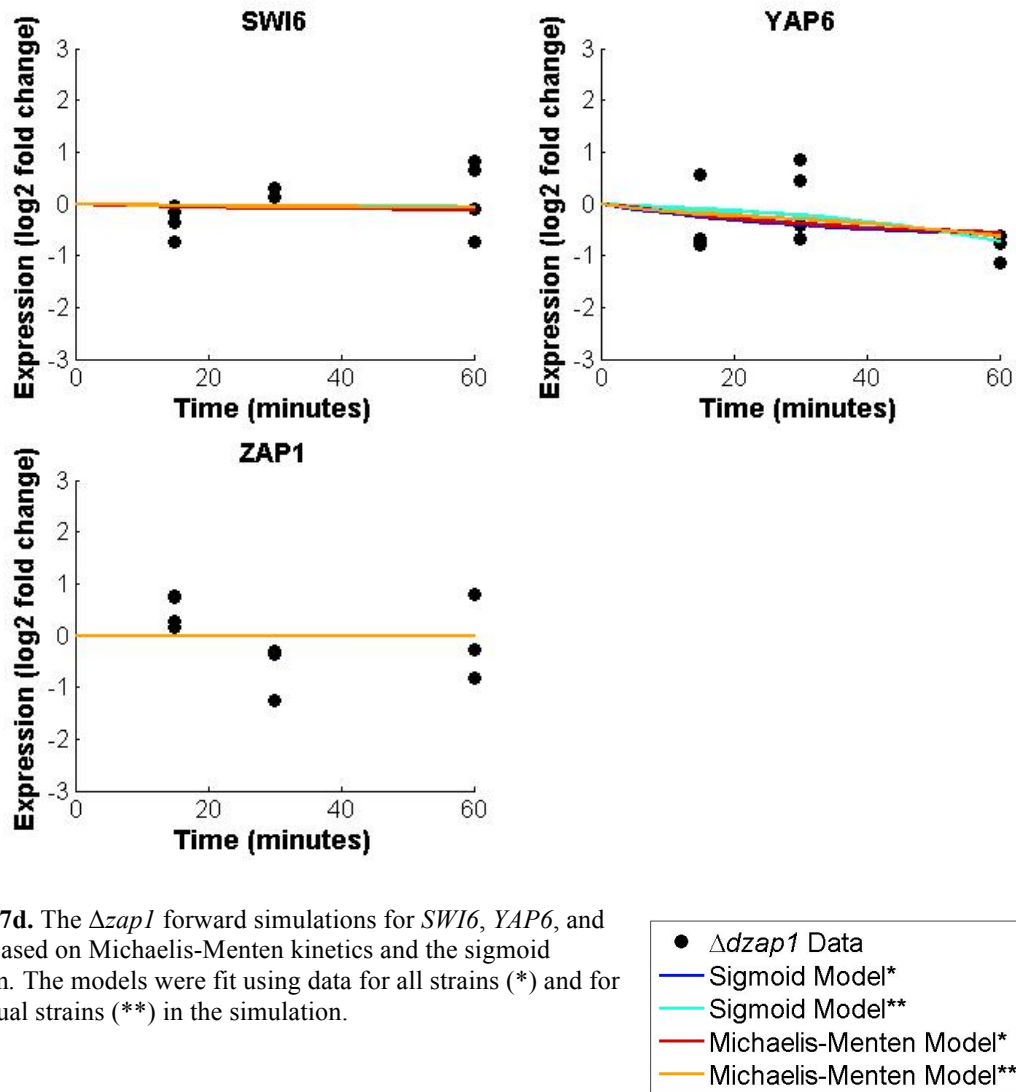


Fig. S27d. The $\Delta zap1$ forward simulations for *SWI6*, *YAP6*, and *ZAP1* based on Michaelis-Menten kinetics and the sigmoid function. The models were fit using data for all strains (*) and for individual strains (**) in the simulation.